Nitrogen Trifluoride-Based Fluoride-Volatility Separations Process: Initial Studies

Fuel Cycle Research & Development

Prepared for
U.S. Department of Energy
Modified Open Cycle
BK McNamara, AM Casella,
RD Scheele, & AE Kozelisky
Pacific Northwest National Laboratory
September 2011
FCR&D-SWF-2011-000390
PNNL-20775

SUMMARY

The use of the low temperature (<100°C) volatility of various fluorides has long been considered a potential approach for separating used nuclear-fuel constituents, particularly uranium and plutonium. The typical fluorinating and oxidizing agent used to produce the volatile fluorides is chemically hazardous and is classified as a reactivity hazard. For example, thermal molecular fluorine and chlorine trifluoride are highly toxic and have the highest National Fire Protection Association chemical and hazard ratings. Because of their aggressive reactivity, when used to fluorinate used nuclear fuel constituent oxides, the volatile fluorides are produced simultaneously. To recover the valuable uranium and plutonium constituents, the volatile fluorides must be separated based on small differences in boiling points, sublimation temperatures, or trapped from the gas phase by selective fluoride salts. Not all chemically trapped constituents can be recovered but for those that can, thermal treatment with or without a fluorinating gas is required, thereby complicating the separations and recovery process for the valuable fuel constituents.

We have been investigating nitrogen trifluoride (NF_3) as the fluorinating and oxidizing agent for a process to recover valuable used nuclear-fuel constituents. Nitrogen trifluoride is minimally hazardous and is not reactive at room temperature, which should simplify a fluoride-volatility based separations process. Because of its lesser reactivity, NF_3 is a thermally-sensitive reactant. In other words, it will react with different compounds at different temperatures. This thermal sensitivity permits the separations approach in which the temperature is controlled at the temperature where a particular compound reacts to form a volatile fluoride. For example, our studies have shown that NF_3 reacts with neat technetium oxide near 300°C to form a volatile fluoride, while neat uranium oxides require temperatures near 500°C to form a volatile fluoride with NF_3.

Thus, in concept, selected fission products and actinides in used nuclear fuel could be released from the fuel when treated with NF_3 at various temperatures. This would eliminate many of the elaborate separations schemes required to purify the valuable constituents released simultaneously with a more aggressive fluorinating agent.

To develop such a process, our overall strategy is to 1) determine whether NF_3 has the potential to produce volatile fluorides or oxyfluorides from potential fuel constituent compounds through thermodynamic calculations, 2) determine experimentally whether and at what temperature NF_3 can convert the neat compounds to volatile fluorides and whether thermally based separations can occur, 3) demonstrate thermally based separations of fission product and actinide volatile fluorides from admixtures with uranium dioxide (UO_2) or U_3O_8 to estimate maximum separation factors, 4) demonstrate separation of fission products and actinides from solid solution-mixed oxides, and 5) demonstrate separations from actual used nuclear fuel. These activities will yield information needed to develop a flowsheet.

Brief descriptions of our FY 2011 accomplishments follow: 1) we evaluated the thermodynamic potential for NF_3 to produce volatile fluorides from fission product and actinide oxides that might be found in used nuclear fuels; 2) we determined experimentally, using thermoanalytical methods, the thermal sensitivities of NF_3 fluorinations of fission product and actinide oxides focusing primarily on those constituents that form volatile or semi-volatile fluorides; and 3) we developed nominal kinetic models for the fluorination reactions. Results from FY 2011 work are listed below:

- Our thermodynamic evaluations indicated that NF_3 could produce volatile fluorides from all known constituents with volatile fluorides.

- Our experimental thermoanalytical studies found that NF_3:
  - could produce volatile fluorides from the oxides of tellurium, niobium, molybdenum, technetium, ruthenium, uranium, and neptunium
  - did not produce the plutonium and rhodium volatile fluorides in observable amounts
  - fluorinated selected constituents that do not form volatile fluorides to fluorides or oxyfluorides. Neither lanthanum oxide nor cerium oxide were converted to volatile fluorides.
- Our thermoanalytical studies found that the volatile fluoride or oxyfluoride production reactions were temperature dependent or were thermally sensitive. Our work with neat compounds indicates that constituents could be selectively separated using different temperatures.
- Our kinetic evaluations found that through temperature selection, constituents can essentially be converted to volatile fluorides in process times <100 min.
- Our in-depth kinetic evaluations and modeling using common gas-solid reaction mechanisms found that different oxides and intermediates reacted via different mechanisms and that the mechanism was temperature sensitive. The predominant gas-solid reaction mechanisms appear to be either one- or two-dimensional phase boundary, three dimensional diffusion, or first-order chemical reactions. The total gas-solid reaction mechanism is dependent on both the chemical reaction mechanism and the various physical characteristics of the solid.

The conceptual process flowsheet developed based on these early experimental studies uses a triuranium octaoxide produced by the voloxidation process as the feed into the first NF_3-fluorination unit, which operates near 300°C, to volatilize molybdenum and technetium; the second NF_3-fluorination unit, which operates near 400°C, to release niobium, ruthenium, and tellurium; the third NF_3-fluorination unit, which operates near 550°C, to release uranium and possibly neptunium; and the final fluorination unit, which uses fluorine or chlorine trifluoride and operates between 400 and 600°C, to release plutonium and possibly neptunium. The alkaline earths, the alkalis, the lanthanides, and lesser fission products remain in the waste residue. The flowsheet proposes the use of a fluidized bed for the fluorination unit.

Overall, our studies show that using the thermal sensitivity of NF_3 as a reactant to produce volatile fluoride is a potentially attractive and viable approach for processing used nuclear fuels to recover valuable constituents or for recovering medical radioisotopes from irradiated materials. The ability of NF_3 to partially fluorinate uranium dioxide to oxyfluorides hints at the possibility that such treatment could be used to release tritium, iodine, and the volatile fission gases from the used fuel matrix.

ACKNOWLEDGEMENTS

The authors would like to thank Cal Delegard for his technical review, and Cary Counts and Meghan Chalk for their editing and document production work, and the Department of Energy for their support of this research.

CONTENTS

FIGURES

TABLES

ACRONYMS

BET	Brunauer-Emmett-Teller
CCD	Thermoelectrical Cooled Charge Coupled Detector
DTA	Differential Thermal Analyzer
EDS	Energy Dispersive Spectroscopy
GEA	Gamma Energy Analysis
ΔG	Gibbs free energy change
ΔH	enthalpy change
ICP/MS	Inductively Coupled Plasma/Mass Spectrometer
MOx	Mixed Oxide (normally uranium and plutonium)
SEM	Scanning Electron Microscope
TG	Thermogravimetric
XRD	X-ray diffraction

SEPARATIONS AND WASTE FORMS/FCR&D PROGRAM

1. INTRODUCTION

Fluorination technologies have been used historically to convert various uranium feedstocks to uranium hexafluoride (UF_6) for ^{235}U isotope enrichment (Schmets 1970; Shatalov et al. 2001; Kamoshida et al. 2000) and have been discussed for nuclear-fuel recycling (Chilenskas 1968; Jonke 1965; Levitz et al. 1969), nuclear materials separations (Galkin et al. 1990), purification (Schmets 1970; Stephenson et al. 1967), and U.S. Department of Energy (DOE) site decontamination (Scheele et al. 2006; Del Cul et al. 2002). The separations processes rely on the ability of some actinides and fission products to form volatile or semi-volatile fluorides to effect separations from other nuclear fuel constituents that do not form volatile fluorides or oxyfluorides. Table 1-1 provides the melting and boiling or sublimation temperatures for fission products and actinide fluorides that are volatile or semi-volatile.

Table 1-1. Volatile fission products and volatile actinide and fission product fluorides (Uhlíř and Mareček 2009).

Highly Volatile			Moderately Volatile		
Substance	T_{melt}, °C	T_{boil}, °C	Fluoride	T_{melt}, °C	T_{boil} or T_{subl}, °C
Kr	-157.2	-153.4	IF_7	5	4
CF_4	-184	-129	MoF_6	17.6	33.9
Xe	-111.8	-108.1	RuF_6	32.1	45.9
TeF_6		-38.6	NpF_6	54.8	55.2
SeF_6		-34.5	TcF_6	37.9	55.2
			UF_6	64	56.5
			PuF_6	51.9	62.2
			IF_5	9.4	98
			SbF_5	6	142.7
			NbF_5	80	235
			RuF_5	101	70
			RhF_5		95.5
			RhF_6	70	73.5

The hexafluorides of uranium, plutonium, and neptunium can be separated from complex matrices and each other by their volatility and the physical properties (boiling point, sublimation point, etc.) of the gaseous products. Large-scale fluorination processes typically have depended on using potent fluorination

reagents that are hazardous to human health, environmentally intrusive, and expensive to produce, transport, and store. The reaction kinetics of several of these molecular fluorine (Iwasaki 1968; Iwasaki 1964; Labaton 1959; Labaton and Johnson 1959; Yahata and Iwasaki 1964; Sakurai 1974), chlorine trifluoride (ClF_3) (Labaton 1959), $BrCl_3$ (Sakurai 1974), dioxygen difluoride (O_2F_2) (Kim and Campbell 1985; Malm et al. 1984; Streng 1963; Burg 1950), and krypton difluoride (KrF_2) (Burg 1950; Ishii and Kita 2000) have been investigated with regard to their utility as fluorinating reagents for uranium and its fission products.

A potential alternative fluorinating reagent nitrogen trifluoride (NF_3) is currently used on an industrial scale to etch and clean microelectronic devices (Golja et al. 1985; Golja et al. 1983; Langan 1998; Kastenmeier 2000). Nitrogen trifluoride is not corrosive and does not react with moisture, acids, or bases at room temperature, is thermally stable to relatively high temperatures, and also is insensitive to shock to pressures above 100,000 psi (Anderson et al. 1977). With its lower chemical and reactivity hazard with respect to other fluorinating agents considered in the past for reprocessing used nuclear fuels, reduced economics associated with transportation, storage, and everyday laboratory or large scale processes could be realized.

In addition to improved safety characteristics, our past studies have shown that NF_3 is a thermally sensitive reagent that reacts with different compounds at different temperatures (McNamara et al. 2009; Scheele et al. 2006). Conceptually, differences in the reaction temperatures of NF_3 with different used nuclear fuel constituents could be used to accomplish selective, temperature-programmed separations of those constituents that form volatile fluorides or oxyfluorides from each other and from those constituents that do not form volatile fluorides or oxyfluorides. The evolved volatile fluorides could be trapped and managed to best utilize the actinide or fission product. The non-volatile residue would be simultaneously fluorinated in this process.

Our strategy for investigating the application of NF_3 to reprocessing used nuclear fuel is to 1) determine through thermodynamic calculations whether NF_3 has the potential to produce volatile fluorides or oxyfluorides from potential fuel constituent compounds, 2) determine experimentally whether and at what temperature NF_3 can convert the neat compounds to volatile fluorides and whether thermally based separations can occur, 3) demonstrate thermally-based separations of fission product and actinide volatile fluorides from admixtures with uranium dioxide (UO_2) or U_3O_8 to estimate maximum separation factors, 4) demonstrate separation of fission products and actinides from solid solution mixed oxides, and 5) demonstrate separations from actual used nuclear fuel. These activities will yield important information needed to develop a flowsheet for processing used nuclear fuel.

This report provides the results of our early investigations into the potential use of the thermally sensitive NF_3 as a replacement fluorinating and oxidizing agent in a fluoride volatility-based used nuclear-fuel treatment process. We provide the results of our thermoanalytical studies, kinetic, and thermodynamic considerations of NF_3 as a fluorinating and oxidizing agent for compounds relevant to the recycle of used nuclear fuel. This report also provides a preliminary flowsheet that applies various possible methods to effect separations of uranium and volatile actinides and fission products from non-volatile ones.

2. Factors Affecting NF_3 Use as a Fluorinator and Oxidizer

Whether NF_3 can be used to fluorinate and/or oxidize used nuclear fuel constituents depends on its reaction thermodynamics and the rates at which the reactions occur. The reaction thermodynamics determine whether a reaction is favored or not. The kinetics determines whether the rates at which a reaction occurs. These two properties determine a reaction's thermal sensitivity or the temperature at which the reaction can and will occur.

Reaction enthalpies and free energies depend on temperature and can range from endothermic (i.e., requiring heat) to exothermic (producing heat) with either an increase or decrease in temperature. For elementary reactions, the rate of a reaction has an exponential dependence on temperature as depicted in the Arrhenius rate equation for the rate constant k.

$$k = A \exp(-E_a/RT) \quad (1)$$

where A is the Arrhenius or frequency factor, E_a is the activation energy, R is the gas constant, and T is temperature in K.

This section provides the calculated reaction enthalpies (ΔH) and free energies (ΔG) and a discussion on the nature of gas-solid reactions.

2.1 Thermodynamics of NF_3 Fluorination

Whether a reaction can and does occur depends respectively on its thermodynamics and its reaction kinetics. The thermodynamic properties and reaction rates are dependent on temperature; thus, calculated reaction enthalpies and free energies based on known thermodynamic properties provide an indication of whether a particular reaction can or cannot occur. To determine if NF_3 had the potential to produce volatile fluorides from the oxides and metals that might occur in used nuclear fuels (Kleykamp 1985; Kleykamp et al. 1985), we used the HSC Chemistry® (Roine et al. 2009) chemical reaction and equilibrium software package to calculate ΔH and ΔG for postulated reactions between NF_3 and uranium, neptunium, plutonium, and other fission product compounds that produce volatile fluorides or oxyfluorides. Table 2-1 provides calculated thermodynamic properties for a median temperature of 300°C as the calculated values did not change more than 10 percent between 200 and 600°C.

Table 2-1. Calculated reaction enthalpies and free energies for NF3 fluorination of selected fission product oxides, metals, and actinide oxides at 300°C.

Postulated Reaction	ΔH, kJ/mol metal	ΔG, kJ/mol metal
$La_2O_{3(s)} + 2NF_{3(g)} = 2LaF_{3(s)} + N_{2(g)} + 1.5O_{2(g)}$	-669	-690
$CeO_{2(s)} + NF_{3(g)} = CeF_{3(s)} + 0.5N_{2(g)} + O_{2(g)}$	-464	-522
$CeO_{2(s)} + 1.33NF_{3(g)} = CeF_{4(s)} + 0.66N_{2(g)} + O_{2(g)}$	-579	-630
$SeO_{2(s)} + 1.33NF_{3(g)} = SeF_{4(g)} + 0.666N_{2(g)} + O_{2(g)}$	-415	-532
$0.5\ Nb_2O_{5(s)} + 1.67\ NF_{3(g)} \rightarrow NbF_{5(g)} + 0.83\ N_{2(g)} + 1.25\ O_{2(g)}$	-571	-705
$0.5\ Nb_2O_{5(g)} + NF_{3(g)} \rightarrow NbOF_{3(g)} + 0.5\ N_{2(g)} + 0.75\ O_{2(g)}$	-277	-412
$Mo_{(s)} + 1.66NF_{3(g)} = MoF_{5(g)} + 0.833N_{2(g)}$	-1023	-1057
$Mo_{(s)} + NF_{3(g)} = MoF_{3(s)} + 0.5N_{2(g)}$	-773	-725
$Mo_{(s)} + 2NF_{3(g)} = MoF_{6(g)} + N_{2(g)}$	-1291	-1291
$MoO_{2(s)} + 2NF_{3(g)} = MoF_{6(g)} + N_{2(g)} + O_{2(g)}$	-706	-810
$MoO_{2(s)} + 1.66NF_{3(g)} = MoF_{5(g)} + 0.833N_{2(g)} + O_{2(g)}$	-262	-345
$MoO_{2(s)} + NF_{3(g)} = MoF_{3(s)} + 0.5N_{2(g)} + O_{2(g)}$	-188	-243
$MoO_{2(s)} + 1.33NF_{3(g)} = MoF_{4(g)} + 0.666N_{2(g)} + O_{2(g)}$	-186	-336
$MoO_{3(s)} + 2NF_{3(g)} = MoF_{6(g)} + N_{2(g)} + 1.5O_{2(g)}$	-550	-694
$MoO_{3(s)} + 1.66NF_{3(g)} = MoF_{5(g)} + 0.833N_{2(g)} + 1.5O_{2(g)}$	-281	-459
$MoO_{3(s)} + 1.33NF_{3(g)} = MoF_{4(g)} + 0.666N_{2(g)} + 1.5O_{2(g)}$	-30	-220
$MoO_{3(s)} + 2NF_{3(g)} = MoF_{3(s)} + 0.5N_{2(g)} + 1.5O_{2(g)}$	-32	-127
$Tc_{(s)} + 1.66NF_{3(g)} = TcF_{5(g)} + 0.833N_{2(g)}$	-849	-860

Postulated Reaction	ΔH, kJ/mol metal	ΔG, kJ/mol metal
$Tc_{(s)} + 2NF_{3(g)} = TcF_{6(g)} + N_{2(g)}$	-993	-989
$TcO_{2(s)} + 2NF_{3(g)} = TcF_{6(g)} + N_{2(g)} + O_{2(g)}$	-538	-638
$RuO_{2(s)} + 1.33\ NF_{3(g)} \rightarrow RuF_{4(s)} + 0.67\ N_{2(g)} + O_{2(g0}$	-477	-530
$RuO_{2(s)} + 1.67\ NF_{3(g)} \rightarrow RuF_{5(g)} + 0.83\ N_{2(g)} + O_{2(g0}$	-289	-406
$0.5\ Rh_2O_{3(s)} + NF_{3(g)} \rightarrow RhF_{3(s)} + 0.5\ N_{2(g)} + 0.75\ O_{2(g)}$	-425	-456
$0.5\ Rh_2O_{3(s)} + 1.33\ NF_{3(g)} \rightarrow RhF_{4(s)} + 0.67\ N_{2(g)} + 0.75\ O_{2(g)}$	-590	-616
$TeO_{2(s)} + 1.33\ NF_{3(g)} \rightarrow TeF_{4(s)} + 0.67\ N_{2(g)} + O_{2(g)}$	-325	-427
$TeO_{2(s)} + 1.33\ NF_{3(g)} \rightarrow TeF_{4(g)} + 0.67\ N_{2(g)} + O_{2(g)}$	-454	-588
$TeO_{2(s)} + 1.67\ NF_{3(g)} \rightarrow TeF_{5(g)} + 0.83\ N_{2(g)} + O_{2(g)}$	-621	-734
$TeO_{2(s)} + 2\ NF_{3(g)} \rightarrow TeF_{6(g)} + N_{2(g)} + O_{2(g)}$	-655	-721
$U_{(s)} + 1.333NF_{3(g)} = UF_{4(s)} + 0.666N_{2(g)}$	-1731	-1673
$U_{(s)} + 2NF_{3(g)} = UF_{6(g)} + N_{2(g)}$	-1895	-1867
$UO_{2(s)} + 2NF_{3(g)} = UF_{6(g)} + N_{2(g)} + O_{2(g)}$	-799	-901
$UO_{2(s)} + 1.33NF_{3(g)} = UF_{4(s)} + 0.666N_{2(g)} + O_{2(g)}$	-983	-1044
$UO_{2(s)} + 0.666NF_{3(g)} = UO_2F_{2(s)} + 0.333N_{2(g)}$	-391	-417
$UO_2F_{2(s)} + 1.333NF_{3(g)} = UF_{6(g)} + 0.666N_{2(g)} + O_{2(g)}$	-334	-431
$UF_{4(s)} + 0.666NF_{3(g)} = UF_{6(g)} + 0.333N_{2(g)}$	-164	-194
$U_3O_{8(s)} + 6NF_{3(g)} = 3UF_{6(g)} + 3N_{2(g)} + 4O_{2(g)}$	-708	-806
$U_3O_{8(s)} + 4NF_{3(g)} = 3UF_{4(s)} + 2N_{2(g)} + 4O_{2(g)}$	-551	-618
$U_3O_{8(s)} + 2NF_{3(g)} = 3UO_2F_{2(s)} + N_{2(g)} + O_{2(g)}$	-374	-374
$UO_{3(s)} + 2NF_{3(g)} = UF_{6(g)} + N_{2(g)} + 1.5O_{2(g)}$	-675	-792
$Pu_{(s)} + 1.333NF_{3(g)} = PuF_{4(s)} + 0.666N_{2(g)}$	-1672	-1604
$Pu_{(s)} + 2NF_{3(g)} = PuF_{6(g)} + N_{2(g)}$	-1569	-1525
$PuO_{2(s)} + 2NF_{3(g)} = PuF_{6(g)} + N_{2(g)} + O_{2(g)}$	-450	-516
$PuO_{2(s)} + 1.33NF_{3(g)} = PuF_{4(s)} + 0.666N_{2(g)} + O_{2(g)}$	-815	-880
$PuF_{4(s)} + 0.666NF_{3(g)} = PuF_{6(g)} + 0.333N_{2(g)}$	+113.2	+54.1
$NpO_{2(s)} + 1.33NF_{3(g)} = NpF_{4(s)} + 0.666N_{2(g)} + O_{2(g)}$	-303	-438
$NpF_{4(s)} + 0.666NF_{3(g)} = NpF_{6(g)} + 0.333N_{2(g)}$	+20.4	-39.2

The thermodynamic data for uranium metal, UO_2, triuranium octoxide (U_3O_8), uranium trioxide (UO_3), uranyl fluoride (UO_2F_2), and uranium tetrafluoride (UF_4) in Table 2-1 indicates that the heats of reaction produced during the fluorination process increase as the uranium oxidation state decreases. The same effect can often be observed for the analogous series for plutonium, molybdenum, and technetium metals and their oxides. For these calculations, we used reactions that would be most thermodynamically favorable thus producing molecular nitrogen (N_2) rather than oxides of nitrogen. In general, the product distributions for fluorination reactions with oxides have not been determined and it should not be construed that these are actual product distributions for each of these systems. However, the oxyfluorides and fluorides, N_2 and O_2 are likely the dominant products based on our limited off-gas characterizations that did not observe any experimentally produced nitrogen oxides.

The ΔH and ΔG for the reactions of NF_3 with metals and metal oxide systems presented in Table 2-1 are generally predicted to be exothermic or have favorable thermodynamic properties. Of note from an

experimental perspective is that the ΔH for the conversion of NpF_4 to NpF_6 is endothermic. In general, the reactions observed in our studies are exothermic. Accordingly, exothermic behavior should be observable in the thermoanalytical results with the potential exception of the PuF_4 to PuF_6 which is not a favorable reaction and NpF_4 to NpF_6 reaction which will be driven by entropy change.

The calculated thermodynamic properties for the sequential fluorination reactions of a metal or its oxide to the fluorinated product suggest that sequential reactions should occur. The observation of sequential reactions will be dictated by the kinetics of each sequential reaction and the response time of the analytical method. Earlier reactions can be obscured by the onset of a subsequent reaction.

In general, the calculated ΔGs indicate that NF_3 should produce the anticipated volatile fluorides. One potential exception to this generalization is the formation of plutonium hexafluoride (PuF_6) should the reaction form plutonium tetrafluoride (PuF_4) as an intermediate. The calculated ΔG for the conversion of PuF_4 to PuF_6 by NF_3 is positive or endothermic and not favorable even though the direct conversion of PuO_2 or Pu to PuF_6 is thermodynamically favorable. This also indicates that should PuF_6 be formed, it will decompose to PuF_4 unless the equilibrium can be shifted to favor PuF_6 by addition of fluorine (F_2) for example.

3. Gas-Solid Reaction Kinetics Considerations

This project investigated using the thermal sensitivity of NF_3 through thermodynamic calculations of temperature effects on sequential fluorination reactions, characterization of fluorinated intermediates through experiment and validation with the fluorination literature, and modeling of gravimetric data to understand factors that govern the temporal evolution of the products of fluorination. Gas-solid reaction kinetics can play an important role in achieving the goal of separating fuel constituents from each other. Simple chemical modeling is inadequate because it does account for the physical characteristics of the solids throughout the conversion and their impact on the access of the gas reactant to the solid reactant.

Physical factors that govern reaction kinetics include gaseous reactant diffusion through the solid reactant, diffusion through an intermediate product barrier, nucleation and growth, and autocatalysis. These physical processes often have temporal existence that masks details of the underlying chemical reactivity. Consequently, measurement of elementary chemical kinetic parameters that we had initially proposed in this project is not rigorously possible for fluorination of the relevant metal and metal oxide systems.

The kinetic behavior described below is well known in other areas of engineering research, but it has not been adapted to fluorination literature until now. It is possible that fluorination of metal and metal oxide surfaces using more aggressive reagents such as fluorine (Ogata et al. 2004; Homma et al. 2008), bromine pentafluoride (BrF_5), ClF_3 (Labaton 1959), etc., follows the "shrinking core" reaction model or similar physical kinetic behavior, but it also could be that the reagent reactivity is such that product barriers, for instance, are fluorinated away with equivalent facility as the starting material. Thermoanalyses of fluorination reaction with aggressive fluorinating agents show little evidence of sequential product formation; rather, volatile production appears to be kinetically favored, and the final process of volatilization likely dominates the observable. Less reactive reagents such as sulfur tetrafluoride (SF_4) or sulfur hexafluoride (SF_6) might have increased thermal sensitivity (Johnson and Fischer 1961; Gray et al. 2010) relative to that described in this report for NF_3.

3.1 Factors Affecting Gas/Solid Reaction Rates

The reaction rate(s) of gas-solid reactions that produce gaseous products are governed by several phenomena of which chemical reactivity is only one. Generally, these phenomena (as described relative to the illustration in Figure 3-1) are associated with:

1. transport of the reactive gas species (i.e., NF_3) from the bulk gas to a stagnant film layer that surrounds the solid reactant (e.g., UO_2)
2. transport of the reactive gas species through the film layer to the surface of the solid reactant
3. adsorption of the reactive gas species onto the surface of the solid reactant
4. reaction between the gas and solid
5. diffusion of the reaction gas species through intermediate solid reaction product(s) that form on the surface
6. adsorption/reaction of the gaseous reactant with the fresh solid reactant beneath the intermediate solid product layer
7. transport of gaseous products away from the solid reactant surface through the stagnant film layer to the bulk gas.

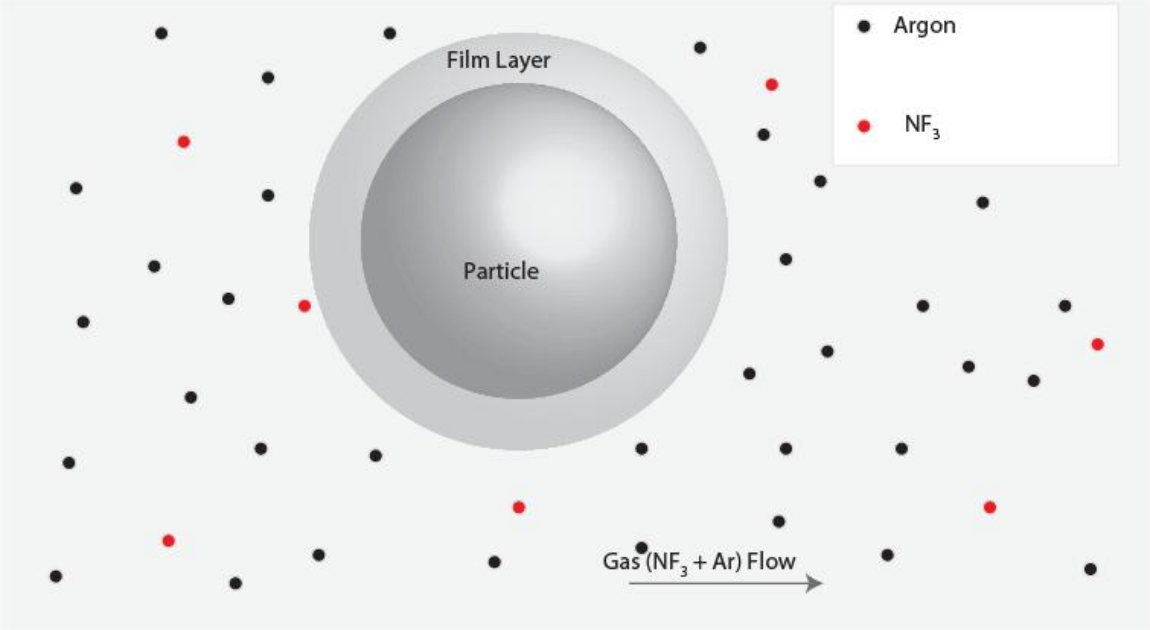

Figure 3-1. Gas-solid interactions.

With any system of reactive gas species, carrier gas species, solid reactant species, and temperature, any of the phenomena listed above may be the limiting step in the overall reaction process. Thus, our objective was to determine which steps are the most important in the control of the gas-solid reaction system of interest and whether they might be used to achieve the desired separation factors.

3.2 Commonly Applied Gas/Solid Kinetic Models

A useful method for determining the rate-limiting step in the overall mechanism of a gas-solid reaction is to compare the shape of the time-dependent fractional conversion curve for the reaction to curves generated for theoretical relations (Sharp et al. 1966). Table 3-1 lists the standard mathematical relationships between the fraction conversion (α), time (t), and half-time (i.e., the time it takes for the reaction to reach 50 percent completion, $t_{0.5}$) for the standard gas-solid reaction models as well as correlations to physical parameters. The shapes of the curves generated by these relations are illustrated in Figure 3-2.

Table 3-1. Common kinetic models for gas-solid reactions (Sharp, Brindley and Achar 1966).

Model	Mathematical Relation
Two-Dimensional Phase-Boundary	$[1-(1-\alpha)^{1/2}] = (u/r)t = 0.2929(t/t_{0.5})$
Three-Dimensional Phase-Boundary	$[1-(1-\alpha)^{1/3}] = (u/r)t = 0.2063(t/t_{0.5})$
One-Dimensional Diffusion	$\alpha^2 = (k/x^2)t = 0.2500(t/t_{0.5})$
Three-Dimensional Diffusion	$[1-(1-\alpha)^{1/3}]^2 = (k/r^2)t = 0.0426(t/t_{0.5})$
First-Order Reaction	$ln(1-\alpha) = -kt = -0.6931(t/t_{0.5})$
Two-Dimensional Nucleation and Growth	$(-\ln(1-\alpha))^{1/2} = kt = 0.8326(t/t_{0.5})$
Three-Dimensional Nucleation and Growth	$(-\ln(1-\alpha))^{1/3} = kt = 0.8850(t/t_{0.5})$

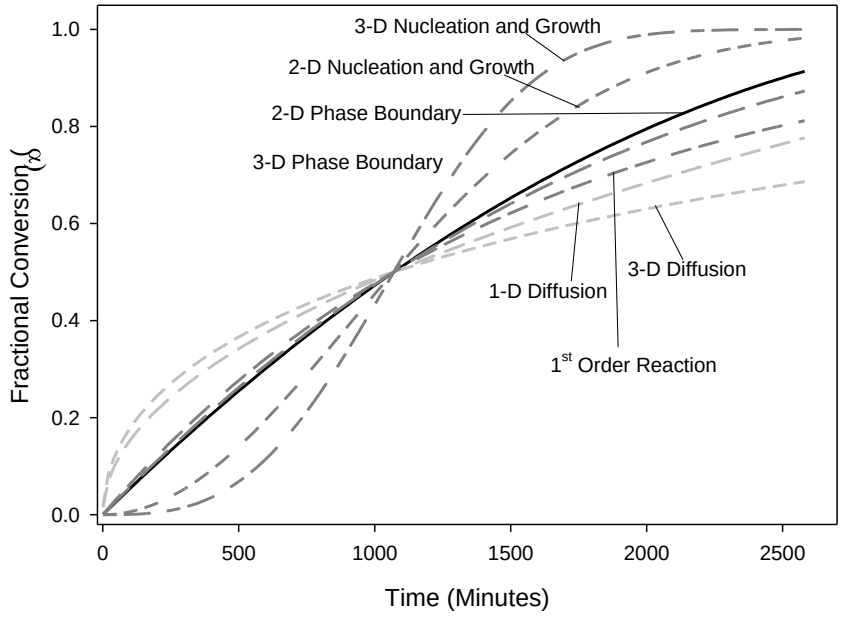

Figure 3-2. Depiction of commonly used kinetic models for gas-solid reactions (See Table 3-1).

The models presented Table 3-1 and Figure 3-2 are further described as:

- *Two-Dimensional Phase-Boundary* − A reaction controlled by the movement of an interface at constant velocity *u* from the edge inward for a disk or a cylinder with radius *r*.
- *Three-Dimensional Phase-Boundary* − A reaction controlled by the movement of an interface at constant velocity *u* from the edge inward for a sphere with radius *r*.
- *One-Dimensional Diffusion* − A reaction controlled by a diffusion process with a constant diffusion coefficient *k* through a reacting layer of thickness 2*x*.
- *Two-Dimensional Diffusion* − A reaction controlled by a diffusion process with a constant diffusion coefficient *k* through a cylinder of radius *r*.
- *Three-Dimensional Diffusion* − A reaction controlled by a diffusion process with a constant diffusion coefficient *k* through a sphere of radius *r*.
- *First-Order Reaction* − A simple first order chemical reaction between the solid and gaseous reactants.

- *Two-Dimensional Nucleation and Growth* − A reaction governed by the nucleation of gaseous reactant upon the solid reactant and subsequent growth outward from this nucleation site in two dimensions.
- *Three-Dimensional Nucleation and Growth* − A reaction governed by the nucleation of gaseous reactant upon the solid reactant and subsequent growth outward from this nucleation site in three dimensions.

The reason that it is useful to consider multiple versions of each model (one-, two-, three-dimensional) is that the overall reaction rate will possibly be affected by the sample geometry (sphere, slab) as well as its arrangement (layers, piles, flat, angled). This point is illustrated by Figure 3-3, which displays two sample arrangement scenarios that present themselves in this work. In the first arrangement, the reactant gas (NF_3) is swept over the sample pan that holds a powder. Although the particulates of the powder are spherical in shape, suggesting the applicability of a three-dimensional model, the NF_3 may simply react down through the powder as though it were a slab, necessitating the application of a one-dimensional model. In addition, the second arrangement shows a slab that is not placed flat on the bottom of the pan so that it is possible for the NF_3 to react with both sides, so that a model other than a one-dimensional model may be more appropriate.

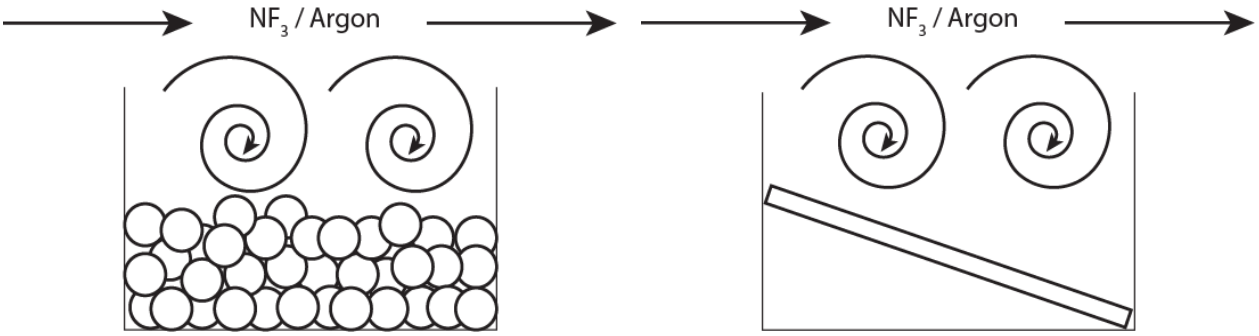

Figure 3-3. Gaseous experimental geometries within the TGA for powders (left) and slab (right).

The method for applying these fractional conversion curves is to first determine α from the M(t) curve generated from the experiment and to then compare the shape of that curve to the theoretical curves in Table 3-1. Once a mechanism has been identified, the characteristic reaction parameter associated with the mechanism can be determined from the reaction half time (the time it takes the reaction to reach 50 percent completion, ($t_{0.5}$). The characteristic parameter is different for each reaction mechanism.

If the characteristic parameter associated with a given reaction can be determined at various temperatures, then one way to determine a temperature dependence of the characteristic parameter for a given equation is to use an equation that is analogous to the Arrhenius equation for a standard chemical reaction. Equation (2) is the standard form of the Arrhenius Equation, and Equation (3) has been modified to a form that is applicable to a phase-boundary governed reaction.

$$k = Ae^{-\frac{E_a}{RT}} \tag{2}$$

$$(u/r) = ae^{-\frac{b}{T}} \tag{3}$$

If plotting the natural log of the determined values of (u/r) versus reciprocal temperature results in a straight line, then the y-intercept of that line will be the natural logarithm of the parameter a and the slope will be the negative value of the parameter b. This fit can then be used much like the Arrhenius equation is used to determine the value of the characteristic parameter for the reaction at other temperatures.

However, caution must be exercised to appropriately apply the significance of this approach. In the case of the Arrhenius equation, well known values of A and E_a that are associated with a pure chemical reaction of interest are generated. The values of *a* and *b* generated by this method for a solid-gas reaction are analogous to the Arrhenius parameters A and E_a, but are distinct as they are governed by the kinetic mechanism controlling the gas-solid reaction, which is affected by the kinetics of the chemical reaction plus the many physical factors of the gas-solid system.

For instance, the three-dimensional, phase-boundary mechanism describes the rate at which a spherical solid reactant (or grouping of several solid reactant spheres) reacts inward with time. As the reaction proceeds inward from the sphere surface toward the center of the sphere, the reaction surface area shrinks according to the sphere radius *r*. According to Table 3-1, the characteristic parameter for the three dimensional- phase-boundary mechanism is *u/r* where *r* is the sphere radius and *u* is literally the velocity (in designated units of length/time such as m/s or µm/min) at which the reaction front travels inward along the shrinking spherical reaction surface. Therefore, *a* and *b* are simply fitting parameters that allow us to determine *u/r* for a reaction of interest once they have been determined.

Ultimately, the method of kinetic modeling involved in this work is to try to match the shape of the fractional conversion curve generated from experimental data with a fractional conversion curve generated from a theoretical relation to gain insight into the dominant mechanisms involved in the reaction. This approach will provide the behavioral models needed to define a processing flowsheet for recovering purified or partially purified valuable constituents based on use of different reaction temperatures. Given the complexity of gas-solid reactions and the many chemical and physical factors that can affect reaction kinetics, we initially tested the models presented in Table 3-1; however, many more models exist and methods for developing new models have long been in existence.

4. Experimental Materials and Methods

For our studies, we used materials from a variety of sources. The fission product oxides and metals were commercially supplied. For the actinide oxide fluorination studies, we used materials from our own inventory.

The UO_2 stock used in the isothermal gravimetric studies was purchased from Johnson and Matthey (Ward Hill, Massachusetts). The UO_2 powder used in these experiments was chosen initially for its relatively small particle size. The Brunauer-Emmett-Teller (BET) surface area of the sample was 0.958 $m^2 \cdot g^{-1}$. X-ray diffraction (XRD) powder patterns of the material indicated that the as-received material was relatively free of primary corrosion products; however as time passed, concentrations of metashoepite increased at the surface. The fresh UO_2 is shown in the scanning electron microscope (SEM) image in Figure 4-1. The material consisted of approximately 200-µm agglomerated spheres that were and easily crushed to <1-µm particles. The particles were crystalline.

The U_3O_8 used in this testing was from the same stocks as described by McNamara et al. (2009). The SEM image presented in Figure 4-2 shows that the National Institute for Standards and Testing U_3O_8 used for testing was typically an aggregate of µm-sized particles.

Two different batches of plutonium dioxide (PuO_2) were used. The first batch was obtained by air oxidization of plutonium metal at 500°C that had partially air-oxidized at room temperature. The second batch of PuO_2 was precipitated from plutonium nitrate solution as the trivalent oxalate. The oxalate product was washed with 0.2 M nitric acid, and calcined to the oxide at 450 to 480°C for 2 h. An SEM image of the PuO_2 from the oxalate presented in Figure 4-3 shows that this PuO_2 had particles ranging from <1 µm to a few µm. The XRD analyses confirmed the product was PuO_2 and a gamma energy analysis (GEA) of a nitric acid solution found 6×10^{-5} kg ^{241}Am/kg Pu.

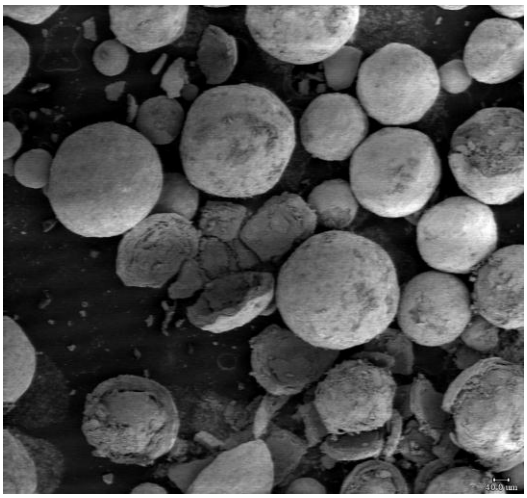

Figure 4-1. 1500 X SEM micrograph of UO_2.

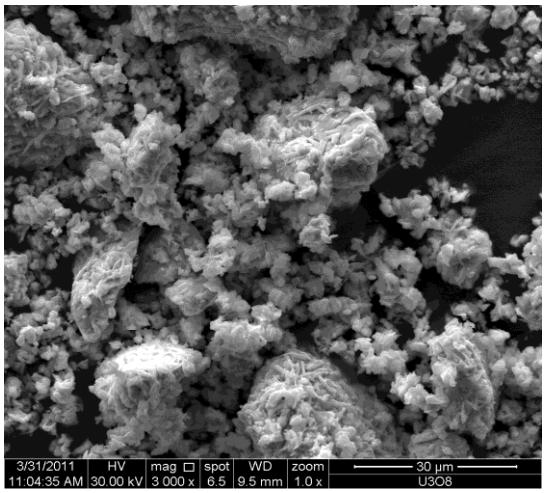

Figure 4-2. 300X SEM micrograph of U_3O_8.

The 99.99-percent pure neptunium dioxide (NpO_2), originally prepared for use as a neutron dosimeter (Adair and Kobisk 1975), was confirmed by XRD analysis to be NpO_2. Figure 4-4 shows that the NpO_2 was an aggregate of 1 to 10 µm-sized particles after crushing using a Wig-L-Bug grinder.

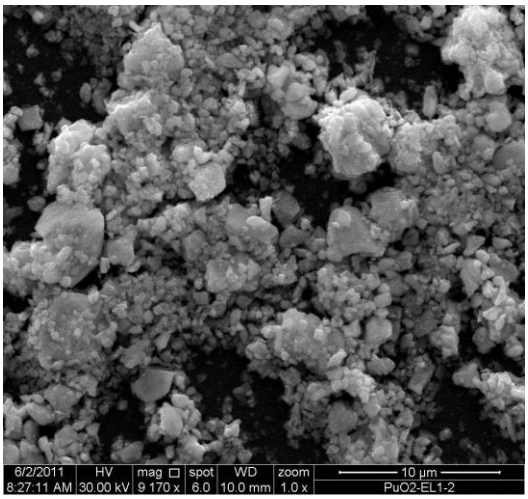

Figure 4-3. 9170X SEM of PuO_2 from oxalate.

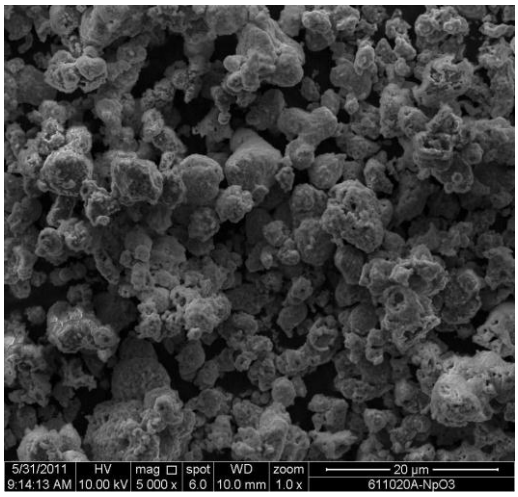

Figure 4-4. 5000X SEM Micrograph of NpO_2.

The mixed uranium and plutonium dioxide (MOx) (ID FS-104) was prepared by Los Alamos National Laboratory (LANL) for analytical laboratory round-robin testing in the 1970s, and was determined by inductively coupled plasma/mass spectrometry (ICP/MS) to be 80% U percent uranium and 20 percent plutonium. SEM analysis coupled with energy dispersive spectroscopy (EDS) analysis of a 600- by 800-µm particle found the plutonium to be distributed uniformly; see Figure 4-5 and Figure 4-6 for a 5000X SEM of the particle and an EDS analysis of the area in the lower left portion. The EDS results show that the MO_X consisted of uranium, plutonium, and oxygen. The unidentified peak is carbon from the carbon coating applied for the SEM analysis.

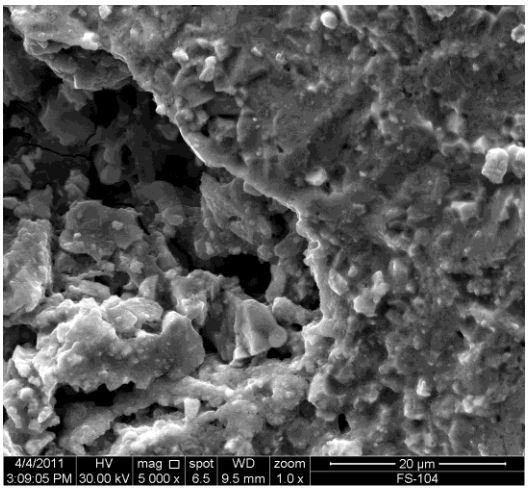

Figure 4-5. 5000X SEM of (0.8 U, 0.2 Pu)O_2.

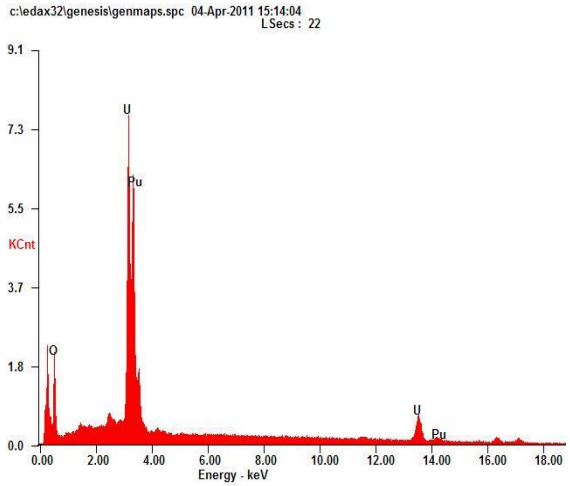

Figure 4-6. EDS Analysis of (0.8 U,0.2 Pu)O_2.

Surrogate non-radioactive fission product oxides were commercially obtained. Alpha Products supplied the 99.9-percent pure ruthenium dioxide (RuO_2), the 99.5-percent pure niobium (V) oxide (Nb_2O_5), and the 99-percent pure molybdenum dioxide (MoO_2). The 99.9-percent purity cerium (IV) oxide (CeO_2) was from GFS Chemicals. Alfa Aesar supplied the 99.999-percent pure lanthanum oxide (La_2O_3), while. EM Science provided the molybdenum trioxide (MoO_3). Fisher Scientific provided the 98-percent pure tellurium dioxide. These materials were used as-received. The Mo-metal was 99.95-percent pure and was from our chemical stock.

TcO_2 was prepared from thermal decomposition of NH_4TcO_4 or by hydrolysis of $(NH_4)_2TcCl_6$. The latter method tended to incur reoxidation of the Tc(IV) to Tc(VI), so it was abandoned for the decomposition method. The particles of the black oxide were determined to be amorphous by XRD analysis. The particles were <1 µm in size but tended to aggregate with aggregate sizes reaching 50 µm. Grey technetium metal powder was prepared by adding 5-percent H_2/Ar to the TcO_2 near 400ºC.

The gases used were 99.995-percent pure NF_3 and either 99.999-percent or 99.9995-percent pure argon.

McNamara et al. (2009) describes older XRD and SEM systems used to characterize materials. XRD analyses were performed using a Rigaku Ultima IV and scan parameters of 10-70 2θ, 0.02 step size, 0.12 sec, 44 mA and 40 kV tube, with a Cu K_α λ= 1.54059 Å. SEM/EDS analyses were performed using an FEI Scanning Electron Microscope, Model Quanta Field Emission Gun 250 coupled with an EDAX Genesis SM2i EDS (energy dispersive x-ray system) with an Apollo silicon drift detector.

Volatile fluorides produced by reacting NF_3 with Mo metal and MoO_2 were condensed in a quartz vessel using a dry ice/acetone bath. The products were characterized using an InPhotonics RS2000, high-resolution, Raman spectrometer using a thermoelectrically cooled charge coupled detector (CCD) operating at -52°C and using a 670 nm, 150 mW diode laser as the excitation source focused using an InPhotonics Raman fiber optic probe operated in a 180° back reflection mode. The spectra and other characteristics of these compounds were compared to those published in the literature (Weaver and Friedman 1967).

Three Seiko 320 and one Seiko 6200 simultaneous thermogravimetric (TG) and differential thermal analyzers (DTA) as described by McNamara et al. (2009) with some small modifications were used. To prevent the denser NF_3, relative to the balance purge Ar, from dropping directly onto the sample and to improve NF_3 concentration control, we moved the mouth of nickel NF_3 delivery tube further back from

2.54 cm to about 3.5 cm from the sample and partially diluted the NF_3 with Ar. The two gases were premixed in the manifold several linear feet from point of entry to the instrument. The total gas flow was typically near 260 mL/min. The sample chamber has a volume of 50 mL. In addition, we also minimized air ingress into the instrument by sealing leaks identified by helium leak testing and eliminating plastic lines, which could be permeable to oxygen.

Volatile neptunium and plutonium fluorides pose special risks that require engineered containment. To mitigate the risk of working with radiotoxic actinides, we installed a Seiko Model 6200 Isoperibol Calorimeter into an actinide glovebox. The TG/DTA exhaust was passed through a water bubbler to hydrolyze the gaseous actinide fluorides. To minimize the instrument's footprint and facilitate operation, the instrument was modified to relocate the control unit outside the glovebox.

Both temperature ramp and isothermal TG/DTA experiments were performed up to 600°C using 5 or 10 vol% NF_3 in argon. Unfortunately for our instrument, NF_3 becomes more chemically aggressive with increasing temperature, ultimately resulting in degradation and eventual failure of the nickel-coated thermocouples. NF_3-pretreated aluminum pans and NF_3-pretreated nickel pans were used for testing.

For all but the PuO_2, NpO_2, and MOx heat ramp studies, we heated the sample to 400°C in argon to remove any tramp water and cooled the sample to 40°C to obtain an accurate mass at conditions used to calibrate the balance. No tramp water was observed for the actinide oxides. For the temperature ramp studies over the range 40°C to the target temperature (typically 550°C), the NF_3 was introduced at the target concentration and held at 40°C to obtain the sample mass in the NF_3; the recorded mass was lower in the NF_3 purge. For the isothermal tests, after measuring a stable mass at 40°C in argon, the sample was heated to the isothermal temperature at which point the temperature was permitted to stabilize before introducing the target NF_3 concentration. After most experiments, the NF_3 flow was stopped and the sample cooled in Ar to 40°C where the mass was stabilized and measured. For the materials that form non-volatile fluorides, this approach provided an accurate measure of the added fluorine content.

5. Results and Discussion

The chemical nature of the fission products and actinides in used nuclear fuel depends on a variety of factors such as burn-up, oxygen potential or O/M-ratio where O is oxygen and M is the metal, and axial and radial temperature gradients in the fuel pin (Kleykamp 1985). Molybdenum, technetium, ruthenium, rhodium, palladium, silver, cadmium, indium, tin, antimony and tellurium) can be present as metallic precipitates. Rubidium, cesium, barium, zirconium, niobium, molybdenum, and technetium can form oxide precipitates. There are continuous transitions between these two groups of metallic and oxide precipitates due to similar oxygen potentials of the fission product oxides and the UO_2 fuel. Fission products that are dissolved in the fuel matrix are strontium, zirconium, niobium, and the rare earths yttrium, lanthanum, cerium, praseodymium, neodymium, promethium, and samarium. The epsilon or 5-metal phase metal precipitates found in irradiated UO_2 are composed of molybdenum, technetium, ruthenium, rhodium, and palladium.

5.1 NF_3-Fluorination of UO_2

UO_2 is the primary commercial nuclear fuel material and will constitute ~95 percent of a used UO_2-based nuclear fuel. The study of the chemistry of UO_2 is complicated by the formation of higher oxides from exposure to air and water.

From the viewpoint of reprocessing, it is important to note that UO_2 is a sintered product. As a result, the crushed material prior to its irradiation is toughened relative to the unsintered powder by sintering and during irradiation it is toughened further through further exposure to high temperatures.

Mechanical pulverization of unirradiated or irradiated fuel encourages powders to oxidize slowly to $UO_{(2+x)}$ and ultimately to U_4O_9 if heated near 250ºC in air. If the fuel is exposed to atmospheric moisture the surface of the fuel will oxidize to hexavalent hydrated forms of uranium such as metaschoepite ($UO_3 \cdot xH_2O$). Radiolytic heat production in the irradiated fuel, when exposed to atmospheric conditions, initiates oxidative changes more readily and is abetted by radiolytically-formed peroxide.

Measurement of the progress of a reaction, reaction kinetics, and heats of reaction depend on well-defined starting materials. Because oxidative changes in air are slow at room temperature, the issue of oxidation of the UO_2 starting material can be managed over the course of experiments. For irradiated fuel, the extent of oxidation during fuel pretreatments might change expectations of reactivity as is discussed in Section 5.1.2.

Discussed in this section are results for the reaction of NF_3 with UO_2 as if it were a material with a stoichiometric composition of $UO_{2.00}$. Because of their reactivity F_2 and more aggressive fluorinating and oxidizing reagents may not discriminate between small differences in oxidation state. In contrast, for NF_3, such changes could alter experimental results as measured by gravimetry.

5.1.1 Thermodynamics of UO_2 Fluorination

The data in Table 2-1 suggest that fluorination of UO_2 by NF_3 might lead to UF_4 as is the case observed for NpO_2 and PuO_2. In fact, the first observable main product of fluorination is always a uranium oxyfluoride and eventually uranyl fluoride (UO_2F_2). Uranyl fluoride occurs with fluorine and other fluorinating reagents (Sakurai 1974; Yahata and Iwasaki 1964). Exothermic heats of formation of UO_2F_2 appear to be derived from the change in oxidation state from tetravalent uranium to hexavalent uranium. Exothermicity in the subsequent reaction to UF_6 appears to be derived from the high fluorine bond strength in UF_6.

5.1.2 Experimental Results for NF_3 Fluorination of UO_2

The overall reaction to produce UF_6 from reaction of fluorine with UO_2 is considered in the literature to be a two-step process (Ogata et al. 2004) with the first step being the formation of UO_2F_2. The reactions with NF_3 are shown in Eqs. 4 and 5. The general observation is that UO_2F_2 is formed preferentially to UF_6 unless the sample heating rate or reaction heat forces a rapid increase in temperature that drives production of UF_6. This is true to the extent that the entire UO_2 sample can be isothermally converted to UO_2F_2 near 400°C. The result allows a purely thermal synthesis of UO_2F_2 (anhydrous) from UO_2.

$$UO_2 + 2/3\ NF_{3(g)} = UO_2F_2 + 1/3\ N_{2(g)} \quad (4)$$

$$UO_2 + 2\ NF_{3(g)} = UF_{6(g)} + N_{2(g)} + O_{2(g)} \quad (5)$$

Thermoanalytical experiments are run in two ways: 1) in ramp mode and 2) in isothermal mode. Each mode produces different information and either mode might be used in a volatility reprocessing scheme. In general, the ramp mode groups thermal events together in time as the ramp rate is increased. In the isothermal mode, heats of product formation are distributed over time so the kinetics of time-separated, individual events can be investigated. Both modes can are discussed here for UO_2.

Figure 5-1 and Figure 5-2 show the TGA/DTA temperature ramp studies of samples of UO_2 powder exposed to a flow of 5-percent NF_3 in argon gas at $5°C \cdot min^{-1}$ and $20°C \cdot min^{-1}$. At the slower heating rate, the DTA in Figure 5-1 shows three discrete exothermic events (marked 1, 2, and 3) as UO_2 was converted to UF_6. This indicates that at least two intermediate oxyfluorides are formed. The total mass increase observed for the slower heating rate was consistent with complete conversion of the UO_2 sample to $UO_2F_{2(anhydrous)}$ (14.1 wt%) to within 0.02 wt%. It is valuable to note that, once the volatilization reaction begins, the heat from the reaction causes the sample temperature to increase slightly. In Figure 5-2 the

significant mass gain and the three exothermic events are not observed because the higher heating rate forces the individual fluorination and oxidation steps to merge. The TGA observed only a slight mass gain near 200°C, which continued to about 457°C.

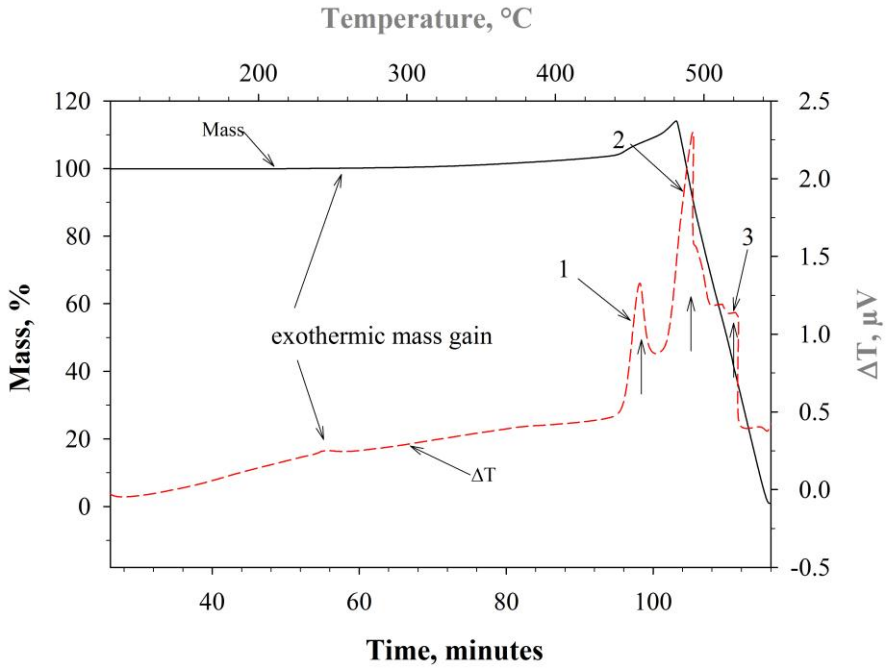

Figure 5-1. Action of 5-percent NF_3 on UO_2 as measured by simultaneous TGA and DTA during heating at 5°C/min.

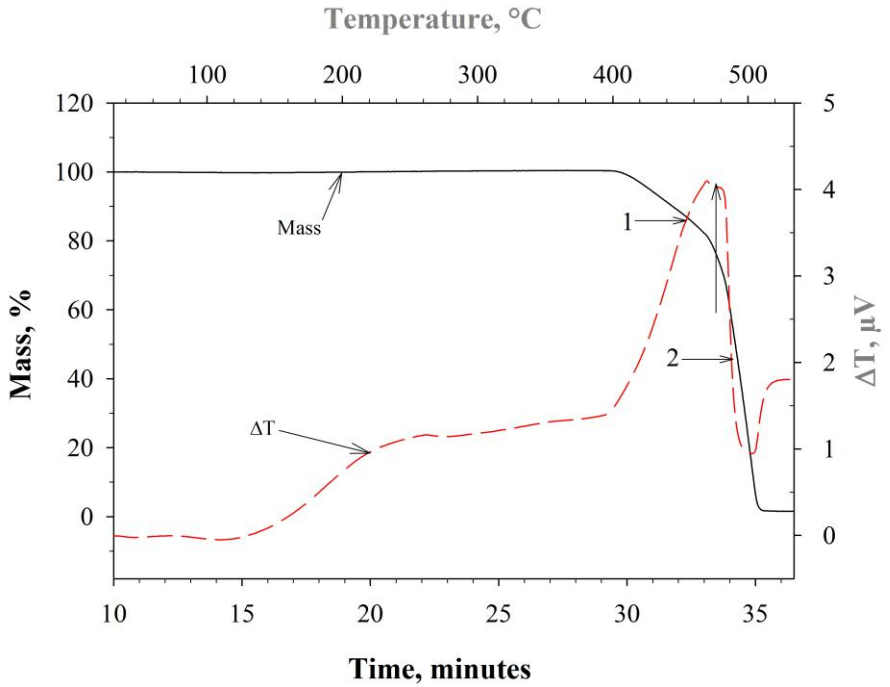

Figure 5-2. Action of 5-percent NF_3 on UO_2 as measured by simultaneous TGA and DTA during heating at 20°C/min.

To obtain a sample of the final intermediate, the reaction was quenched by cooling the sample near 440°C to room temperature under an NF_3/argon purge. An XRD powder pattern acquired from the sample confirmed the presence of UO_2F_2 as the only air-stable product. The mass change and XRD analysis support the finding that the final uranium oxyfluoride formed before UF_6 formation is UO_2F_2.

As shown in Figure 5-1, the final mass increase was followed by rapid, exothermic mass loss, indicating release of UF_6 near 492°C, until 100 percent of the sample was volatilized. On the high-temperature side of the DTA curve, a feature (marked 2) indicates that at least one other chemical species or other thermal event is involved in the release of UF_6. The presence of a third exothermic event has not been cited for fluorination of UO_2 with use of other fluorinating reagents (Ogata et al. 2004). It is not yet understood if the third exotherm as shown was a chemically distinct product or rather was due to physical changes in the evolving sample. Intermediate products of uranium oxide fluorination that have been identified in the literature include UOF_4 (Paine et al. 1975; O'Hare and Malm 1982; Lau et al. 1985; Wilson 1974a; Armstrong et al. 1989), $U_2O_3F_6$ (Wilson 1974b), and $U_3O_5F_8$ (Otey and LeDoux 1967). The distinctive orange coloration of UOF_4 and $U_3O_5F_8$ (Paine, Ryan and Asprey 1975; Otey and LeDoux 1967) has not been observed in our (quenched) experiments.

The higher heating rate of 20°C/min, shown in the TGA scan in Figure 5-2, does not show the mass buildup of UO_2F_2 because the increased sample heat rate accelerated heat and mass transport throughout the sample. In the mass-loss portion of the TG curve, two distinct rate contributions marked (1) and (2) in Figure 5-2 comprise the release of UF_6. The higher heating rate allows observation of a rate-limited region (1), which suggests formation of a product or product barrier, and a region (2) of more facile UF_6 production. These data are aptly described by gas-solid models developed recently for fluorination UO_2 (Ogata et al. 2004) by fluorine. For the fluorine reaction, the formation of UO_2F_2 can be observed, but it appears that the higher reactivity of fluorine, and likely, more aggressive fluorination reagents forces UF_6 production at a rate faster than the build-up of UO_2F_2.

Our isothermal TG studies suggest that the first exotherm observed in Figure 5-1 is due to the formation of a stable uranium oxyfluoride which indicates that NF_3 is able to deliver fluorine into the UO_2 which in turn implies that other constituents will be exposed to fluorine. This suggests that any volatile fluoride will be able to escape from the fluorinated UO_2 at its temperature of formation. This sequential build-up to UO_2F_2 indicates that a UO_2 fuel could be treated with NF_3 at temperatures lower than 390ºC with very little loss of uranium to volatile UF_6. This finding indicates that the temporal build-up of uranium oxyfluoride could be used to separate species such as molybdenum and technetium that would volatilize at faster rate and at lower temperature; other constituents such as tritium, iodine, and the noble gases may also be released.

5.1.3 Kinetic Modeling of NF_3-Fluorination of UO_2

It is well documented that the molecular fluorine-fluorination of UO_2 to form UF_6 proceeds through the intermediate UO_2F_2 (Ogata et al. 2004; Homma et al. 2005). In the case of the fluorine-fluorination of UO_2, it is reasonable to consider the primary reaction as written in Eq 4 above, which leads to an expected time-dependent mass ratio of

$$\frac{m(t)}{m_0} = \frac{N^0_{UO_2} M_{UO_2} (1-\alpha) + N^0_{UO_2} M_{UO_2F_2} \alpha}{N^0_{UO_2} M_{UO_2}} \tag{6}$$

which can be rearranged into

$$\alpha = \left(\frac{m(t)}{m_0} - 1\right)\left(\frac{M_{UO_2}}{M_{UO_2F_2} - M_{UO_2}}\right) \tag{7}$$

where $m(t)$ is the measured mass at time t, m_0 is the initial measured mass at time $t = 0$, M_{UO_2} is the molecular mass of UO_2, and $M_{UO_2F_2}$ is the molecular mass of UO_2F_2.

As Figure 5-1 shows, the reaction of NF_3 with UO_2 is a multi-step process with individual kinetics contributing to the overall conversion to UF_6. The total mathematical equation for the kinetic model will be a linear combination of the kinetics for the various steps. Our attempts to apply the kinetics development strategy provided in Section 3 to UO_2 indicated that we needed to acquire additional data before a representative set of models for each step can be developed to permit an accurate calculation of separation factors. As we discuss the behavior of other fuel constituents, we will provide comparisons of thermal behavior during NF_3 treatment to illustrate its power to separate.

5.2 NF_3 Fluorination of U_3O_8

If voloxidation is used to release tritium and other volatiles and semi-volatiles, U_3O_8 will be the likely feed for the fluorination process. Voloxidation is a fuel preprocessing step under consideration for removal of fission products in irradiated nuclear fuel. The process heats uranium oxide fuel using an oxidizing gas purge, typically air or oxygen, and provides three major advantages as a head-end processing of uranium oxide fuel: 1) Separation of the fuel/cladding interface, which results in a lowered quantity of cladding constituents in downstream processing and also generation of less high level waste adhered to the cladding surface; 2) a decrease in the particle size of the fuel, which increases the surface area of the fuel for more efficient downstream processing; and 3) complete removal of ^{14}C, ^{85}Kr, Xe, ^{129}I, and tritium (^{3}H) below 950°C, and partial or full removal of fission products cesium, molybdenum, technetium, ruthenium, and rhodium at temperatures below 1200°C. Individual capture technologies for the off-gas fission products are interfaced to the voloxidation furnace.

Voloxidation pulverizes the fuel by the decrease in the fuel density of 11.0 g/cm^3 (UO_2) to 8.3 g/cm^3 (U_3O_8), thereby increasing its volume. As McEachern and Taylor (1998) report, the particle sizes will increase by about 36% relative to parent UO_2 particles. The elimination yields of fission products to high temperature are reproduced from Yoo et al. (2008) in Table 5-1. Notably, even fission gas products such as krypton are difficult to remove until temperatures in excess of 950ºC are reached.

Table 5-1. Voloxidation elimination yields of radionuclides from irradiated fuel (Yoo et al. 2008).

Temperature	Elimination yields (wt%)										
°C	H	Kr	Xe	C	I	Cs	Tc	Ru	Rh	Te	Mo
500	99	15	5	20	5	21	53	81	39	2	-
700			90	95	60	21	53	81	39	2	-
950			100	100	90	90	98	94	78	32	12
1200					100	100	100	100	80	90	80
1500							100	100	90	100	90

Temperatures in excess of 950°C begin to alter the voloxidation product to a high-fired uranium product that is more difficult to process by solution, gas phase, or electrolytic methods (Yoo et al. 2008) and depending on exposure time, induces phase alteration of the α-U_3O_8 ultimately to β-U_3O_8.

The thermodynamic data in Table 2-1 for the reaction of NF_3 with U_3O_8 to produce UF_6 indicates that the overall enthalpy will be exothermic with an enthalpy below that of UO_2, but considerably greater than that for NF_3's reaction with UO_2F_2 or UF_4 to produce UF_6. Accordingly, the experimental DTA data should observe heat production.

5.2.1 Experimental Results for NF_3 Fluorination of U_3O_8

As for the case of UO_2, temperature ramp and isothermal gravimetric experiments are described that provide information on the general behaviors of the reaction of NF_3 with U_3O_8. Depending on the reprocessing design, both approaches are important.

The source of α-U_3O_8 used in this study was a powder with a mean (uniform) particle size of 1 µm and a BET surface area of 0.299 $m^2 \cdot g^{-1}$. When α-U_3O_8 is heated to above 1000ºC, such as might happen during voloxidation, the more chemically resistant β-U_3O_8 forms. When we heated our α-U_3O_8 to above 1000°C, particles were produced which were glassy like obsidian and had a particle size distribution of 1 to 20 µm as aggregates of the α-U_3O_8 source.

The plot of the DTA curve with respect to temperature (top axis) in Figure 5-3 allows visualization of the rapid heat evolution as was commonly observed from these samples for sample heating ramp rates above 10°C/min. The inset in Figure 5-3 shows an expanded view of the DTA curve to either side of the UF_6 production event. Two small thermal signatures, marked (1) and (3), lie to either side of the major thermal release of UF_6, marked (2). A uranium oxyfluoride had likely formed on the low-temperature side, and the decrease in the mass gradient toward the high-temperature side, marked (3) in Figure 5-3 is consistent with (exothermic) formation of a third product that appeared to be rate limiting with respect to UF_6 production.

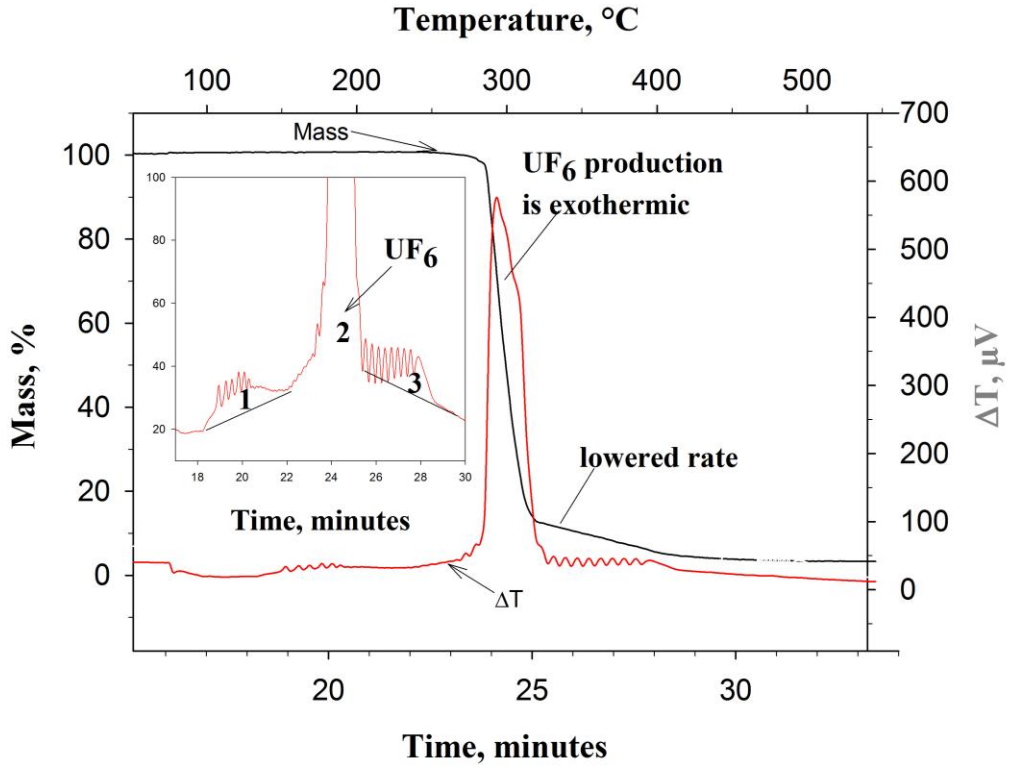

Figure 5-3. Action of 10-percent NF_3/Ar on α-U_3O_8 as measured by simultaneous TGA and DTA during heating at 10°C/min. Three signatures were observed: 1) mass gain, 2) rapid mass loss, and 3) slower mass loss.

According to neutron diffraction data (Herak 1969), the structure of β-U_3O_8 is pseudohexagonal or rigorously, orthorhombic. Our SEM images indicate that heating the α-U_3O_8 to the β-U_3O_8 form caused an increase in the size of the particles even creating elongated particles. These data are consistent with an

interpretation in which the crystal grains of α-U_3O_8 were sintered on heating and coalesced with other grains. As a result, larger particles of this more refractory β-U_3O_8 form were produced. The ß-U_3O_8 could be important depending on the temperature used for the voloxidation pretreatment.

Changes in particle size could change the rate of UF_6 production, but should not greatly alter the onset temperature for conversion. Changes in crystallinity might change the onset temperature by allowing preferential attack along a crystallographic axis, However, the crystallinity change between α-U_3O_8 and β-U_3O_8 is rather subtle (Loopstra 1970; Herak 1969).

The reaction of NF_3 with β-U_3O_8 was similar to that of α-U_3O_8 with the exception that the onset temperature was about 100°C higher using the same temperature ramp rate of 10°C·min^{-1}. The experiment confirms that changes in crystallinity, particle size, surface area, and other physical characteristics can influence the reactivity of NF_3 with uranium materials. Our evolving understanding of the physiochemical kinetics of these reactions would suggest that the diffusion time for NF_3 to penetrate the β-U_3O_8 particle is such that the chemical reaction does occur at lower temperature but that it is not observable for a long "induction period". In any case, the heat treatment adversely decreases fluorination rates. A similar dissolution rate decrease is known when comparing α-U_3O_8 with ß-U_3O_8.

Isothermal experiments using 10-percent NF_3 indicate behavior similar to that from the temperature ramp tests. As shown in Figure 5-4, the reaction can be controlled to produce very low amounts of UF_6 for greater than 20 hours. The abrupt changes in rate of curvature at 475ºC indicates the existence of at least two or three precursors producing UF_6. The change in the curvature as the temperature was increased from 475 to 500ºC likely indicates that a product barrier was removed with greater facility at the higher temperature. At 525 ºC, very rapid production of UF_6 is observed.

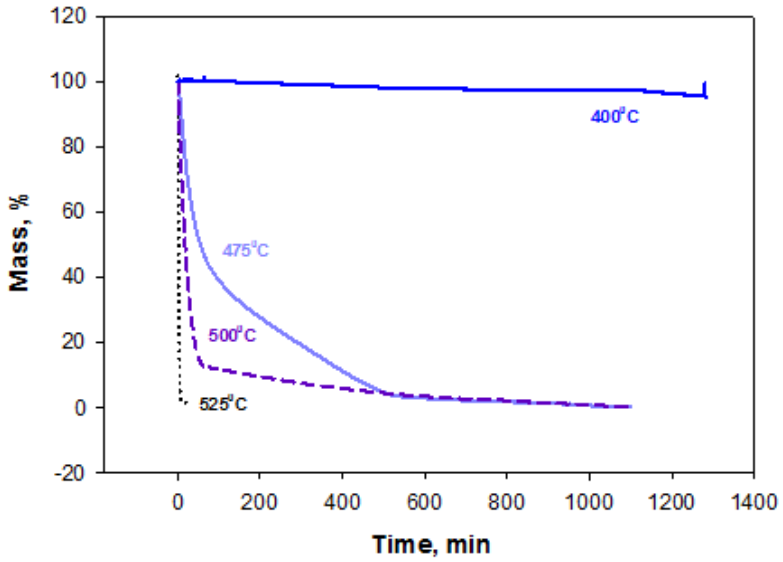

Figure 5-4. The effect of temperature on action of 10-percent NF_3 on α-U_3O_8 as measured by isothermal TG at 400, 475, 500, and 525°C.

Because NF_3 requires temperatures >400°C to effectively volatilize α-U_3O_8 and β-U_3O_8 it may be easy to effectively remove the low volatile fluorides used nuclear fuel constituents, such as technetium, molybdenum, ruthenium, and their oxides from the voloxidized fuel.

5.2.2 Kinetic Modeling of the NF_3-Fluorination of U_3O_8 Reaction

To identify a kinetic model to apply to the NF_3fluorination of U_3O_8, we compared the isothermal TG-measured reaction profile with common gas-solid kinetic models presented in Table 3-1. Inspection of Figure 5-5 suggests that in the current geometric configuration of our experiment, the reaction between NF_3 and U_3O_8 to produce UF_6, proceeds through a phase-boundary reaction mechanism. The fractional conversion of a phase-boundary controlled mechanism is described by the general equation

$$\alpha = 1 - \xi^{F_p} \tag{8}$$

where

$$\xi = \left(\frac{A_p}{F_p V_p}\right) r_c \tag{9}$$

and A_p is the original surface area of the solid reactant, V_p is the original volume of the solid reactant, F_p is the shape factor (representing the number of dimensions along which the reaction front is traveling (i.e., one for sphere, two for cylinder, one for slab), and r_c is the distance from the center of the geometry to the solid surface. For the reaction characterized in the representative isothermal scan at 525ºC shown in Figure 5-5, the data aligns well with a phase-boundary model for one, two, or three dimensions.

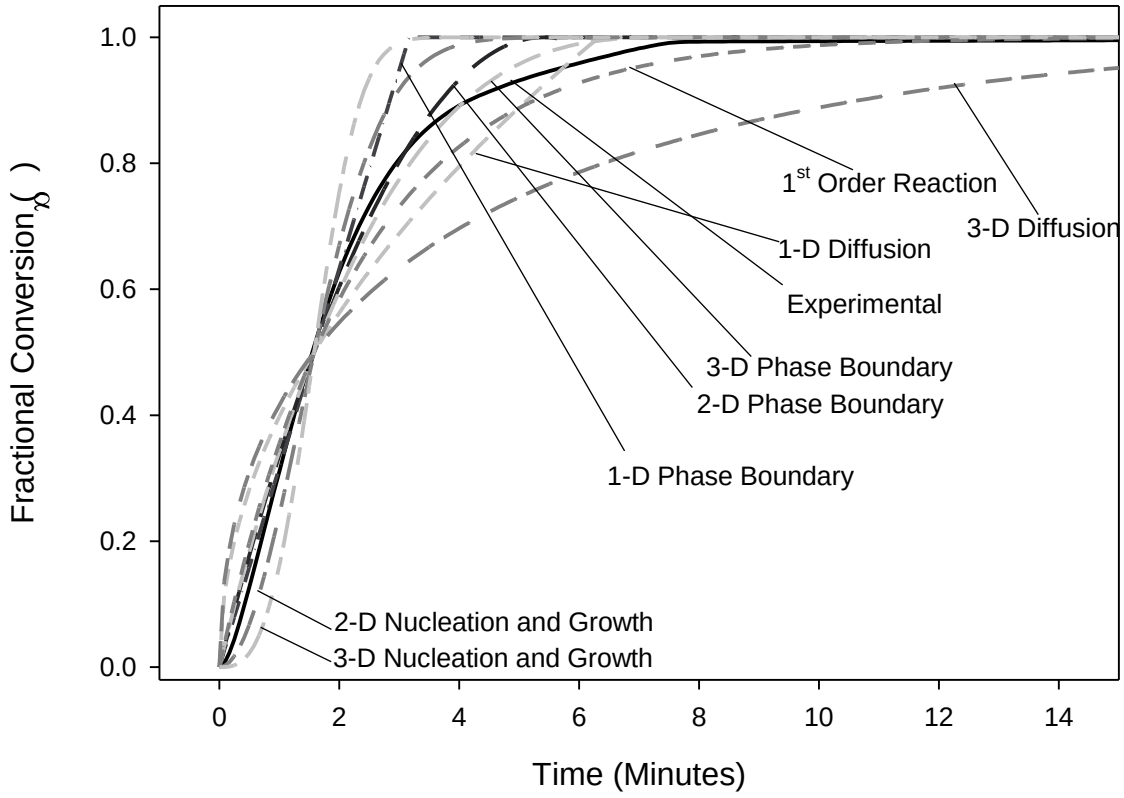

Figure 5-5. Comparison of the thermal action of 10-percent NF_3 on U_3O_8 as measured by isothermal TG at 525°C with common gas-solid reaction mechanisms.

The best fit was obtained using the equation with a non-integral dimension numbers such as 1.5. This suggests that, as the NF_3 drops down on the U_3O_8 powder, it systematically reacts downward as though attacking a slab of material, except that the powder is porous resulting in a slightly higher reaction rate. The product is volatile. The sharp bend near the end of the fractional conversion curve suggests the

presence of an impurity or diffusion barrier imposed by an intermediate solid or the formation of an intermediate that forms a volatile product at a slower rate. The temperature-dependent reaction rate can be characterized using the following equations (Sharp, Brindley and Achar 1966):

2 Dimensions: $[1-(1-\alpha)^{1/2}] = (u/r)t = 0.2929(t/t_{0.5})$ (10)

3 Dimensions: $[1-(1-\alpha)^{1/3}] = (u/r)t = 0.2063(t/t_{0.5})$ (11)

and (as derived by authors)

1 Dimension: $\alpha = (u/r)t = 0.5\left(t/t_{0.5}\right)$ (12)

1.5 Dimensions: $[1-(1-\alpha)^{2/3}] = (u/r)t = 0.37(t/t_{0.5})$ (13)

where *u* is the velocity at which the reaction front moves across the solid reactant (in this case, it is essentially, the overall kinetic reaction rate), *r* is equivalent to the r_c that occurs in Eq. 9, and $t_{0.5}$ is the time at which a fractional conversion of 0.5 is reached. Table 5-2 is a comparison of the value of $t_{0.5}$ and *(u/r)* for each of the reaction temperatures tested and for each of the phase-boundary mechanisms described by Eq. 10 through 13.

Table 5-2. Values of the model dependent rate (u/r) for action of 10-percent NF_3 on U_3O_8 at various temperatures.

Temperature	$t_{0.5}$ min	(u/r) 1-D, min^{-1}	(u/r) 1.5-D, min^{-1}	(u/r) 2-D, min^{-1}	(u/r) 3-D, min^{-1}
475°C	196	0.003	0.002	0.0015	0.001
500°C	17.5	0.029	0.021	0.017	0.012
525°C	1.58	0.316	0.234	0.185	0.131

Treating the value of a single model type (*u*/*r*) as though it were the rate constant *k*, the values in Table 5-2 can be plotted in the form of the Arrhenius equation with the results presented in Table 5-3 and Figure 5-6.

$$k = Ae^{-\frac{E_a}{RT}} \quad (14)$$

For the kinetic analysis performed here, it is necessary to understand that the half-time of the entire experiment was used, but it is evident from fits to several isothermal scans that the phase-boundary fits are more accurate for the beginning of the reactions than at the end.

Table 5-3. Arrhenius parameterization of model dependent (u/r) values for action of 10% NF_3 on U_3O_8

Arrhenius Parameter	Gas-Solid Model Type			
	1D	1.5D	2D	3D
ln(a), min^{-1}	68.429	69.719	70.305	70.879
b, K	55562	56824	57466	58192
Model Fit R^2	0.9989	0.9993	0.9998	0.9999

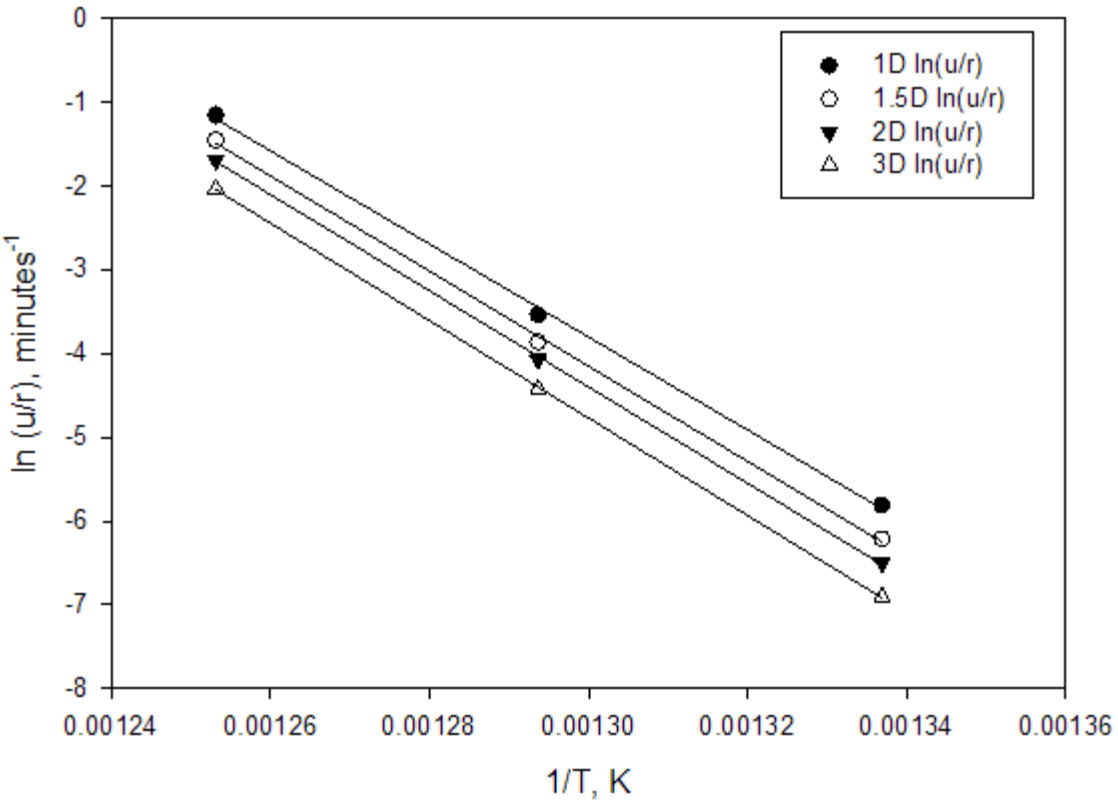

Figure 5-6. Arrhenius-type plot for action of 10-percent NF_3 on U_3O_8; (u/r) is treated as k.

Taking the average of all four models results in the following equation:

$$\ln(u/r) = 68.833 - \frac{57011}{T} \quad (15)$$

5.3 NF_3-Fluorination of NpO_2

Neptunium arises from nuclear reactor operations by neutron capture by ^{238}U with subsequent ß-decay to ^{237}Np. In a UO_2 fuel, neptunium likely forms NpO_2. Our studies on the action of NF_3 on Np to produce a volatile fluoride used NpO_2.

5.3.1 Thermodynamics for NF_3 Fluorination of NpO_2

Two of the most stable forms of neptunium are the tetravalent oxide and the tetravalent fluoride. The oxide NpO_2 is quite stable to hydration or oxidation to high temperature so the impurity content in the sample can be passively managed. As such, thermodynamic calculations for the reaction of NpO_2 with fluorinating reagents to produce NpF_4 and NpF_6 indicate that these reactions are considerably less favored than the analogous reactions for uranium. Nevertheless, the reaction is well known to produce NpF_4 and NpF_6 as well as the oxyfluorides NpO_2F_2 and $NpOF_4$ with many fluorinating reagents and under various conditions of temperature and reagent concentration.

Neptunium hexafluoride is an orange solid that melts at 327.8 K. Both the solid and the liquid evaporate to reddish-brown gas. The volatility of NpF_6 presents possible separation schemes to recover neptunium from spent nuclear fuel and led to early interest in preparations and characterization of NpF_6 (Malm et al. 1958; Seaborg and Brown 1961; Trevorrow et al. 1968). The volatility of NpF_6 is similar to that of UF_6

and PuF_6, but the kinetics of its volatilization can differ widely as a result of the reactivity of the fluorinating reagent that is used. Of interest here is whether NF_3 be used to separate neptunium from uranium in particular and not simply by trapping methods or distillation, but rather by its thermal reactivity

5.3.2 Experimental Results for NF_3 Fluorination of NpO_2

Treverrow and coworkers (1968) found that NpO_2 and NpF_4 are volatilized as NpF_6 by treatment with fluorine, BrF_5, or BrF_3. They found that NpO_2 fluorination proceeds through NpF_4 with no indication of either oxyfluorides such as observed for UO_2 or intermediate fluorides as it is converted to NpF_6. In contrast, Henrion and Leurs (1971) found that NpO_2 is converted by fluorine to NpO_2F_2 with no formation of NpF_4. Gibson and Haire (1992) found that NpF_6 forms when NpO_2 was treated with fluorine between 400 and 700°C. Above 700°C, they observed only NpF_5. More aggressive reagents such as KrF_2 and O_2F_2 can produce NpF_6 well below room temperature, but with cooling (to 197 K), they produce NpO_2F_2.

The TGA results provided in Figure 5-7 showed that, when heated at 5°C/min in 10-percent NF_3/Ar, NpO_2 began to fluorinate at 420°C but the maximum mass gain of >14 percent was not reached until 560°C when the neptunium obviously began to volatilize. As Figure 5-7 shows, powdered NpO_2, when heated isothermally at 470°C in 5-percent NF_3/Ar, gained about 15 mass% or intermediate between the 14 percent gain for conversion to NpO_2F_2 and the 16% for conversion to NpF_4. XRD characterization of this green powder determined that it was NpF_4 in contrast to the NpO_2F_2 reported in the literature. It is known that hydrolysis of NpF_6 can produce NpO_2F_2 or $NpOF_4$. That is, there is not a further reaction that might account for the presence of NpF_4 as the major product of fluorination, for instance, from the decomposition of NpF_6 to an admixture of a neptunium oxyfluoride and NpF_4. Consequently, we believe the fluorination with NF_3 proceeds through a nearly pure NpF_4 product to NpF_6.

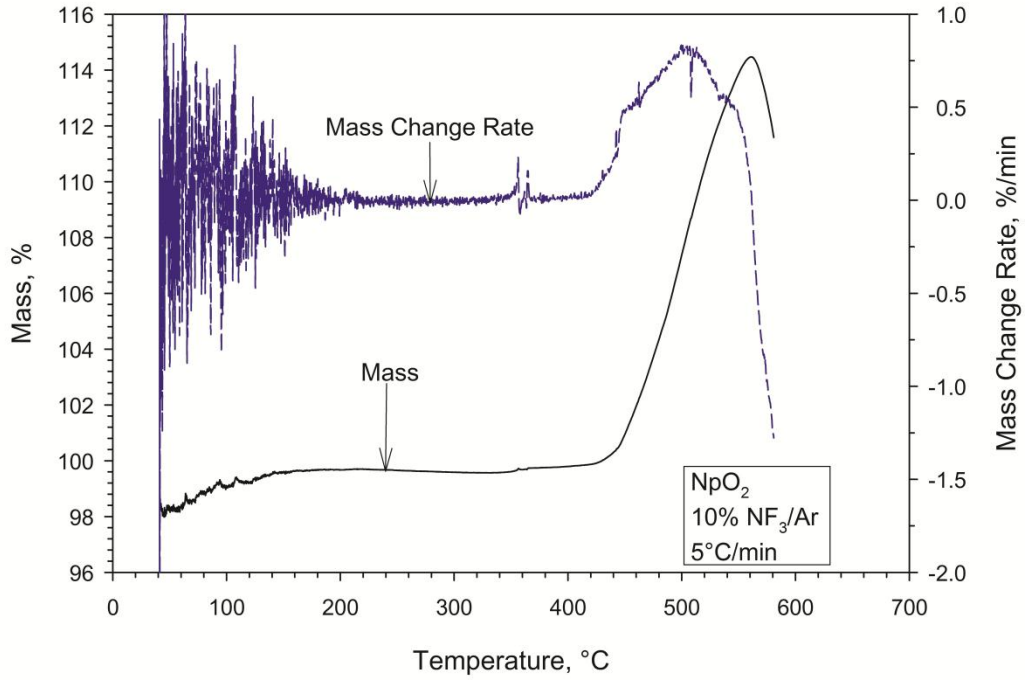

Figure 5-7. Thermal action of 10-percent NF_3 on NpO_2 as measured by simultaneous TG and DTA during heating at 5°C/min.

Figure 5-7 shows that after what appears to be a stable mass, the fluorinated NpO_2 began to lose mass, likely as the volatile NpF_6. We attribute the lower than expected mass gain to simultaneous NpF_4 and volatile NpF_6 formation. The region of stable mass also may be due to the rate-controlling formation of a higher fluoride that was rapidly converted to NpF_6. The general reaction profile also may be explained by the complexity of heterogeneous gas solid reaction kinetics (Kwon et al. 2002; Galwey 2004).

As Figure 5-8 shows, powdered NpO_2 when heated isothermally at 470°C in 5 percent NF_3 in argon gained about 15 mass percent or intermediate between the 14-percent gain for conversion to NpO_2F_2 and the 16 percent for conversion to NpF_4. The XRD characterization of this green powder found that it was NpF_4. After what appears to be a stable mass, the fluorinated NpO_2 began to lose mass likely forming the volatile NpF_6. The lower than expected mass gain could be attributed to simultaneous formation of NpF_4 and NpF_6. The region of stable mass may also be due to the rate controlling formation of a higher fluoride that was rapidly converted to NpF_6. The general reaction profile may also be explained by the complexity of heterogeneous gas solid reaction kinetics (Kwon et al. 2002; Galwey 2004).

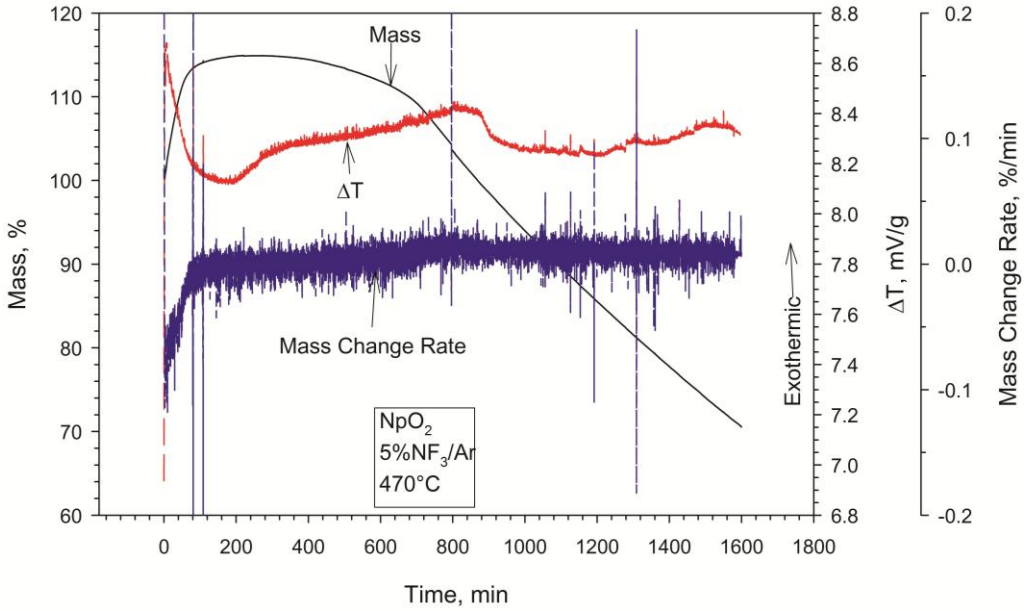

Figure 5-8. Thermal action of 5-percent NF_3 on NpO_2 at 470ºC as measured by simultaneous TGA and DTA.

5.3.3 Kinetic Modeling of NF_3-Fluorination of NpO_2 to NpF_4

The NpO_2 fluorinated with NF_3 in this work was in the form of 2-5 µm spherical particles illustrated in Figure 4-4. Results from experiments measuring the fluorination of NpO_2 with NF_3 have indicated that a nearly complete conversion to NpF_4 is achieved before the conversion to NpF_6 as indicated by mass loss. In the case of the fluorination of NpO_2, it is reasonable to consider the primary reaction to be:

$$3NpO_2 + 4NF_3 \rightarrow 3NpF_4 + 2N_2 + 3O_2 \tag{16}$$

which leads to an expected time-dependent mass ratio of:

$$\frac{m(t)}{m_0} = \frac{N^0_{NpO_2} M_{NpO_2}(1-\alpha) + N^0_{NpO_2} M_{NpF_4}\alpha}{N^0_{NpO_2} M_{NpO_2}} \tag{17}$$

which can be rearranged into:

$$\alpha = \left(\frac{m(t)}{m_0} - 1\right)\left(\frac{M_{NpO_2}}{M_{NpF_4} - M_{NpO_2}}\right) \quad (18)$$

Comparison of the 470°C isothermal mass curve for the initial fluorination of NpO_2 to NpF_4 with the common gas-solid kinetic models of Table 3-1 is presented in Figure 5-9. At 470°C the complete conversion of NpO_2 to NpF_4 requires about 200 minutes. This reaction appears to be a blend of the First-Order Reaction and Three-Dimensional Diffusion models. A possible explanation for the match with a pure first-order chemical reaction for the first 75 percent of the experiment followed by a slowdown for the final 25 percent may be due to differences in access of the NF_3 to fresh material. In the beginning smaller particles or particles with greater porosity would react quickly. With the consumption of the smaller or more porous particles the reaction would regress to a diffusion limited reaction. This comparison highlights the complexities of gas-solid reactions and the potential influences of physical properties and the importance of head-end processing to size the particle.

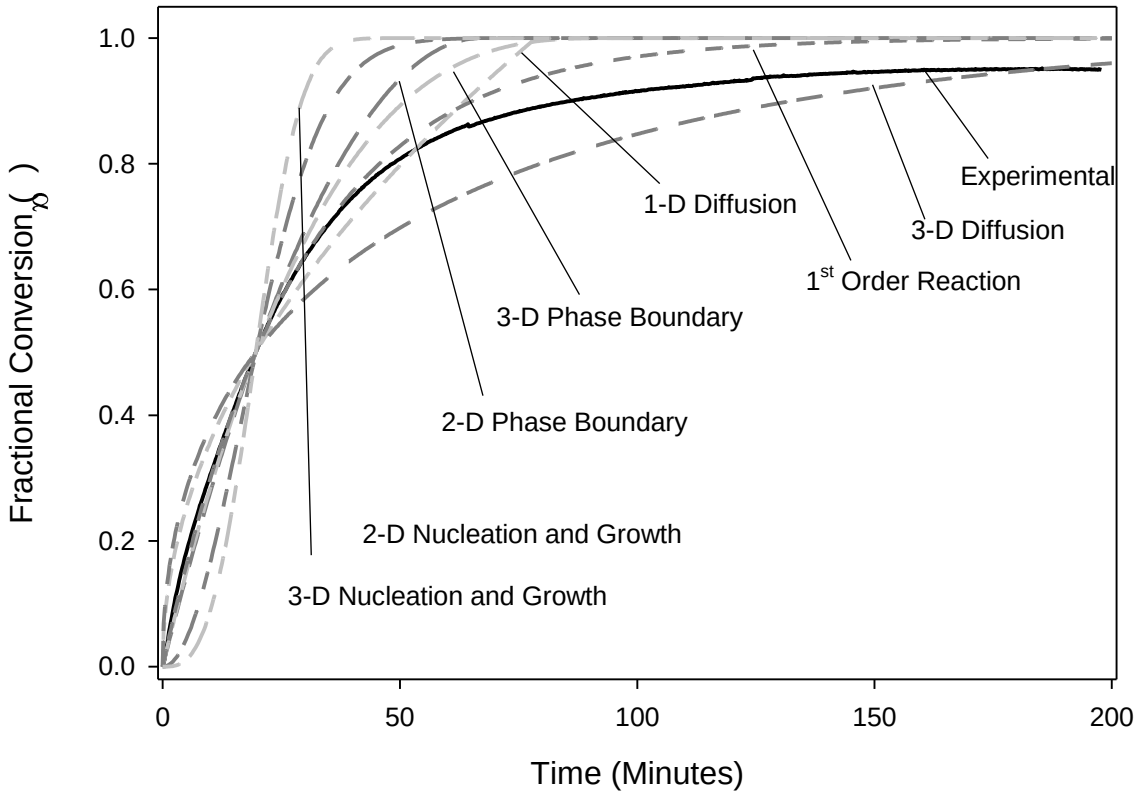

Figure 5-9. Comparison of the action of 470°C 5-percent NF_3/Ar on NpO_2 to product NpF_4 as measured by TGA with gas-solid kinetic models.

From a processing perspective related to separation of uranium and neptunium, this end-of-conversion slowdown in reaction rate, may benefit separation of these two constituents. The slow conversion of NpO_2 to NpF_4 will subsequently slow the conversion of the NpF_4 to the volatile NpF_6 and could improve the separation of uranium and neptunium.

5.3.4 Kinetic Modeling of NF3 Fluorination of NpF4 to NpF6

With neptunium and uranium having similar volatile fluoride production temperatures, the reaction rates become very critical for separating the two elements. To obtain the needed temperature dependence, we performed three isothermal TGA experiments for the conversion of NpO_2 to NpF_4 to NpF_6 using 10-percent NF_3/Ar at 450, 475, and 500°C (Figure 5-10).

In these single experiments, the behavior at 450 and 475°C were very similar, requiring very long times >2500 min to completely convert the NpO_2 to NpF_6. In contrast, at 500°C, the conversion was nearly complete in 200 min.

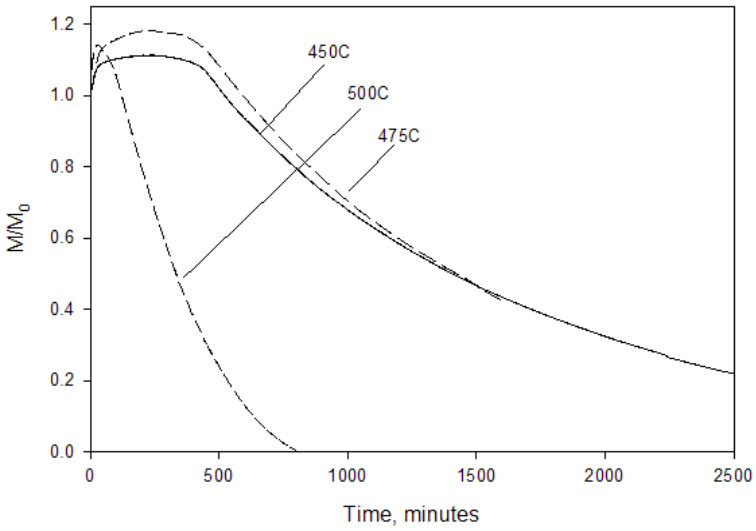

Figure 5-10. Action of thermal 10-percent NF_3/Ar on NpO_2 as measured by isothermal TG at 450, 475, and 500°C.

To develop a representative gas-solid reaction model, we compared the TG-behavior at the different temperatures of the NpF_4 to NpF_6 conversion with the gas-kinetic models of Table 3-1 to identify the likely kinetic mechanism. Figure 5-11 compares the 450°C isothermal reaction producing NpF_6 from NpF_4 with a first-order chemical reaction model and a two-dimensional phase-boundary model. This comparison suggests that the first-order chemical model provides the best fit. Similar comparisons at the higher temperatures showed a gradual shift to the two-dimensional phase-boundary model for the best fit. We do not have an explanation for the difference at this time. Because of the apparently changing mechanism, we did not develop the Arrhenius type temperature dependence for this set of data.

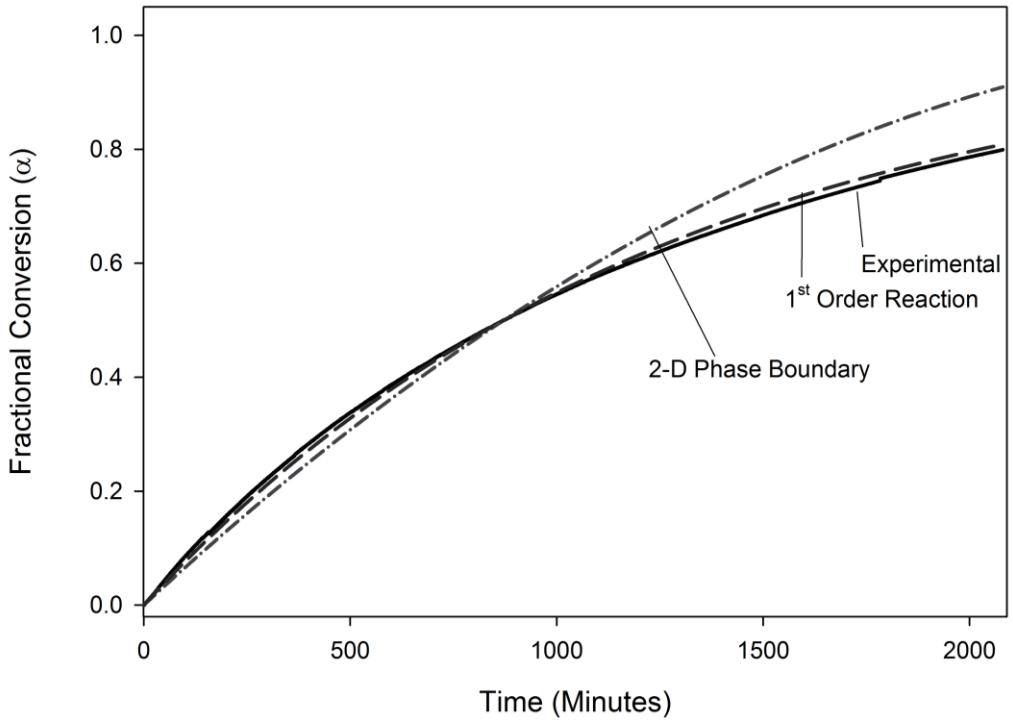

Figure 5-11. Comparison of thermal action of 10% NF_3/Ar on NpF_4 to form NpF_6 as measured by 450°C isothermal TG with a 1st order chemical reaction model and 2-D Phase Boundary model.

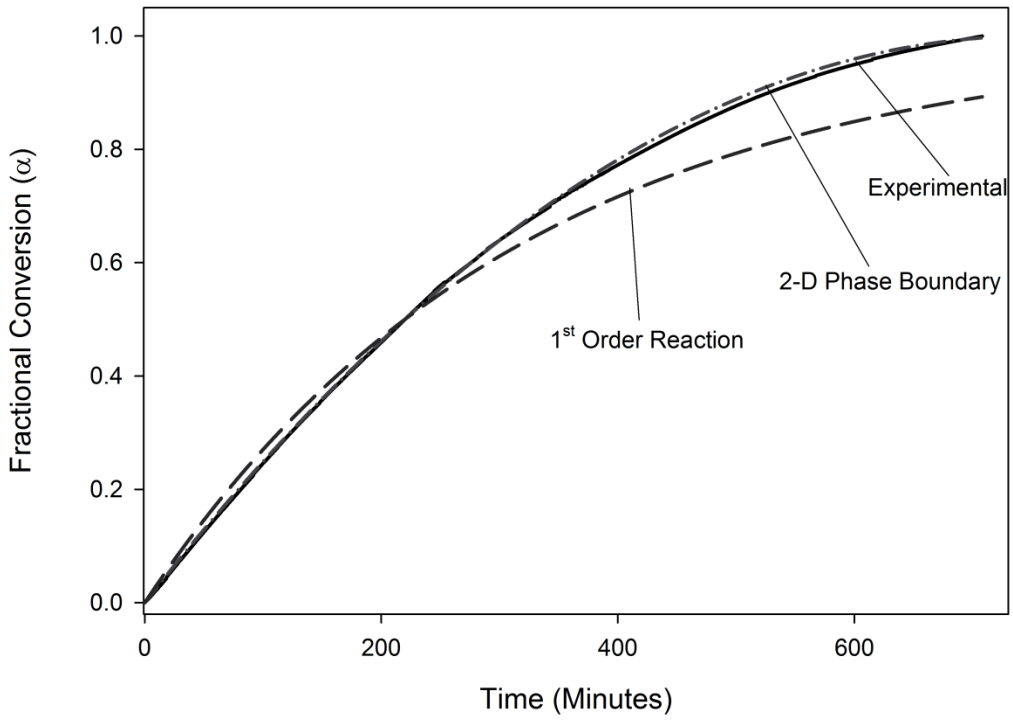

Figure 5-12. Comparison of thermal action of 10% NF_3/Ar on NpF_4 to form NpF_6 as measured by 500°C isothermal TG with a 1st order chemical reaction model and 2-D Phase Boundary model.

The fractional conversion for each data set was calculated from the inflection point on the right side of the top of the curve assuming that, at the inflection point, the material in the pan was 100-percent NpF_4 and was converted to NpF_6. For the lower temperature reactions at 450 and 475°C, the data aligned extraordinarily well with a first-order reaction kinetics theoretical curve. Strangely, the 500°C-case aligned extraordinarily well with the two-dimensional phase-boundary theoretical curve. For the first-order reaction mechanism, the fractional conversion model equation is:

$$ln(1-\alpha) = -kt = -0.6931(t/t_{0.5}) \quad (19)$$

Table 5-4 was generated for a first-order reaction model:

Table 5-4. Kinetic parameters for NF_3 fluorination of NpF_4 to NpF_6.

T(K)	t0.5 minutes	k minutes-1
450	871.2	7.96E-4
475	839	8.26E-4

To understand these results in regards to the separation of pure UO_2 and NpO_2 as their volatile hexafluorides, Figure 5-13 compares the reaction of both pure compounds under exposure to 10-percent NF_3 at 450°C; note that the reaction times at this temperature are too long for use as an efficient separations approach. We present the 450°C results because at temperatures > 500°C, the UO_2 reaction becomes very fast, and it is difficult to fit the data. After the initial buildup of product (i.e., UO_2 to UO_2F_2 and NpO_2 to NpF_4), the reaction to produce the volatile hexafluoride is initiated. The initial step is rate limiting in the case of the NpO_2 with respect to that of UO_2. This is a good example of why the whole curve fitting approach is important to understanding the thermal sensitivity of NF_3 towards reprocessing.

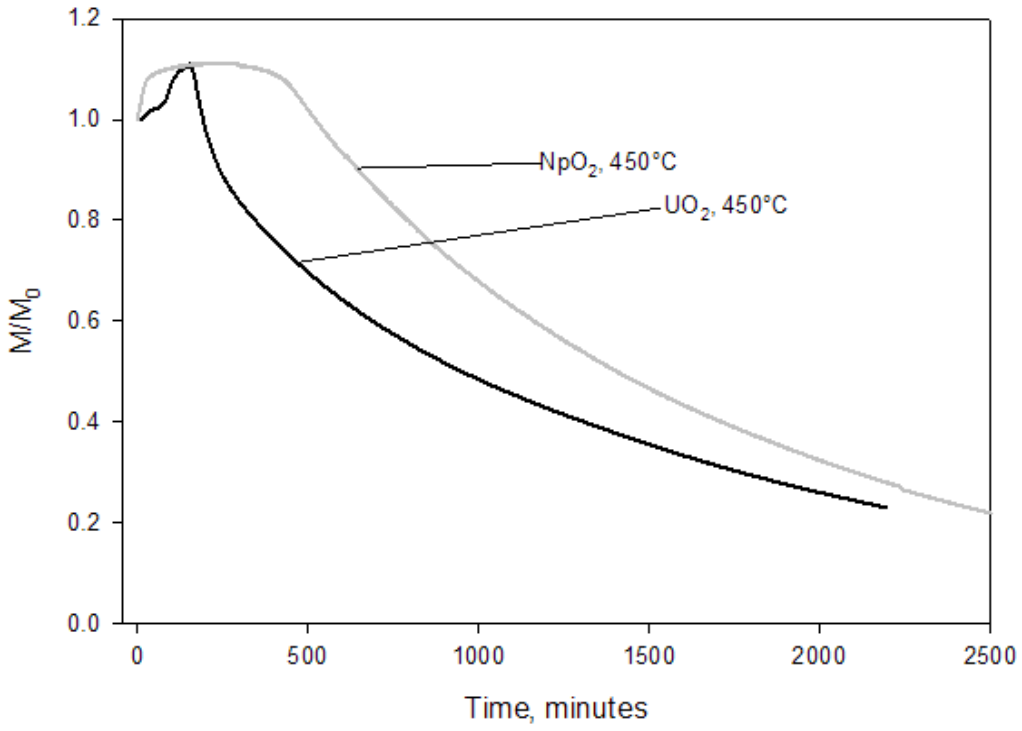

Figure 5-13. Comparison of the thermal action of 10% NF_3/Ar on NpO_2 and UO_2 as measured by 450°C isothermal TG.

After the initial buildup of the intermediate solid product, UO_2F_2 and NpF_4, the reactions producing the volatile hexafluorides begin. The initial formation of NpF_4 limits the overall production of a volatile fluoride. While the UO_2 is quickly converted to UO_2F_2 and very quickly begins to convert to UF_6. The initial fluorination to NpF_4 may limit the heat of the reaction that would drive NpF_4 to NpF_6. However, a similar heat is produced (Table 2-1) to produce the UO_2F_2 from UO_2. It appears that kinetic factors increase the overall reaction rate of UO_2 to UF_6. It appears that separation of U and Np using thermal sensitivity differences will require refinement.

With respect to separation of neptunium from uranium after the fuel has been voloxidized to U_3O_8, Figure 5-14 compares the fluorination behaviors of NpO_2 and α-U_3O_8 as they are exposed to 10-percent NF_3/Ar. As hoped, at comparable temperatures, the uranium is volatilized at a faster rate than the neptunium. For example, at 500°C, the uranium is 90 percent volatilized in <100 min, while neptunium has not yet begun to volatilize. The change in the rate of uranium volatilization after 90 percent loss is not understood at this time. Comparison of these experiments indicates that neptunium and uranium can be separated effectively by controlling temperature.

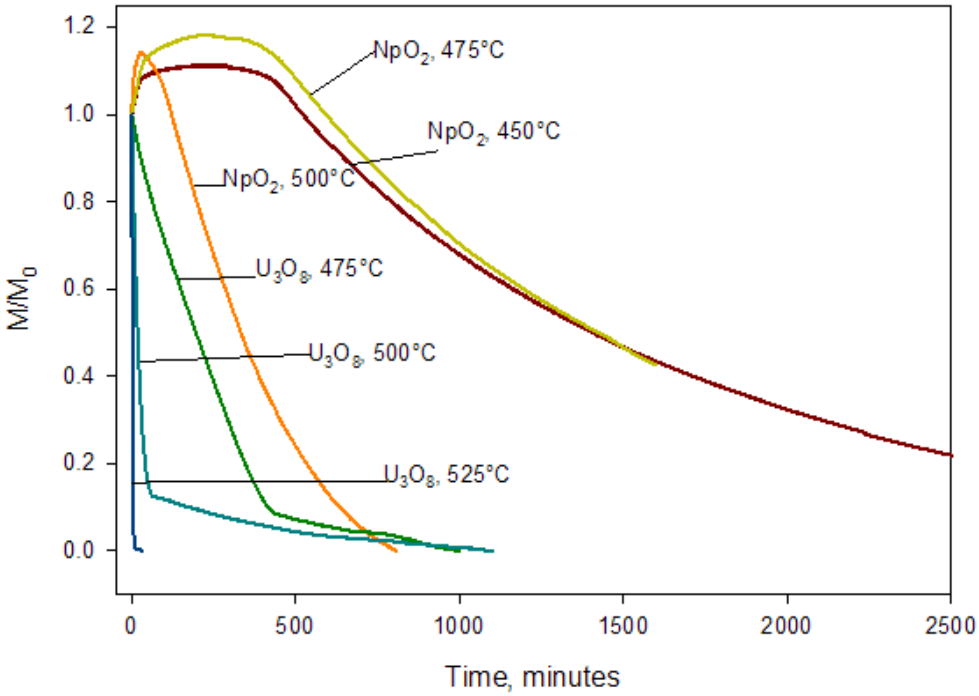

Figure 5-14. Comparison of the effects of temperature on the NF_3 volatilization of neptunium and uranium as α-U_3O_8.

5.4 NF_3 Fluorination of PuO_2

Being a major and important constituent in used nuclear fuel that forms a volatile fluoride and often the target with respect to proliferation controls , the action of NF_3 on plutonium is of significant importance. This section discusses the behavior of PuO_2 when exposed to NF_3 and more aggressive fluorinating agents in terms of the thermodynamic properties, measured thermal behavior, and kinetic models.

5.4.1 Thermodynamics for Fluorination of PuO_2

In one sense, PuO_2 ought to be the easiest of materials to work with experimentally. Like neptunium, the oxide PuO_2 is quite resistant to hydration or oxidation at very high temperature such that the impurity

content in the sample can be easily managed. Of the volatile hexafluorides, formation of PuF_6 is clearly one of the more difficult to accomplish and to maintain.

The thermodynamic data in Table 5-5 show that the reaction is exothermic from PuO_2 to PuF_6 but that formation of the tetrafluoride, PuF_4 is the favored fluorinated form. The free energy difference between PuF_4 and PuF_6 indicates that PuF_6 should decompose to PuF_4 unless special actions are taken such as maintaining an over pressure of molecular fluorine to shift the equilibrium to favor PuF_6. It is possible that PuO_2 is fluorinated to $PuO_2F_2$when more aggressive reagents are used at colder temperatures as was discussed for the reaction of such reagents with NpO_2. Table 5-6 provides calculated reaction enthalpies and free energies for the reaction of PuO_2 with selected aggressive fluorinating agents and the fluorination and oxidation of PuF_4 to PuF_6. As might be predicted from chemical reactivities, the more aggressive fluorinators have ΔGs that favor the formation of PuF_6 when compared to NF_3.

Table 5-5. Calculated enthalpy and free energy changes for reaction of NF_3 with PuO_2 and PuF_4 to produce PuF_6.

Postulated Reaction	ΔH, kJ/mole Pu	ΔG, kJ/mole Pu
$PuO_{2(s)} + 2NF_{3(g)} = PuF_{6(g)} + N_{2(g)} + O_{2(g)}$	-450	-516
$PuO_{2(s)} + 1.33NF_{3(g)} = PuF_4 + 0.666N_{2(g)} + O_{2(g)}$	-815	-880
$PuO_{2(s)} + 1.5NF_{3(g)} = PuO_2F_2 + 0.75N_{2(g)}$	-472	-278
$PuF_{4(s)} + 0.666NF_{3(g)} = PuF_{6(g)} + 0.333N_{2(g)}$	+113.2	+54.1

Table 5-6. Calculated enthalpy and free energy changes for reaction of other fluorinating agents with PuO_2 and PuF_4 to produce PuF_6.

Postulated Reaction	ΔH, kJ/mole Pu	ΔG, kJ/mole Pu
$PuO_{2(s)} + 3F_{2(g)} = PuF_{6(g)} + O_{2(g)}$	-757	-917
$PuO_{2(s)} + 3O_2F_{2(g)} = PuF_{6(g)} + 4O_{2(g)}$	-695	-636
$PuO_{2(s)} + 1.5N_2F_{4(g)} = PuF_{6(g)} + O_{2(g)} + 1.5N_{2(g)}$	-682	-864
$PuO_{2(s)} + F_{2(g)} = PuO_2F_{2(s)} + 2O_{2(g)}$	-581	-366
$PuO_{2(s)} + O_2F_{2(g)} = PuO_2F_{2(s)} + O_{2(g)}$	-561	-273
$PuO_{2(s)} + 0.5N_2F_{4(g)} = PuO_2F_{2(s)} + 0.5N_{2(g)}$	-557	-349
$PuF_{4(s)} + F_{2(g)} = PuF_{6(g)}$	+97	+91
$PuF_{4\,(s)} + O_2F_{2(g)} = PuF_{6(g)} + O_{2(g)}$	+76	-2.2
$PuF_{4\,(s)} + 0.5N_2F_{4(g)} = PuF_{6(g)} + 0.5N_{2(g)}$	+101	+15
$PuF_{4(s)} + F_{2(g)} = PuF_{6(g)}$	+97	+91
$PuF_{4\,(s)} + O_2F_{2(g)} = PuF_{6(g)} + O_{2(g)}$	+76	-2.2
$PuF_{4\,(s)} + 0.5N_2F_{4(g)} = PuF_{6(g)} + 0.5N_{2(g)}$	+101	+15

Table 5-6 shows that except for O_2F_2 the more aggressive fluorinating and oxidizing agents should have trouble converting PuF_4 to PuF_6. The extra localized heat provided may help raise the temperature to drive the reaction beyond PuF_4. If this is the case, it may be possible to use NF_3 to produce PuF_6 at a higher temperature. With a ΔG of +91 kJ/mol Pu for the F_2 fluorination of PuF_4 to PuF_6 shows that PuF_6 will

spontaneously decompose to PuF_4 and F_2. To control or minimize this decomposition, special measures such as increasing the overpressure of F_2 to shift the equilibrium to favor or partially favor PuF_6. Thermodynamic calculations can provide the necessary level to maintain a target PuF_6 concentration.

Several researchers have demonstrated that the formation of PuF_6 can be achieved near room temperature or lower (Malm, Eller and Asprey 1984; Asprey et al. 1986). Very aggressive reagents such as KrF_2, O_2F_2, and perhaps N_2F_4 are required. Apparently, these reagents avoid a stable PuF_4 buildup by their extraordinary reactivity and the rates of their reaction with PuO_2. Fluorination of PuO_2 and the formation and stability of PuF_6 has been studied extensively. Using BrF_5, PuF_4 is reported to be the only product of fluorination (Jarry and Stockbar 1966). Gibson and Haire (1992) reacted PuO_2 with F_2, F_2/O_2, and ClF_3 and found only PuF_4 and no higher fluorides; however the preparation of PuF_6 is well documented. (Trevorrow et al. 1961; Weinstock and Malm 1956; Fischer et al. 1962; Weinstock et al. 1959).

Ogata et al. (2004)and Homma et al. (2005) estimated the rate of PuF_6 formation using a shrinking core model. Anastasia et al. (1967; 1968; 1969) have shown that the fluorination of PuF_6 in a fluidized-bed reactor is affected by the conditions used in the fluorination of uranium with fluorine, by the conditions used for the fluorination of plutonium, and by the presence of the added fission products (Gendre 1962; Steindler and Steidl 1957; Vandenbussche 1966). Use of aggressive fluorinating reagents essentially should fluorinate everything such that the plutonium should be last to be removed in the overall design of a fluoride volatility reprocessing scheme.

5.4.2 Experimental Results for NF_3 Fluorination of PuO_2

Figure 5-15 presents the results of our TG experiment where the PuO_2 from oxidation of partially oxidized plutonium metal was treated with 5-percent NF_3/Ar as it was heated at 5°C/min up to 650°C. The PuO_2 was converted starting near 450°C to pink PuF_4 based on XRD analysis of a similar experiment. No plutonium volatility was observed.

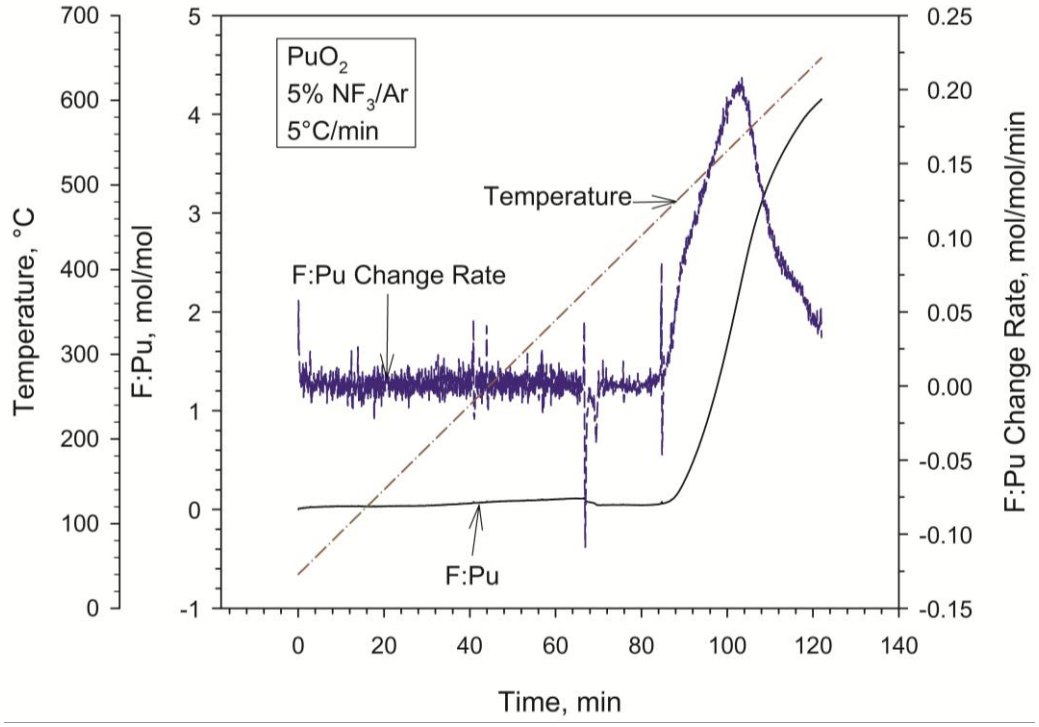

Figure 5-15. Thermal action of 5-percent NF3/Ar on PuO2 from metal as measured by TGA during heating at 5°C/min.

Figure 5-16 presents the results of a 445°C isothermal experiment where PuO_2 from calcination of oxalate was exposed to 10-percent NF_3/Ar. The final product was pink and had an fluorine:plutonium atom ratio of 3.9:1, while in other duplicate experiments, the final ratio reached 4:1. This result, in combination with our XRD results, indicates that PuF_4 was formed. In other experiments, there was no detectable indication of plutonium volatility even with up to 30-percent NF_3/Ar at a variety of isothermal temperatures up to 500°C.

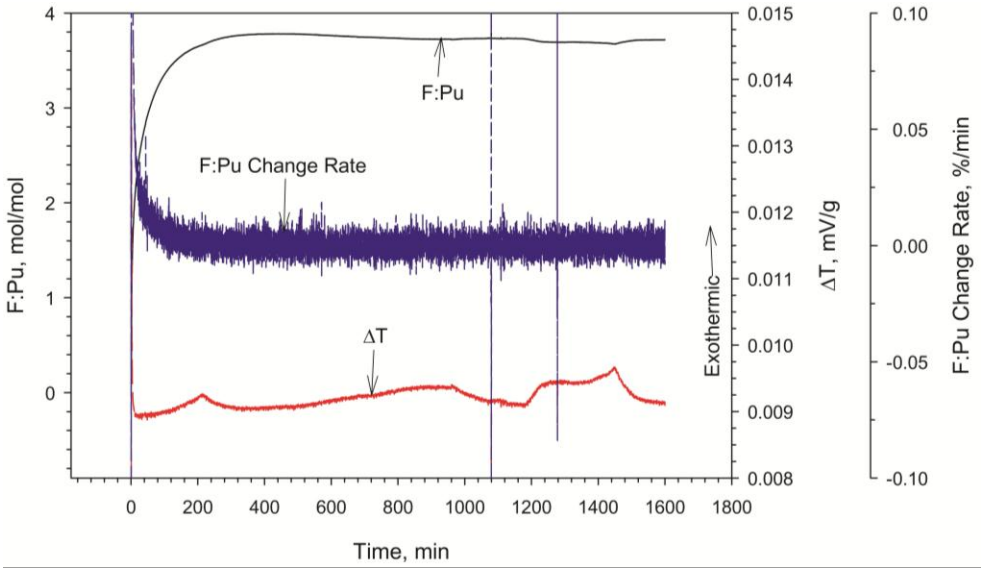

Figure 5-16. Thermal action of 10-percent NF_3/Ar on PuO_2 (from oxalate) as measured by isothermal TGA at 445°C.

The absence of PuF_6 volatility due to NF_3 treatment is consistent with the endothermic ΔG values at 300°C of +126 kJ/mol Pu indicate that PuF_6 is not the preferred fluoride relative to PuF_4. Thus, if PuF_4 is formed as an intermediate, NF_3 will be challenged to produce PuF_6 without a significant overpressure. Higher temperatures may be required to increase the reaction rate to bypass PuF_4 formation. Both the endothermic ΔH and ΔG values at 300°C of 97 and 91 kJ/mol Pu for the F_2-fluorination of PuF_4 to PuF_6 also indicate that PuF_6 under equilibrium conditions should decompose to PuF_4. This is consistent with Treverrow et al.'s (1961) equilibrium studies using PuF_6 prepared by treating PuF_4 with F_2 at 550°C . They measured equilibrium constants (mol PuF_6/mol F_2) ranging from 4.55×10^{-4} to 50.5×10^{-4} for the temperature range 150 to 425°C, respectively.

The absence of significant mass loss in the presence of NF_3 indicates that NF_3 is not an effective agent for producing and maintaining the volatile PuF_6 at concentrations up to 30-percent NF_3/Ar. The neat uranium oxides and PuO_2 testing indicates that treatment of a mixed plutonium and uranium oxide with NF_3 would cause the uranium to volatilize leaving the non-volatile PuF_4. The plutonium would thus remain with the non-volatile fission products and actinides as is discussed in Section 5.5.

5.4.3 Kinetic Modeling of NF_3 Fluorination of PuO_2

The fractional conversion of PuO_2 to PuF_4 was determined using the methodology developed for UO_2 and NpO_2 and was compared to the theoretical curves. Two identical experiments were run at 450ºC to determine the kinetic reaction mechanism of the NF_3 with the PuO_2. The results of these isothermal TG experiments are presented in Figure 5-17 and Figure 5-18. While the experimental behavior was bounded by the models in Table 3-1, the fits indicated that the two experiments were irreproducible and worse, seemed to indicate two different dominant reaction mechanisms, with three-dimensional diffusion for the

first and possibly phase boundary for the second reaction. This was particularly evident during the early reaction time.

Given the complexity of gas-solid reaction mechanisms, the lack of reproducibilty might be due to the wide variety of particle sizes in the initial sample (see Figure 4-3). Using this hypothesis, the initial jump in the fraction conversion relative to the three-dimensional diffusion model may be due to the rapid fluorination of the large surface area afforded by the small particles, while the seemingly very slow conversion fraction later in the reaction is due to the diffusion through the much larger particles. It can be justifiably hypothesized that if all of the particles in the original sample were of uniform shape and size, then the resulting fractional conversion curve would match up very well with the three-dimensional diffusion model. One way to attempt to account for this discrepancy is to realize that if the smaller particles were to be removed from the sample prior to fluorination, then the fractional conversion would be much slower at the beginning of the reaction, resulting in a longer reaction half time.

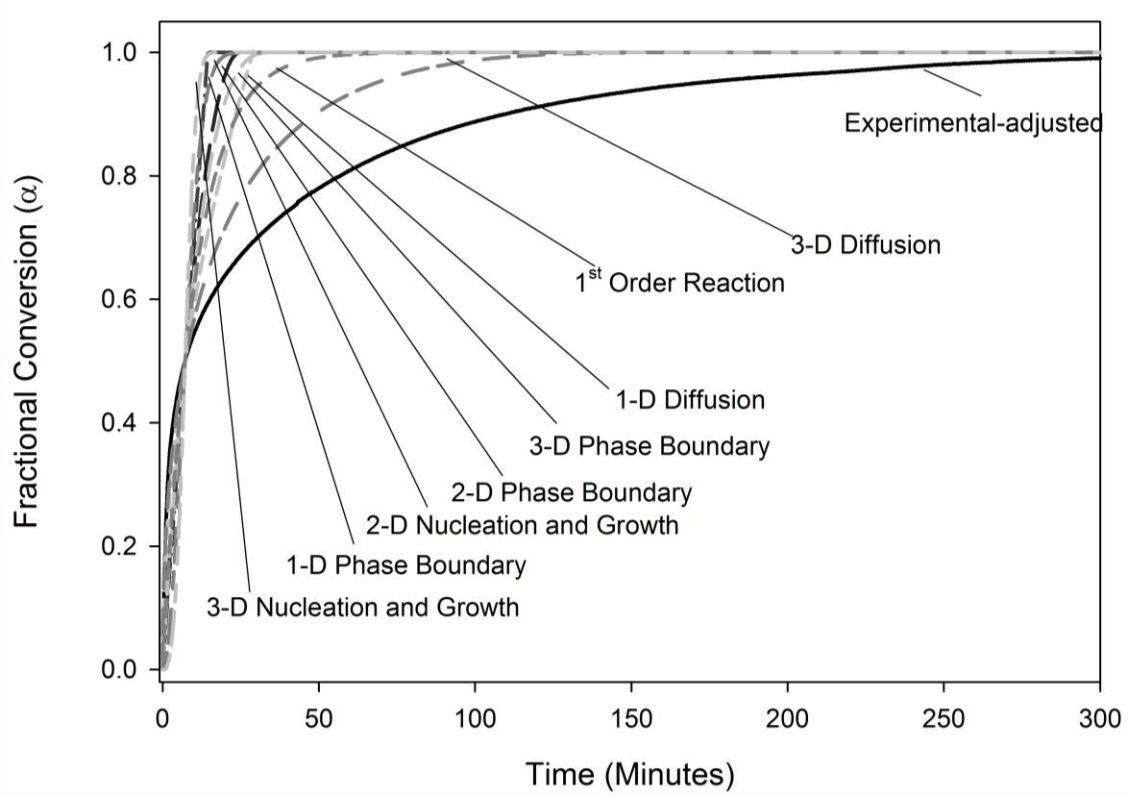

Figure 5-17. Kinetic models of the action of 10-percent NF_3/Ar on PuO_2 (from oxalate) at 450°C (Experiment 1 $t_{0.5}$ = 7.25 min).

Another potential explanation for the rapid reaction at the beginning of exposure to NF_3 and the later slowdown is that an intermediate plutonium oxyfluoride rapidly forms and is more slowly converted to PuF_4. This possibility is consistent with the observed thermal sensitivity of NF_3 as a fluorinating and oxidizing agent. We have no evidence yet that an oxyfluoride is formed.

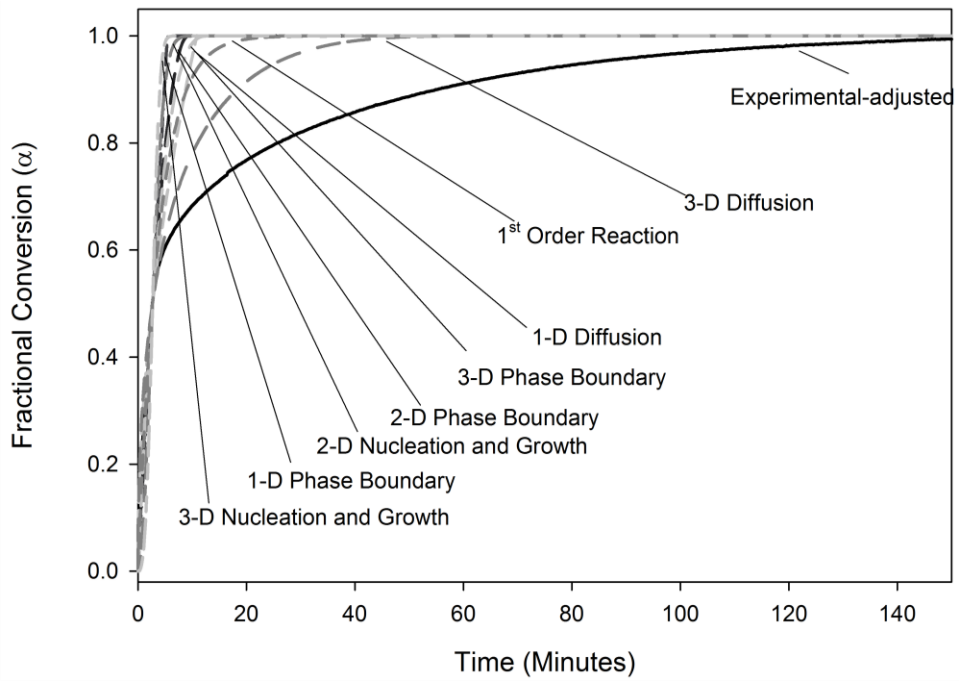

Figure 5-18. Kinetic models of the action of 10-percent NF_3/Ar on PuO_2 (from oxalate) at 450°C (Experiment 2 $t_{0.5}$ = 2.7 min).

It can be seen in the figures that, although the initial jump in the fractional conversion in the experimental curve is quite severe, the subsequent fit to the three-dimensional diffusion theoretical curve is much better. These results must be considered when attempting to determine the kinetic parameters associated with the kinetic data for the reaction of NF_3 with PuO_2. For very small particles as might be found in irradiated UO_2, it is likely that the kinetic parameters can be determined using a one-dimensional or two-dimensional phase-boundary model, and for the larger particles, the kinetic parameters can be determined using the thre-dimensional diffusion model

It seems reasonable to conclude that if the entire sample would have been comprised of very small particles, then the half time of reaction of the sample for the conditions tested would have been roughly 2 minutes. Likewise, if the sample would have been comprised of only large particles, then the half time of the reaction would have been roughly 13 minutes. The resulting values of the kinetic parameters using these estimates are presented in Table 5-7.

Table 5-7. Arrhenius-type kinetic paramaters for the action of 10-percent NF_3/Ar on PuO_2.

Model Conditions	One-Dimensional Phase-Boundary $t_{0.5}$=2 minutes, T=450C	Two-Dimensional Phase-Boundary $t_{0.5}$=2 minutes, T=450C	Three-Dimensional Diffusion $t_{0.5}$=13 minutes, T=450C
Kinetic Parameter Value	(u/r)=0.25 minutes^{-1}	(u/r)=0.146 minutes^{-1}	(k/r^2)=0.0035 minutes^{-1}

Our efforts to model reactions of NF_3 with PuO_2, NpO_2, and UO_2 are not yet complete. It does seem clear that the reactions are diffusion or phase-boundary limited in nature for the pure compounds. Whether or not this result can be extended to systems with intimately mixed components that form volatile fluorides remains uncertain at this time. The next section discussing the results of our studies on intimately mixed uranium and plutonium oxide does show that a volatile can effectively be separated from a lesser non-volatile fluoride.

5.5 NF_3 Fluorination of $(U_{0.8}Pu_{0.2})O_2$

Mixed uranium and plutonium oxide fuels are candidates for use in liquid metal breeder and light water reactors. We had some mixed oxide pellets that were prepared for analytical round robin testing in the 1970s for the Liquid Metal Breeder Reactor development program. These mixed oxides provided us with an opportunity to investigate the individual behaviors of these two volatile fluoride-forming actinides when intimately mixed.

5.5.1 Experimental Results for NF_3 Fluorination of $(U_{0.8}Pu_{0.2})O_2$

Figure 5-19 presents the results of a TG/DTA experiment where a $(U_{0.8}Pu_{0.2})O_2$ mixed oxide was heated at 5°C/min in 5-percent NF_3/Ar up to 630°C. This experiment found that uranium was quantitatively separated from the plutonium assuming that a heel of PuF_4 remains. The thermal behavior of the mixed oxide was not strictly a linear combination of the UO_2 and PuO_2 behaviors. The MOx has a small exothermic mass gain near 300 and 450°C and a sharp exothermic mass loss after 500°C that could be attributed to reaction with UO_2 but also exhibits an exotherm near 400°C. The exothermic reaction of PuO_2 with NF_3 that occurs near 500°C may be masked by the UO_2 reaction.

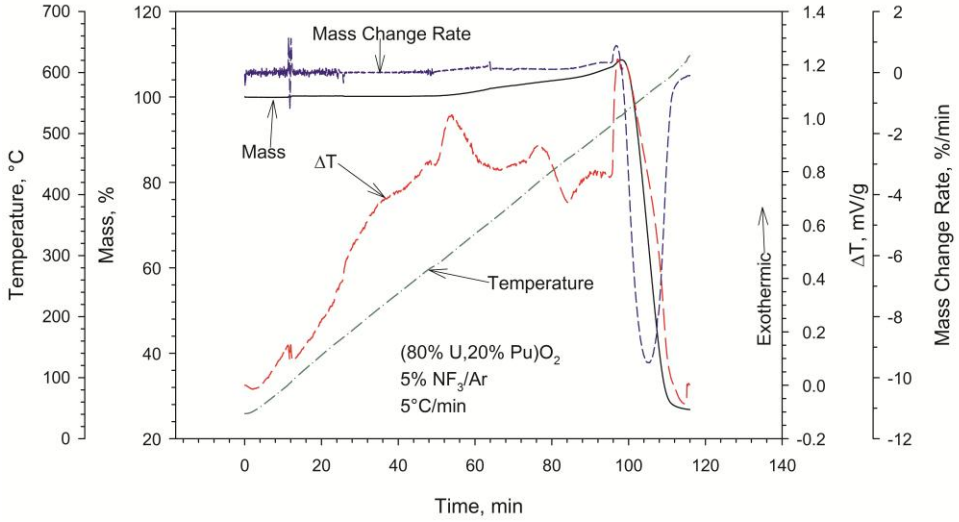

Figure 5-19. Thermal action of 5-percent NF_3/Ar on (0.80 U,0.2 Pu)O_2 as measured by simultaneous TG and DTA during heating at 5°C/min.

Figure 5-20 and Figure 5-22 provide SEM 1470X and SEM 16000X images of the product of the NF_3 treatment of the MOx, respectively. These micrographs show that the product is very porous. The EDS analyses for the particles in these micrographs are presented in Figure 5-21 and Figure 5-23. No uranium is found in the product by EDS analysis, indicating that the bulk uranium is effectively removed by NF_3 treatment.

That we can effectively remove the bulk uranium from the non-volatile PuO_2 that is in solid solution in UO_2, shows that thermal NF_3 will be able to obtain near quantitative removal of fuel constituents that form volatile fluorides or oxyfluorides from the non-volatile constituents. These results are very encouraging because it demonstrates that a volatile can be extracted from an intimately mixed co-ingredient.

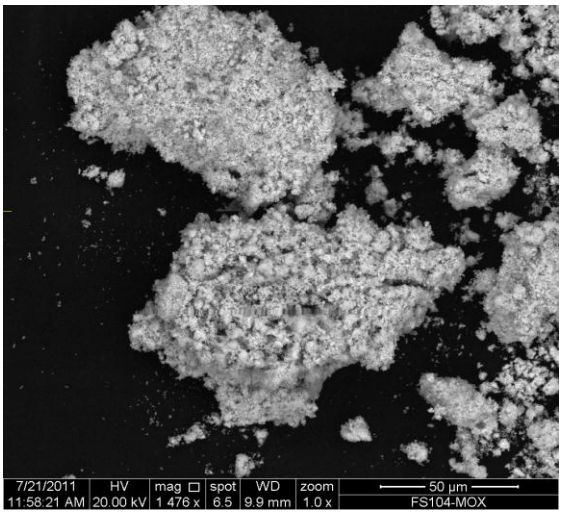

Figure 5-20. 1470X SEM Micrograph of $(U_{0.8}Pu_{0.2})O_2$ after treatment with NF_3.

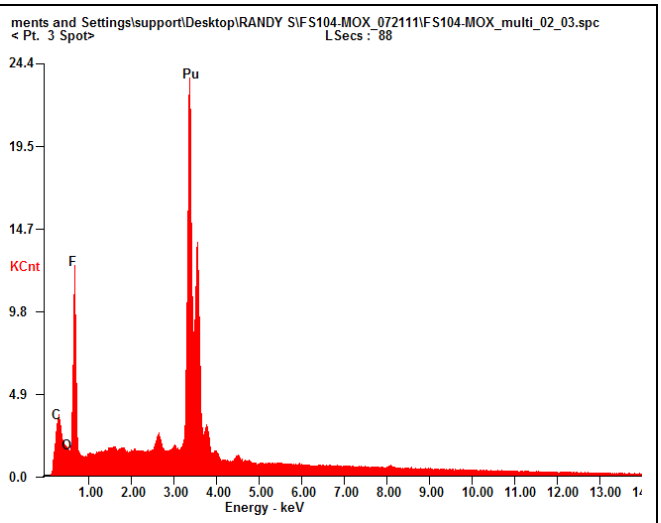

Figure 5-21. EDS analysis of large NF_3-treated particle at bottom left of Figure 5-20.

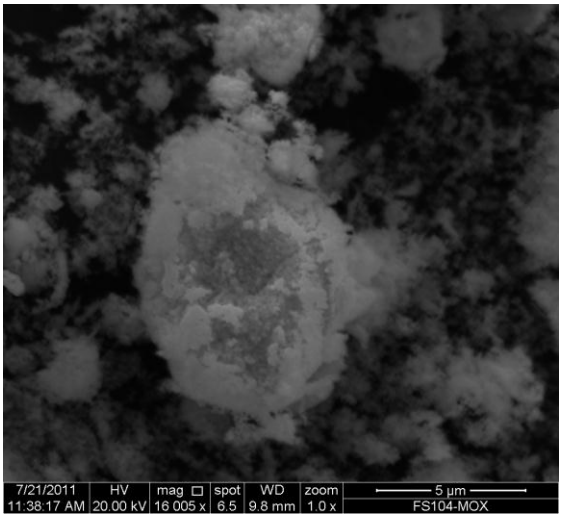

Figure 5-22. 16000X SEM Micrograph of $(U_{0.8}Pu_{0.2})O_2$ after treatment with NF_3.

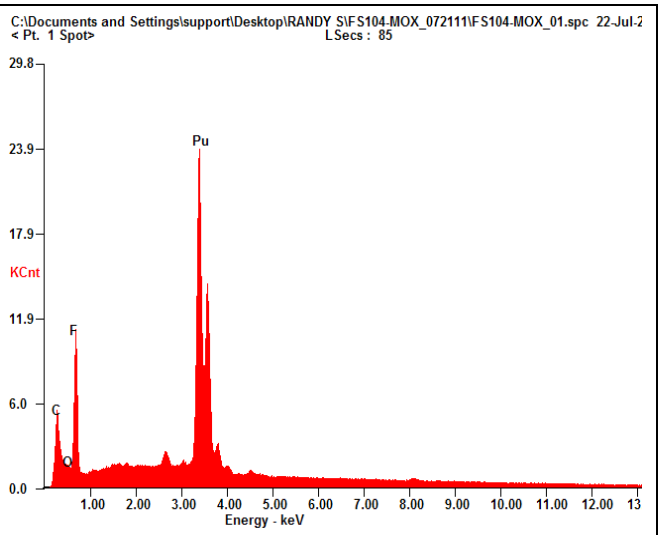

Figure 5-23. EDS analysis of large NF_3-treated particle at center of Figure 5-21.

5.6 NF3 Fluorination of Molybdenum Metal and Oxides

5.6.1 Thermodynamics and Speciation of Mo, MoO_2

Molybdenum and technetium may be found in a variety of oxidation states in irradiated nuclear fuel. For that reason, we investigated the fluorination of molybdenum metal, MoO_2, and MoO_3. Molybdenum metal has been reported to be 40 percent of the epsilon or five-metal phase (Kleykamp et al. 1985; Kleykamp 1985). If a voloxidation process was used to pretreat the irradiated fuel molybdenum or technetium metal and tetravalent molybdenum or technetium would be encouraged to oxidize further. If alternative pretreatment schemes are considered, then the effect on varied molybdenum and technetium speciation is important.

The chemistries of Molybdenum fluorides and oxyfluorides were reviewed by Weaver and Friedman (1967) then at Oakridge National Laboratory, and little new information has been added to the literature since then. The pure fluorides are MoF_5 (b.p.= 213.6ºC) and MoF_6 (b.p.=33ºC). The volatile oxyfluorides of interest here are $MoOF_4$ and MoO_2F_2 (sublimes at 270ºC). There are little data on the latter oxyfluoride, the former is a white compound with a boiling point of 180ºC. Vapor pressure data for these compounds have been published and the Raman and infrared frequencies for MoF_5 and MoF_6 are published.

We acquired the Raman spectra of the molybdenum compounds as a first identification of the products of reaction of molybdenum metal with NF_3. The Raman spectrum from the material, as captured in a flow-through quartz cell and using dry ice and acetone as the refrigerant, confirmed the yellow compound as MoF_6. Reaction of MoO_2 with NF_3 led to the formation of the white $MoOF_4$ as determined by Raman. An alternative approach is to further identify these products using their known vapor pressure behavior. This approach has the advantage in that provides an understanding of how the volatilized fluorides and oxy fluorides can be transported and trapped.

It is important to note that the reaction of molybdenum compounds with NF_3 in a TG flow-through experiment will produce one of the four known molybdenum volatile fluorides or oxyfluorides, and the product is essentially the final product because it is removed by the sweep gas. In a static reactor, the oxyfluorides can continue to react with the fluorinating reagent to ultimately produce MoF_6. Similar behavior can be expected for technetium compounds.

Chilenskas (1968) found in several experiments that < 51 to 76 percent of the molybdenum was released during fluidized-bed treatment with BrF_5 of irradiated UO_2. In contrast, Table 5-1 shows that molybdenum is not volatilized by voloxidation even at 1500ºC. Because the voloxidation process relies on full oxidation of all molybdenum species to MoO_3 (=1155ºC) and removal from particle inclusions, high temperature would be required for molybdenum removal. BrF_5 and more aggressive fluorinating reagents are superior at lower temperature but remove uranium at the same temperature.

5.6.2 Experimental Results for NF_3 Fluorination of Molybdenum Metal, MoO_2, and MoO_3

Figure 5-24 shows that molybdenum metal began to react exothermically when heated at 5°C/min with 5-percent NF_3/Ar near 300°C and was completely converted to a volatile fluoride (formation of any intermediates are not rate-limiting). The DTA results show that the reaction was sufficiently fast and exothermic that self-heating of the sample occurred as evidenced by the increase in temperature at 330°C and the temperature drop at 390°C as the program temperature catches up to the sample temperature. Because of this small increase in temperature, a small mass increase occurred simultaneously indicating the formation of an intermediate non-volatile fluoride. As mentioned earlier, Raman analysis indicated that the product was MoF_6. This experiment shows that NF_3 is an effective fluorinating and oxidizing agent for converting molybdenum metal to a volatile fluoride.

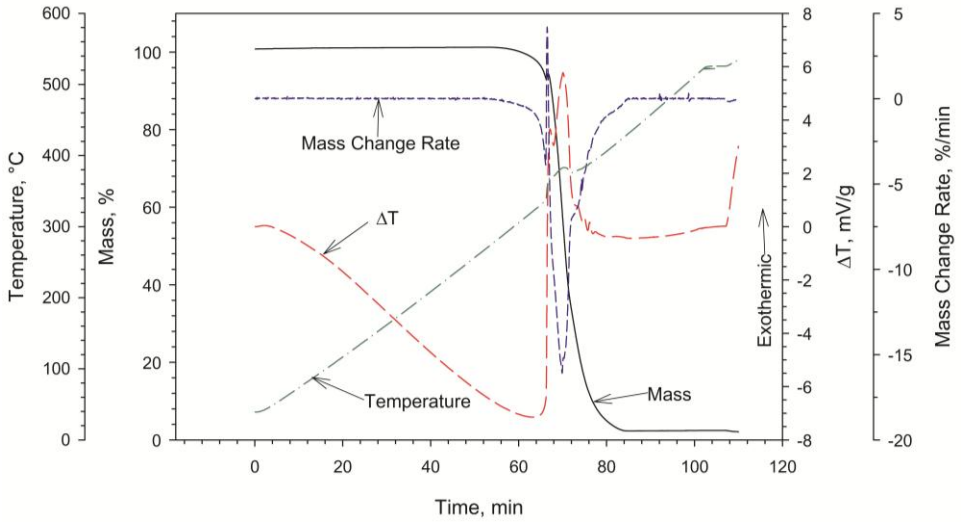

Figure 5-24. Action of thermal 5-percent NF_3/Ar on Mo metal as measured by simultaneous TG and DTA.

Figure 5-25 shows that 5-percent NF_3/Ar began to fluorinate MoO_2 near 260°C when heated at 5°C/min. The reaction was exothermic as predicted by our thermodynamic properties calculations. The DTG results suggest that the fluorination/oxidation proceeds via a two-step reaction. The DTA results do not provide that same indication at this ramp rate. Raman analysis found $MoOF_4$. Again NF_3 proves to be an effective fluorinating and oxidizing agent for producing a volatile molybdenum fluoride.

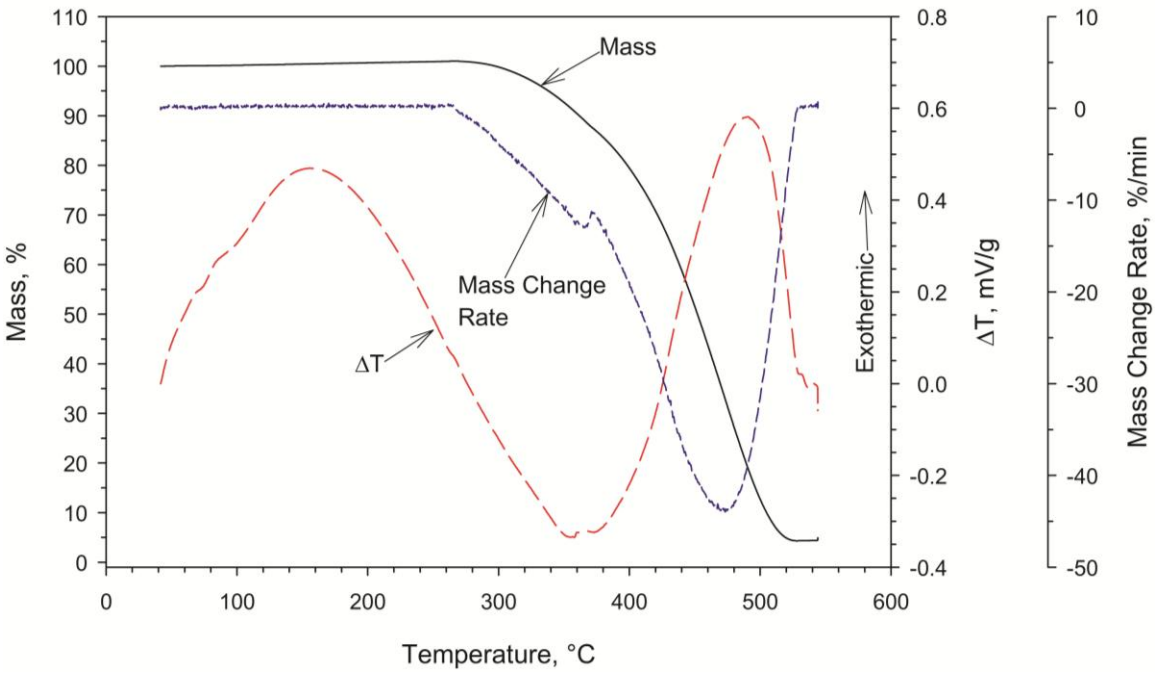

Figure 5-25. Thermal action of 5-percent NF_3/Ar on MoO_2 as measured by simultaneous TGA and DTA.

Using the mass change rate as a guide in Figure 5-26, MoO_3 began to react rapidly and lose mass at 320°C; the exothermicity becomes obvious after 75 min (~400°C). The sample lost 30 percent of its original 13 mg mass after being heated in 5-percent NF_3/Ar at 5°C/min and held isothermally for 20 min.

When compared to the other molybdenum compounds tested, the fluorination rate was slower for MoO_3. This experiment indicates that NF_3 is an effective fluorinating agent for MoO_3.

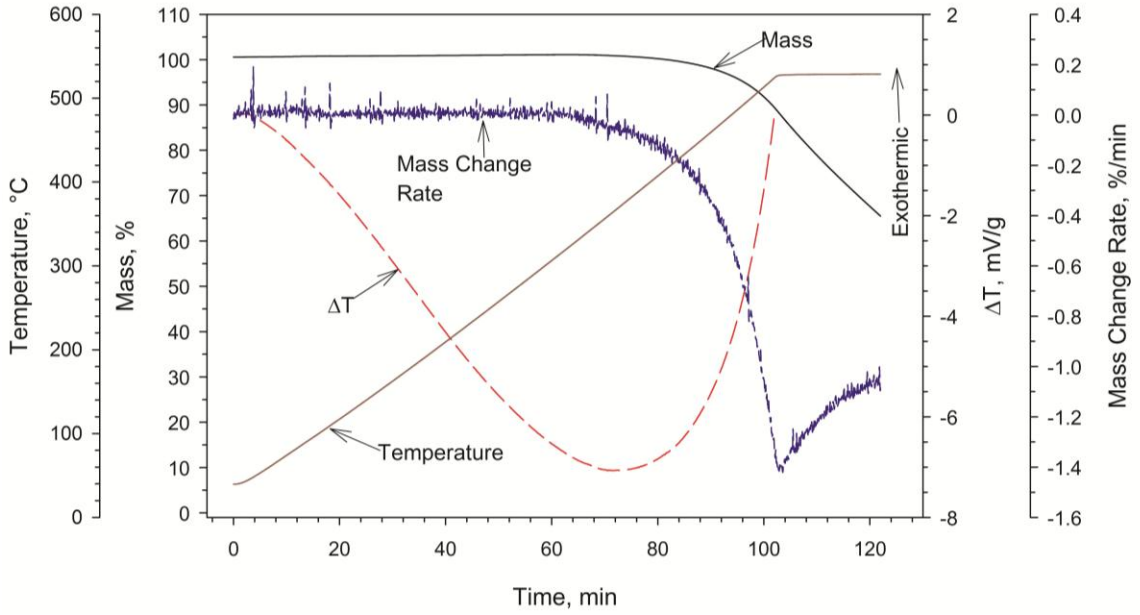

Figure 5-26. Thermal action of 5-percent NF_3/Ar on MoO_3 as measured by TGA and DTA during heating at 5°C/min.

Comparison of the NF_3-reaction profiles of the molybdenum compounds with those of the uranium oxides finds significant differences in behavior. The molybdenum compounds appear to proceed by direct conversion to a volatile fluoride near 300°C while UO_2 must proceed through an intermediate at 550°C and U_3O_8 began to volatilize near 520°C. These differences in the reaction pathway and volatilization temperatures between the molybdenum compounds and uranium oxides indicate that molybdenum could be separated from uranium oxides by NF_3 treatment near 300°C.

5.7 NF_3 Fluorination of Tc Metal and TcO_2

Technetium might exist in irradiated fuel in different oxidation states (Kleykamp 1985; Kleykamp et al. 1985) and these would be altered by fuel pretreatments such as voloxidation. Therefore we investigated Tc metal and TcO_2 as likely fuel constituents.

5.7.1 Thermodynamics for Fluorination of Tc and TcO_2

Quite a bit of thermodynamic data are available in the literature from vapor-pressure measurements made on the volatile fluorides and oxyfluorides of technetium (Rard et al. 1999; Schwochau 2000). The speciation is similar to that of the molybdenum system with TcO_3F and $TcOF_4$ being the predominant oxyfluorides and TcF_5 and TcF_6 the homoleptic fluorides. TcF_5 is a yellow solid that melts at 50ºC and decomposes at 60ºC (Peacock 1983). It can be purified by sublimation. Raman bands at 749, 693, 669, 282, 225,and 139 cm^{-1} (Schwochau 2000) help to distinguish it from TcF_6. The yellow TcF_6 can be prepared in high yields from technetium metal at 400ºC with fluorine gas (Selig et al. 1961). It boils at 55.3ºC and vapor pressure measurements have been reported (Selig, Chernick and Malm 1961). Raman fundamentals are reported as 712.9, 639, 748, 265, 297, and 145 cm^{-1} (Claassen et al. 1970) $TcOF_4$ is formed as a byproduct of technetium metal fluorination. It has two phases (blue and green), but relevant to separations chemistry, they can be separated from TcF_5 and TcF_6 because of the higher boiling point of

165ºC (Edwards et al. 1968; Edwards et al. 1970). TcO_3F is prepared from TcO_2 using fluorine gas, yielding about 56 percent product. It also is yellow, and vapor-pressure measurements have been reported (Selig and Malm 1963). The boiling point of TcO_3F is about 100ºC. Its Raman spectrum is as follows: 696, 962, 317, 951, 347, and 231 cm^{-1} (Binenboym et al. 1974; Selig and Malm 1963).

5.7.2 Nature of Technetium Fluorides and Oxyfluorides

Fluorination of the metal and the oxide produces different volatile fluorides: TcF_5, TcF_6 or the oxyfluorides: $TcOF_4$, TcO_3F. TcF_6 undergoes a solid-solid transition at -4.54ºC, melts at 37.4ºC, and boils at 55.3ºC. $TcOF_4$ forms in two phases, one blue and one more green in color. They have been separated from each other by vacuum sublimation. The blue phase boils near 165ºC. TcO_3F is a yellow compound that boils near 100ºC. The significance of these data concerning the volatility behavior of the technetium or molybdenum fluorides and the oxyfluorides is that they should all be removed readily form the uranium fuel matrix once they have been formed. It is rather remarkable that not only are all of these the species of fluorination are volatile but also that they are thermally stable in most cases, as are $UF_{6(g)}$ and $NpF_{6(g)}$. Ultimately, in a static reactor, all products should be driven to TcF_6. It is quite likely, however, that in a flow system technetium compounds mixtures are formed. We have not yet identified the major species of fluorination of TcO_2 by NF_3. The pure metal appears to be predominantly TcF_6.

5.7.3 Experimental Results for NF_3 Fluorination of Tc Metal and TcO_2

Figure 5-27 compares the effects of NF_3-treatment of neat TcO_2 at 256°C and UO_2 at 425°C and illustrates the potential for the use of simple differences in temperature to separate Tc as TcO_2 from UO_2. The UO_2 requires temperatures in excess of 390ºC to begin the initial formation of UO_2F_2 and to produce UF_6 at a significant rate. TcO_2 on the other hand, is rather quickly removed here as TcO_3F, based on fluorine-fluorination studies (Selig and Malm 1963).

Figure 5-27. Comparison of TG-measured thermal behavior TcO_2 at 256°C and UO_2 at 425°C. TcO_3 product based on fluorine fluorination (Selig and Malm 1963).

We looked a bit more deeply at the removal rates of TcO_2 and have begun repeating these experiments with Tc metal. In Figure 5-28 are plotted the volatilization curves for TcO_2 using NF_3 and show the effects of temperature. These are the first such data known for TcO_2. The kinetics of volatilization were investigated. As in the case of UO_2 and especially U_3O_8 we again observed diffusion-controlled behavior as opposed to chemical kinetics. We also note that in contrast with UO_2 thermal scans of fluorination of TcO_2 or Tc metal show little preliminary mass gain before volatilizing. In the case of the metal, the product of fluorination was TcF_6 was determined by its Raman spectrum.

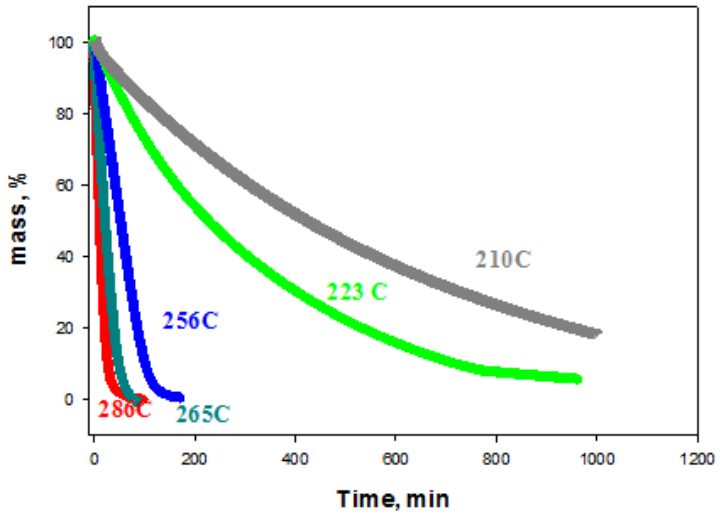

Figure 5-28. Effect of temperature on the action of NF_3 on TcO_2 to produce a volatile oxyfluoride or fluoride.

5.7.4 Kinetics of NF_3 Fluorination of TcO_2

It appears that the reaction between NF_3 and TcO_2 proceeds through a phase-boundary reaction mechanism similar to that described for U_3O_8. The fractional conversion of a phase-boundary controlled mechanism (Szekely et al. 1976a; Szekely et al. 1976b) is described by the same Eqs. (8) through (13). For the reaction characterized in the representative isothermal scan taken at 280ºC in Figure 5-29, the data aligns well with phase boundary reactions for one or two dimensions. Using non-integral dimension numbers such as 1.5 resulted in closer fits. The interpretation of this result is that the NF_3 drops down on the TcO_2 powder and systematically reacts downward as though attacking a slab of material, except that the powder is porous resulting in a slightly higher reaction rate. The sharp bend near the end of the fractional conversion curve is indicative of the presence of an impurity or the formation of an intermediate that forms a volatile product at a slower rate or survival of larger particles. Using the same methodology as described for U_3O_8 the fractional conversion $t_{0.5}$ was estimated. Table 5-8 compares the values of $t_{0.5}$ and (u/r) for four reaction temperatures and for each of the phase-boundary mechanisms described by Equations (10) through (13).

Table 5-8. Comparison of Arrhenius-type parameters for action of 10-percent NF_3/Ar on TcO_2 at various temperatures.

Temperature	$t_{0.5}$, min	(u/r) 1-D, min^{-1}	(u/r) 1.5-D, min^{-1}	(u/r) 2-D, min^{-1}	(u/r) 3-D, min^{-1}
256°C	48.2	0.010	0.008	0.006	0.004
265°C	23.4	0.021	0.016	0.013	0.009
286°C	13.2	0.038	0.028	0.022	0.016
323°C	2.40	0.208	0.154	0.122	0.086

Treating the value of (u/r) as though it were a rate k, the values above can be plotted in the form of the Arrhenius equation with the results presented in Figure 5-29 and Table 5-9.

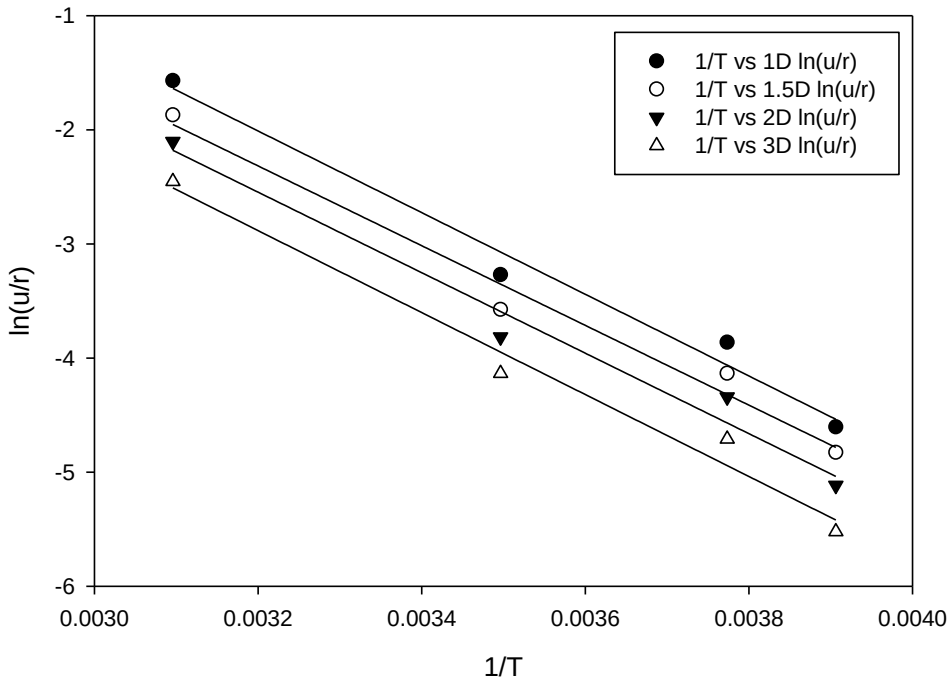

Figure 5-29. Arrhenius-type plot for thermal action of 10-percent NF_3/Ar on TcO_2.

Table 5-9. Arrhenius-type parameters for action of NF_3 on TcO_2.

Temperature	1D	1.5D	2D	3D
ln(a), min^{-1}	9.4375	8.8615	8.7372	8.6071
B, K	3577.5	3493.2	3526.3	3590.8
R^2	0.9823	0.9806	0.9768	0.9797

Taking the average of all four models results in the following equation:

$$\ln(u/r) = 68.833 - \frac{57011}{T}, \quad (20)$$

From a comparison of the values of the estimated removal rate (u/r) for TcO_2 and U_3O_8 at various temperatures it can be seen in Table 5-10 that removal of pure technetium occurs several orders of magnitude than for pure U_3O_8. A similar comparison is valid for UO_2 and TcO_2 as described above. The molybdenum appear to be very similar to the technetium results.

Table 5-10. Comparison of reaction rates (u/r) for action of NF_3 on TcO_2 and U_3O_8.

Temperature (C)	u/r for TcO_2	u/r for U_3O_8
200	0.000354	3.53178E-23
225	0.001483	1.49898E-20
250	0.005425	3.56757E-18
275	0.017625	5.15357E-16
300	0.051668	4.82376E-14
325	0.138442	3.08916E-12
350	0.342738	1.41682E-10

Temperature (C)	u/r for TcO_2	u/r for U_3O_8
375	0.791186	4.83716E-09
400	1.716336	1.27043E-07
425	3.522362	2.64021E-06
450	6.87817	4.44837E-05
475	12.84352	0.000620544
500	23.03311	0.007299782

5.8 NF_3 Fluorination of Transition Metal Oxides Having the Potential to form Volatile fluorides

To date, we have only performed temperature ramping studies of other transition metal oxides that have the potential to form volatile fluorides and have not done the isothermal studies needed to determine the reaction kinetics. In this section, we provide the results of our thermoanalytical studies on the NF_3 fluorination of Nb_2O_5, RuO_2, Rh_2O_3, and TeO_2.

5.8.1 Experimental Results for NF_3 Fluorination of Nb_2O_5

As Figure 5-30 shows, when Nb_2O_5 was exposed to 5-percent NF_3/Ar and heated at 5°C/min to 550°C and held isothermally for 20 min, the niobium volatilized, likely as NbF_5 which boils at 235°C. The slightly increasing mass suggests that Nb_2O_5 reacted almost immediately upon being exposed to NF_3 at 40°C. The mass change rate (DTG) indicates that the reaction accelerated near 360°C. The DTA indicates that the reaction was exothermic. The final mass gain of 4.5 percent corresponds to a maximum measured fluorine:niobium atom ratio of 0.55:1. Brown (1968) reports that a variety of niobium (V) oxyfluorides NbO_2F, Nb_3O_7F, $Nb_5O_{12}F$, $Nb_{17}O_{42}F$, and $Nb_{31}O_{77}F$ have been identified but none with a fluorine:niobium ratio atom ratio of 0.6:1. It was unlikely that the fluorination to form a full non-volatile fluoride went to completion before the niobium began to volatilize.

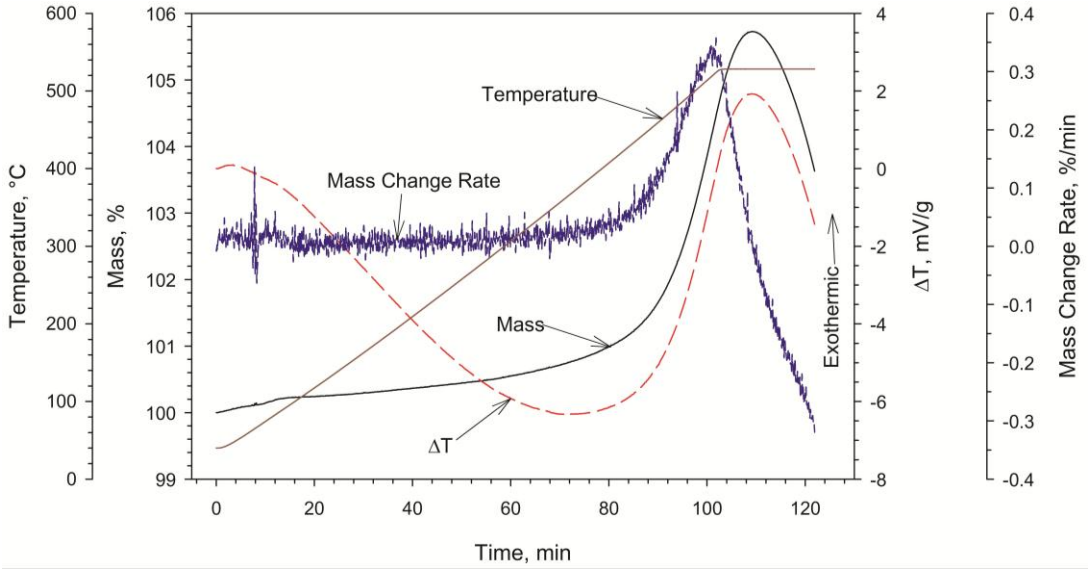

Figure 5-30. Thermal action of 5-percent NF_3/Ar on Nb_2O_5 as measured by simultaneous TGA and DTA during heating at 5°C/min.

The DTG maximum was earlier than that observed for the maximum mass which indicates that mass loss was occurring simultaneously with formation of a non-volatile fluoride or oxyfluoride. Without the 550°C isotherm, the niobium volatilization would not have been obvious.

Chilenskas (1968) reports that using bromine pentafluoride (BrF_5) removed 0 to 1.9% of the niobium in irradiated UO_2 in five fluidized bed experiments and molecular fluorine removed 0 to 5.8% of the niobium from the heel remaining after BrF_5 treatment to remove the uranium.

This experiment indicates that NF_3 is a sufficiently strong fluorinating agent to convert Nb_2O_5 to a volatile fluoride before it is fully converted to its intermediate. The closeness of the volatilization temperatures for uranium and niobium suggest that niobium may volatilize simultaneously with uranium when treated with thermal NF_3. Differences in the susceptibility of non-volatile intermediates to reaction with NF_3 might be used to achieve separation by treatment at slightly different temperatures. Isothermal experiments to gain further information on the reaction profile and to develop kinetic models are required to determine optimum temperatures to achieve separation of niobium using thermal NF_3.

5.8.2 Experimental Results for NF_3 Fluorination of RuO_2

Ruthenium forms one or more volatile fluorides; two of which are RuF_6 with a boiling point of 46°C and RuF_5 with a sublimation temperature of 70°C. Ruthenium is found both as the metal in the five-metal phase and as RuO_2 in the oxide fuel matrix. We only report our results for RuO_2 here.

Claassen and coworkers (1961) first prepared RuF_6 by heating ruthenium metal in 40 kPa (300 mm) fluorine at a 49-percent yield with RuF_5 also forming. They found the RuF_6 to be unstable, decomposing to RuF_5 and fluorine, although they found that they could store it at room temperature in a nickel can.

As Figure 5-31 shows, when heated in 5-percent NF_3/Ar at 5°C/min up to 540°C, RuO_2 began to react exothermically at 330°C with what appears to be some volatilization. However, the RuO_2 began to gain mass near 460°C and eventually began to rapidly lose mass at 500°C with a near total mass loss after 20 min at 540°C. The product(s) remain to be characterized and, based on volatilities either RuF_5 or RuF_6, could be the volatile fluoride formed.

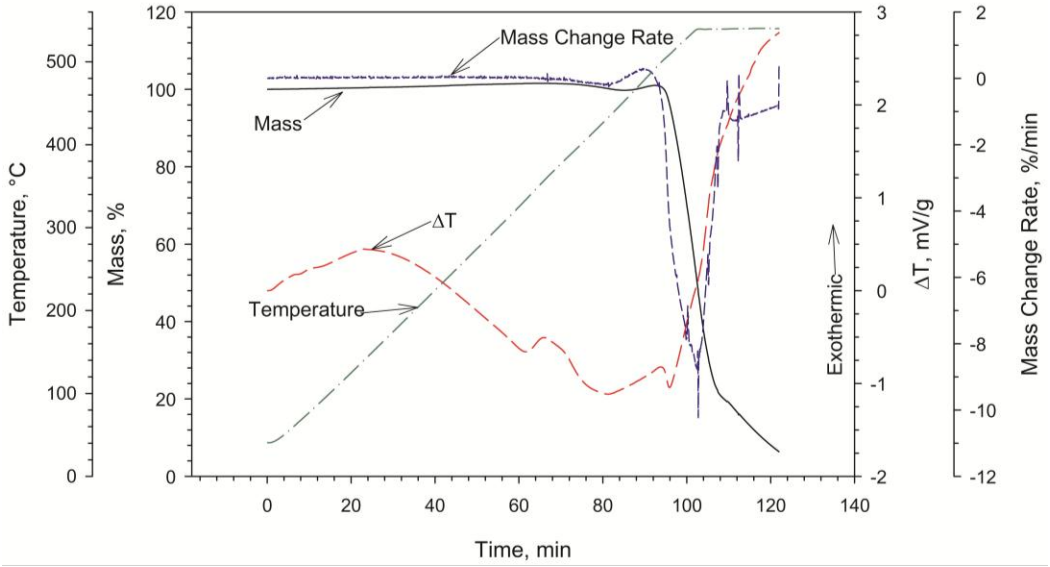

Figure 5-31. Thermal action of 5-percent NF_3/Ar on RuO_2 as measured by simultaneous TGA and DTA during heating at 5°C/min.

The differences in the NF_3 reaction temperatures between RuO_2 and the uranium oxides are not great suggesting that separations based solely on reaction temperatures may be difficult. The differences in temperature and pathway, particularly for UO_2, suggest that, through careful temperature control, separations could be achieved. Isothermal testing to provide a more precise thermal reaction profile and to develop kinetic models are needed.

Chilenskas (1968) found that 44 to 71 percent of the ruthenium was volatilized when they treated irradiated UO_2 with BrF_5 and that fluorine treatment released 3.2 to 14 percent of the total ruthenium. The complexity of the ruthenium fluorination reaction with fluorine was highlighted by investigations of Corbin et al. (1980) on fluorine-fluorination at 800°C of RuF_3, RuO_2, and RuO_2 mixed with an excess of UO_2 or yttrium oxide (Y_2O_3). When treating RuF_3, RuF_5 was produced. When treating RuO_2, a mixture of RuF_4, RuF_5, and $RuOF_4$ formed. In the presence of excess UO_2 or Y_2O_3, RuO_2 reacted with fluorine to produce mixtures of RuF_4, RuF_5, $RuOF_4$, RuO_2, and RuF_6.

Our initial studies indicate that NF_3 will fluorinate and oxidize RuO_2 to a volatile fluoride. The work of Corbin et al. (1980) work indicates that more detailed studies are required to determine the fraction of RuO_2 that can be volatilized from used fuel.

5.8.3 Experimental Results for NF3 Fluorination of Rh_2O_3

Rhodium forms two volatile fluorides RhF_5 and RhF_6 with boiling or sublimation temperatures of 95.5 and 73.5°C, respectively. Rhodium is found in used nuclear fuel as an oxide dissolved in the oxide matrix or as a metal in the five-metal particles. We only report on the NF_3 fluorination of Rh_2O_3.

Chernik et al. (33) first reported volatile RhF_6 by burning rhodium metal in a liquid nitrogen-cooled quartz vessel. They found it to be unstable at room temperature.

As Figure 5-32 shows, when heated in 5-percent NF_3 to 550°C at 5°C/min and held isothermally for 20 min, Rh_2O_3 was fluorinated to a nominal fluorine:rhodium atom ratio of 1.6:1. Based on the fluorine:rhodium change rate, the reaction was a series of two exothermic reactions with the first beginning near 220°C and the second near 350°C. After 20 min at 550°C, the mass continues to increase, suggesting the formation of a higher fluoride or oxyfluoride.

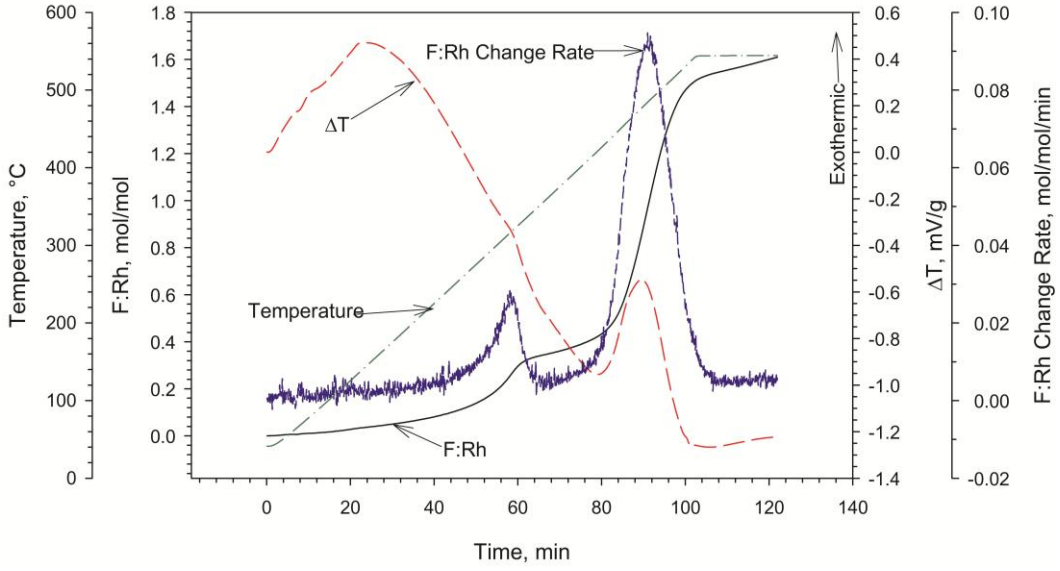

Figure 5-32. Thermal action of 5-percent NF_3/Ar on Rh_2O_3 as measured by simultaneous TGA and DTA during heating at 5°C/min.

Based on this temperature ramp study, although rhodium has volatile fluorides, NF_3 is not a sufficiently strong fluorinating and oxidizing agent to produce a volatile fluoride by heating to 550°C. In a fluoride volatility-based separations process, the rhodium oxide would fluorinate but would remain with the non-volatile fraction.

5.8.4 Experimental Results for NF_3 Fluorination of TeO_2

Tellurium has a single reported volatile fluoride that has a boiling point of -34.5°C. Figure 5-33 shows that as TeO_2 was heated at 5°C/min in 5-percent NF_3/Ar to 550°C and held for 20 min, tellurium was fluorinated and volatilized beginning near 260°C. After the experiment, 40 percent of the TeO_2 remained, but the mass curve indicates that the reaction would continue if the NF_3 atmosphere continued to be maintained at 550°C. The DTA curve suggests that the reaction was exothermic.

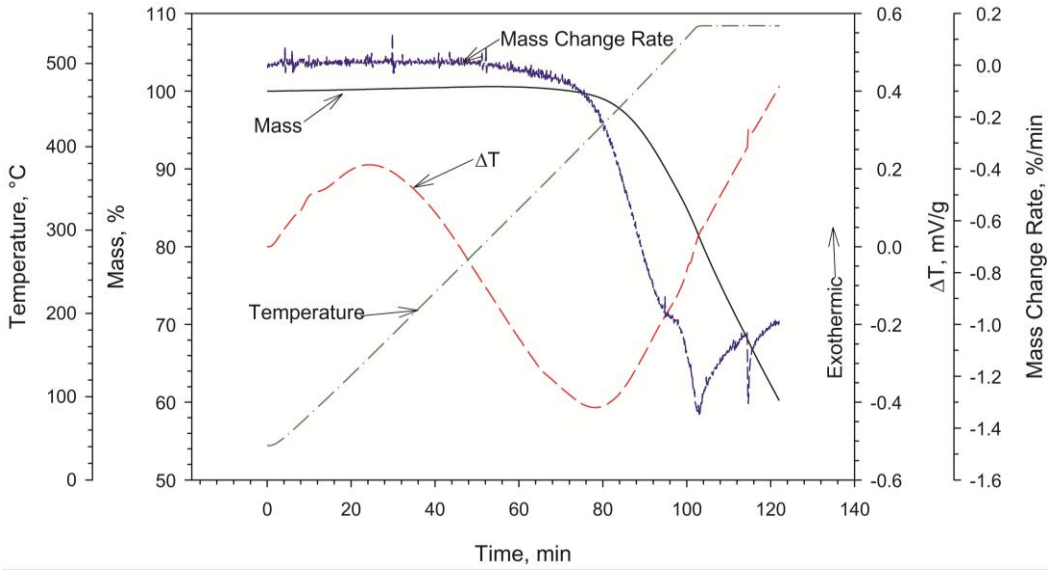

Figure 5-33. Thermal action of 5-percent NF_3/Ar on TeO_2 as measured by simultaneous TGA and DTA during heating at 5°C/min.

The significant differences between the reaction and volatilization temperatures between TeO_2 and UO_2 or U_3O_8 indicate that tellurium could be separated from uranium oxides by treatment near 260°C. Whether the tellurium could be separated from the other fission products that form volatile fluorides at temperatures significantly less than uranium compounds would require additional more precise isothermal testing to develop kinetic models.

5.9 NF_3 Fluorination of Non-Volatile Fission Products

Other than those fission products and actinides identified in Table 1-1, the other used fuel constituents do not form volatile fluorides and would be expected to remain in the fluorinator heel. For this year, we provide the results of our thermoanalytical on the NF_3 fluorination of La_2O_3 and CeO_2 representative of the oxidation state 3 and 4 lanthanides.

5.9.1 NF_3 Fluorination of La_2O_3

Although not presented here, the La_2O_3 lost significant amounts of water by drying at 400°C. As shown in Figure 5-34, NF_3 fluorinated La_2O_3 to a nominal fluorine:lanthanum atom ratio of 1.64:1 and was trending up when heated in 5-percent NF_3/Ar at 5°C/min to 550°C and then held isothermally at 550°C for 20 min.

The mass change rate curve (DTG) indicates that the La_2O_3 was fluorinated in a two-step reaction with the first reaction beginning near 230°C and ending with the formation of an fluorine:lanthanum atom ratio of 1:1 or LaOF. Based on extrapolation of the DTG curve, the second step began near 330°C and, based on the upward slow mass gain trend, would have produced a non-volatile lanthanum oxyfluoride having the nominal composition $La_3O_2F_5$. Brown (1968) and Moeller (1973) both report the existence of LaF_3 and LaOF, but they do not report any intermediate oxyfluorides. The product needs to be characterized to confirm its final composition.

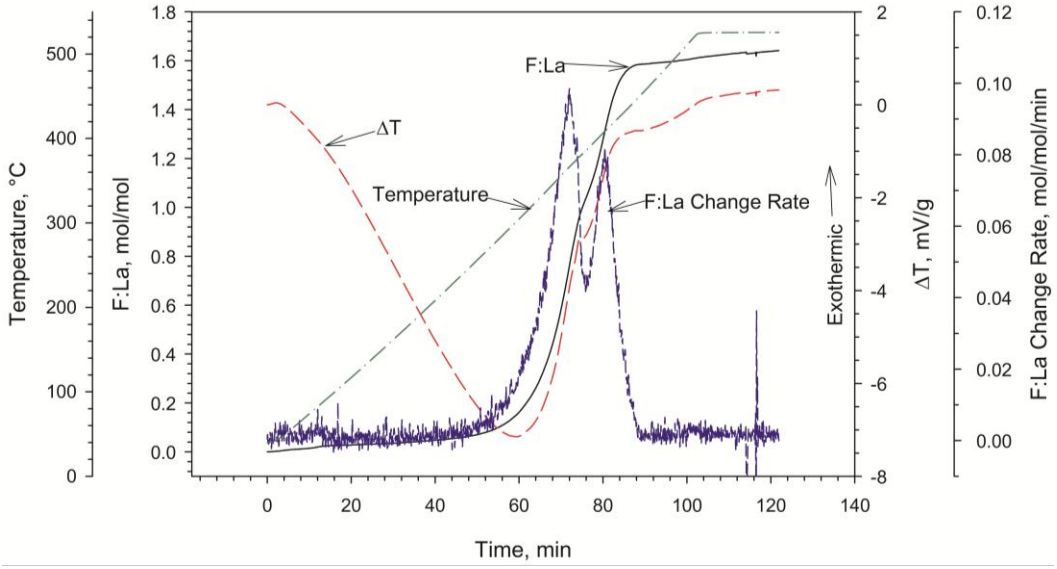

Figure 5-34. Thermal action of 5-percent NF_3/Ar on La_2O_3 as measured by simultaneous TGA and DTA during heating at 5°C/min.

The DTA (ΔT curve) observed small exotherms consistent with our thermodynamic calculations that the overall fluorination reaction was exothermic although it does not completely react to LaF_3, which is the postulated product for our thermodynamic calculations. Other similar experiments observed significant exothermic behavior. The ΔT curve Figure 5-34 illustrates one of the complications in the use of DTA to observe reactions that produce (exothermic) or require (endothermic) heat to proceed. Typically over broad temperature ranges, the baseline is curved and, from our own experience, varies from experiment to experiment, which complicates the interpretation of the DTA results. Detection of heat changes requires the interpreter to couple the data with the coincident information provided by the TG or DTG curves to be able to identify deviations from previous and succeeding data.

This experiment shows that even when heated to temperatures where NF_3 converts UO_2 and UO_3 to volatile UF_6, the lanthanum does not volatilize. This indicates that uranium can be separated from lanthanum by treatment with thermal NF_3.

5.9.2 NF_3 Fluorination of CeO_2

Figure 5-35 shows that when heated in 5-percent NF_3/Ar at 5°C/min and held at 550°C for 20 min, CeO_2 was converted in two steps to CeF_4. Based on the fluorine:cerium change rate (DTG), near 320°C, NF_3 began to react exothermically with the CeO_2 to produce $CeOF_2$. Before the CeO_2 was completely converted to $CeOF_2$, the non-volatile CeF_4 began to form near 400°C. The product has not been characterized.

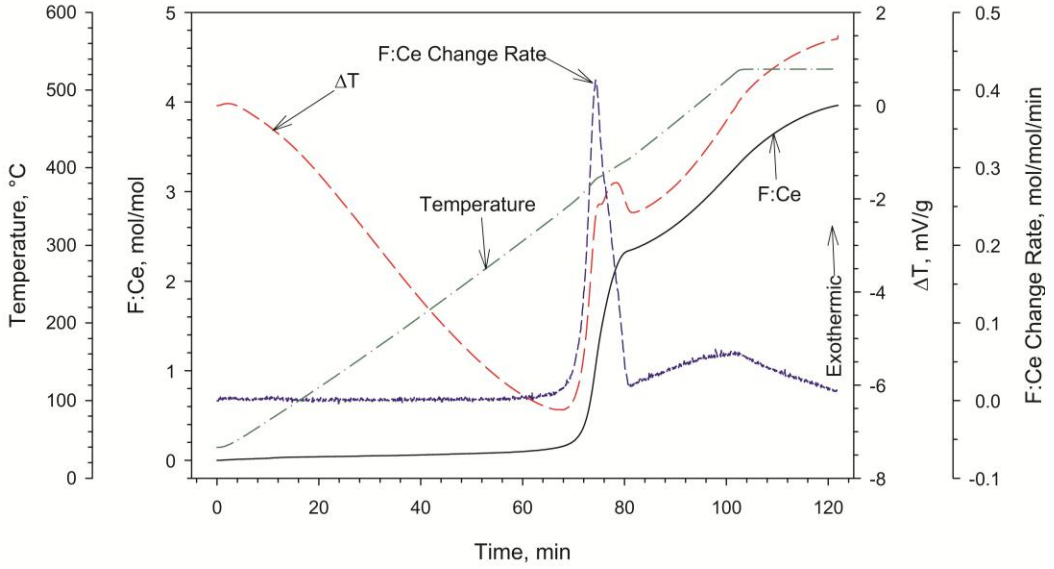

Figure 5-35. Thermal action of 5-percent NF_3/Ar on CeO_2 as measured by simultaneous TGA and DTA during heating at 5°C/min.

Brown (1968) reported the preparation of CeF_4 by fluorine treatment of the trifluoride and the oxide. Moeller (1973) reported the preparation of CeF_4 from the trifluoride. Brown reported that no oxyfluorides of the tetravalent lanthanides or actinides other than $ThOF_2$ have been observed. Kwon et al. (2002) found in their hydrogen fluoride (HF)-fluorination studies that to fluorinate CeO_2 that they had to use a combination of HF and molecular hydrogen (H_2) to produce CeF_3.

As with lanthanum oxide, cerium does not form a volatile fluoride or oxyfluorides. Cerium will remain in the non-volatile solids when the uranium is volatilized.

6. NF_3 Costs Regulations, Recycle and Facility Design Considerations.

In support of the program to investigate and develop a molten salt cooled reactor, Scheele and Casella (2010) considered the use of NF_3 as a replacement for a mixture of H_2 and HF to remove oxygen and water contaminants from the various fluoride salts that are candidates for the primary and secondary coolants. Scheele and Casella discuss current industrial uses of NF_3 and various operational considerations such as costs, strategies for managing NF_3 releases (recycle or destruction), safety, materials of construction, and environmental aspects of NF_3 use.

NF_3 is mildly toxic, non-corrosive, and non-reactive at room temperature,thus making it easy to manage the chemical and reactivity hazards during transportation, storage, and normal operations. Industrial experience with NF_3 also is extensive, with NF_3 commonly used as an etchant and chamber cleaner in the electronics industry.

From an industrial operations perspective, care appears to be necessary when using NF_3 in a plant. Precautions must be taken to prevent adiabatic compression and make sure that NF_3 thermal decomposition does not occur in unplanned locations. The system must be engineered to avoid the use of ball valves and sharp bends.

The materials of construction that will be required to contain NF_3 would include nickel or nickel-based alloys similar to other fluorinating and oxidizing agents. Fluorinating agents become more reactive with

increasing temperature and would require pure nickel or nickel-based alloys for containment until the gas stream has cooled. NF_3 is compatible with stainless steel at temperatures below 100°C.

With respect to the cost of the fluoride, HF is about one third the cost of NF_3 on a fluorine basis. Of the fluorine-containing chemicals, more HF is produced than any other. NF_3 is produced on an industrial scale, and its capacity has grown each year since being identified as a useful etchant.

Because of its value and being identified as a potential global warming contributor, managing recycling and releases of NF_3 should be evaluated. Because of its importance to the electronics industry, commercial technologies using incineration or plasmas have been developed and are used to destroy the NF_3 in a facility's gaseous effluent stream. A process also has been developed and used to recover and recycle NF_3. In addition, the electronics industry is actively pursuing alternative methods to control NF_3 releases.

For a more detailed discussion on these aspects of NF_3 use, we refer the reader to Scheele and Casella (2010).

7. Conceptual Flowsheet Design

The process flowsheets that have been proposed for fluoride volatility-based reprocessing vary from totally dry processes (Levitz et al. 1969) to a hybrid process that combines fluorination with solvent extraction (Kamoshida et al. 2000; Kobayashi et al. 2005; Kani et al. 2009).

The totally dry process described by Levitz et. al. (1969) consists of 1) a mechanical head-end to separate the fuel from the cladding, 2) a 350°C fluidized-bed fluorinator for removing the uranium by controlling the fluorine concentration, 3) a fluidized-bed fluorator to volatilize the plutonium using fluorine, and 4) trapping and purification systems for the voltilized uranium and plutonium. They assumed that 90 percent of the volatile fission product fluorides followed the uranium while the remaining 10 percent followed the plutonium. Purification of the uranium and plutonium is achieved using cold traps and fluoride salt traps. The non-volatile fission products remain in the fluidizer heel and are treated as waste.

Kamoshida (2000), Kobayashi (2005), and Kani (2009) in their so-called FLUOREX reprocessing technology uses a hybrid system of first fluorinating the preconditioned fuel using fluorine to remove the uranium that makes up the bulk of the fuel followed by conversion of the fluorination residuals back to oxides that are dissolved in nitric acid. Valuable constituents are recovered by solvent extraction. Following mechanical head-end treatment, they propose treating the sheared and chopped fuel by an oxidation-reduction process to pulverize the used fuel. The pulverized fuel then is fluorinated in a flame-reactor to volatilize most of the uranium as UF_6; some of the plutonium and volatile fission product fluorides will contaminate this UF_6. The UF_6 is purified by rectification and passing through a sodium fluoride trap (decontamination factor 10^7). The residual solids from the fluorination process then are pyro-hyrolyzed to convert the residual uranium, plutonium, and fission products to oxides or oxyfluorides, dissolved in nitric acid, and fed into a PUREX solvent extraction process to recover the uranium and plutonium.

In our initial conception of fluoride-volatility reprocessing using NF_3, the different thermal sensitivities of NF_3 reactions (different reaction temperatures and kinetics) with uranium, plutonium, neptunium, and fission products that form volatile fluorides will be used to achieve needed separations. As presented, NF_3 is used to fluorinate used fuel that has been pretreated by voloxidation to convert the uranium to U_3O_8. We have considered other possibilities where the thermal sensitivity of NF_3 would be applied to the concepts proposed by Kamoshida (2000), Kobayashi (2005), and Kani (2009).

Although we focus here on treatment of U_3O_8, NF_3 is an effective fluorinating/oxidizing agent for UO_2 converting UO_2 to UF_6 through a sequential series of oxyfluoride. It may prove unnecessary to chemically

pretreat the used fuel provided the used fuel can be adequately pulverized. The possibility exists that such chemical and structural changes caused by NF_3treatment could be used to release volatile fission products such as tritium, iodine, and the noble gases from UO_2 directly.

7.1 Conceptual Dry-Process Description

Our NF_3-based conceptual process uses thermal sensitivity for the formation of volatile fluorides to first sequentially remove fission products, then remove the uranium that makes up the bulk of the used fuel, followed by a final treatment of the <5-percent residual with fluorine and/or ClF_3 to simultaneously volatilize plutonium and neptunium; neptunium can be removed with NF_3 after the uranium is removed. Previous concepts using aggressive fluorination agents used inorganic fluoride salts and/or fractional distillation to separate the concurrently volatilized fluorides. The residual non-volatile fluorides would be immobilized and disposed of as waste.

The conceptual process described is for treatment of used UO_2 fuel, the current predominant nuclear fuel. As presented schematically in Figure 7-1, the spent fuel is first processed using voloxidation which converts the UO_2 to U_3O_8 powder by reaction with air, oxygen, or oxides of nitrogen to release the volatile fission products and oxides. The voloxidized fuel is then treated with 10-percent NF_3/Ar at 300 to 350°C to volatilize technetium and molybdenum; the U_3O_8 and other fission products (FP) or actinide oxides do not react with NF_3 to form volatile fluorides until higher temperatures are achieved. The temperature then is increased to 400 to 450°C to remove the niobium, ruthenium, and technetium. Tellurium oxide begins to react slowly with NF_3 to form a volatile fluoride at 260°C, but the reaction is slow and requires higher temperatures to volatilize at an acceptable rate so some technetium may be mixed with the molybdenum and technetium. The uranium then is volatilized by increasing the temperature to 500 to 550°C. Plutonium and neptunium would then be volatilized from the remaining non-volatile fluorides and oxyfluorides by treatment at 400 to 600°C with fluorine or ClF_3. Alternatively, neptunium would be removed with further treatment with NF_3 after the uranium is volatilized by increasing the temperature to 600°C, and the plutonium would be volatilized with fluorine and/or ClF_3. We propose to condense the volatile fluorides using cold traps. Other options for trapping the volatile fluorides include fluoride or oxyfluoride beds. A more detailed discussion follows.

The voloxidation process converts the UO_2 to U_3O_8 thus releasing all or nearly all the volatile fission products xenon, krypton (^{85}Kr), tritium (^{3}H), and iodine; we expect selenium oxide to volatilize during this operation also. The radioactive volatile fission products will be captured and managed using established or to be developed capture and immobilization technologies.

The oxides of niobium and ruthenium react with NF_3 to form volatile fluorides or oxyfluorides at temperatures ranging from 400 to 550°C. U_3O_8 begins to volatilize in the presence of NF_3 near 530°C under similar experimental conditions. The mixture will be treated with 10-percent NF_3 at 400 to 450°C to leverage differences in fluorination and oxidation kinetics to remove the niobium and ruthenium from the uranium and minimize uranium volatilization. The volatile niobium and ruthenium will be captured using a cold trap and the residual NF_3 will be recycled.

The treated mixture will be exposed to 10-percent NF_3 at 550°C to convert the U_3O_8 to volatile UF_6. The PuO_2 and NpO_2 will be converted to the tetrafluorides at this temperature. Because of slower reaction kinetics for the conversion of NpF_4 to NpF_6 and an incubation period compared to the U_3O_8 – NF_3 reaction kinetics, the uranium recovered by cold trapping should have only traces of neptunium.

If neptunium recovery is desired, the temperature can be increased to >600°C to improve reaction kinetics for the conversion of NpF_4 to NpF_6 with recovery by cold trapping. The plutonium remains with the non-volatiles.

If a mixture of neptunium and plutonium is desired, a more aggressive fluorinating agent such as fluorine or ClF_3 will be required to convert the plutonium to the volatile PuF_6. Thus, based on work by others, in our baseline conceptual process, the uranium-free residual is treated with fluorine or ClF_3 at 400 to 600°C to produce the volatile PuF_6 and NpF_6. The PuF_6 and NpF_6 would be co-collected in a cold trap. To date, volatile PuF_6 has not been produced by NF_3 treatment even though the formation from the oxide is thermodynamically favorable; however, the conversion of PuF_6 from PuF_4 by NF_3 is not thermodynamically favored.

The residual lanthanide-, strontium-, cesium-, americium-, zirconium-, and lesser fission product-containing fluorides and oxyfluorides will incorporated into a waste form to be developed. Immobilization candidates include fluoro-apatite, borosilicate glass, or a combination of a ceramic and phosphate glass.

The conceptual process flowsheet is constructed to provide as much separation of the volatile fission products and actinides as possible. The flowsheet could be modified to simultaneously remove the low-temperature forming volatile fission product fluorides from the uranium by increasing the initial NF_3 treatment temperature to between 400 and 450°C. Another potential modification would be to use the ability of NF_3 to form stable uranium oxyfluorides from UO_2 as an intermediate(s) before the formation of volatile UF_6 at higher temperatures; this chemical conversion might release the volatile fission products (tritium, krypton, xenon, and iodine).

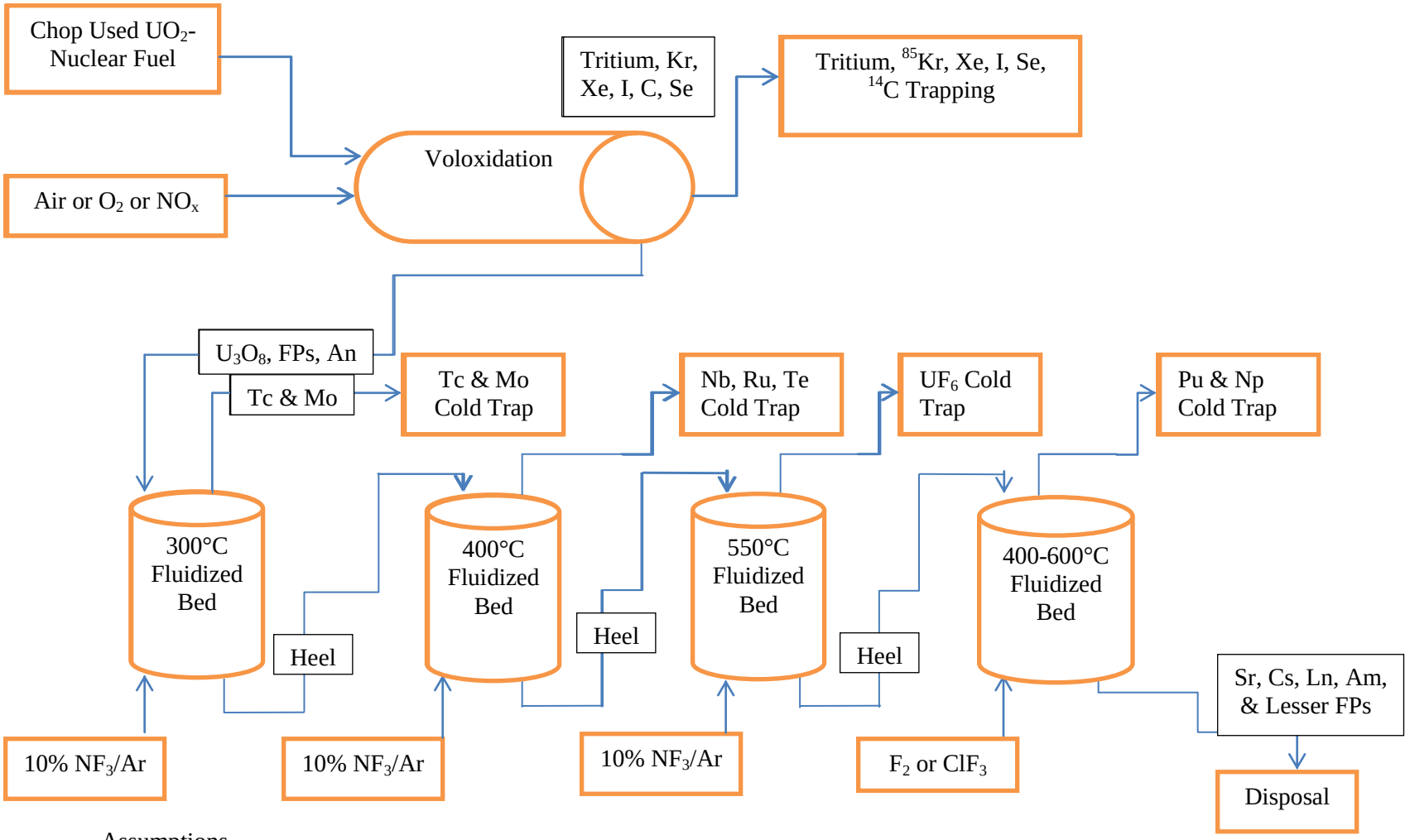

Assumptions

1) NF_3 is recycled.
2) Assume neptunium is not desired as a pure product.
3) Oxygen and nitrogen are the gaseous waste products.
4) Technetium, molybdenum, niobium, ruthenium, and tellurium will be managed as wastes

Figure 7-1. Conceptual NF_3-based flowsheet relying on reactions thermal sensitivities for separations.

8. Conclusions

Our early investigation of the potential use of NF_3 as a fluorinating and oxidizing agent in fluoride volatility-based nuclear fuels reprocessing has shown that NF3 can successfully fluorinate likely chemical forms of the used nuclear-fuel constituents. With the exceptions of rhodium and plutonium, NF3 can effectively convert neat fuel constituent compounds that form volatile fluorides to volatile fluorides or oxyfluorides. The volatilization reaction is temperature sensitive with transition metal oxides such as technetium and molybdenum being volatilized near 300°C and actinides such as uranium and neptunium being volatilized near 500°C. There are sufficient differences in volatilization reaction rates such that separations of those constituents such as uranium and neptunium can be easily separated from each other.

Our kinetic modeling studies have shown that the reactions of NF3 with UO2, NpO2, and PuO2 are complex likely being affected by uncontrolled physical factors. The nature of the kinetic gas-solid reactions depends on whether it is a volatile-forming reaction or simply the addition of fluorine, the substitution of fluorine for oxygen, and/or oxidation coupled with fluorination. The predominant gas-solid reaction mechanisms appear to be either two-dimensional or three-dimensional phase-boundary reactions, diffusion, or first-order chemical reaction.

With respect to process applications, we found that, depending on temperature, volatilization can be driven to completion in <100 minutes. The temperature to achieve these potential processing times varies depending on the target fuel constituent. For complete release of all fuel constituents including the important plutonium, a more aggressive fluorinating and oxidizing agent would be required for separation from the non-volatile fluorides. We have proposed a conceptual flowsheet that would use fluorine or ClF3, both of which the nuclear industry has experience with, to treat the 5 mass% residual after removal of the volatile fluorides.

In general, our studies have shown that NF3 continues to be an attractive potential approach for recovering valuable constituents in used nuclear fuel or for recovering medical radioisotopes from irradiated materials. The ability of NF3 to partially fluorinate UO2 to oxyfluorides hints at the possibility that such treatment could be used to release tritium, iodine, and the volatile fission gases from the used-fuel matrix.

9. References

Adair, HL, and EH Kobisk. 1975. "Preparation and Characterizaton of Neutron Dosimeter Materials." Nuclear Technology 25:224-36.

Anastasia, LJ, PG alfredson, and MJ Steindler. 1968. "Fluidized-Bed Fluorination of UO_2-PuO_2 Fission Product Pellets with Fluorine." Nucl. Appl. Technol. 4:320-9.

Anastasia, LJ, PG Alfredson, and MJ Steindler. 1969. "Fluidized-Bed Fluorination of UO_2-PuO_2 Fission Product Pellets with BrF_5 and Fluorine. Part 1. The Fluorination of Uranium, Neptunium, and Plutonium." Nucl. Appl. Technol. 7:425-32.

Anastasia, LJ, PG Alfredson, MJ Steindler, GW Redding, JG Riha, and M Haas. 1967. *Laboratory Investigations in Support of Fluid-Bed Fluoride Volatility Processes. Part XVI. The Fluorination Of UO2—PuO2-Fission-Product Oxide Pellets With Fluorine in a 2-Inch-Diameter Fluid-Bed Reactor*. ANL-7372. Argonne National Laboratory, Argonne Illinois.

Anderson, RE, EM Vander Wall, and RK Schaplowsky. 1977. Nitrogen Trifluoride. Technical Rpt. AFRPL-TR-77-71, Aerojet Liquid Rocket Co, Sacramento, CA.

Armstrong, DP, RJ Jarabek, and WH Fletcher. 1989. "Micro-Raman Spectroscopy of Selected Solid UxOyFz Compounds." Applied Spectroscopy 43:461-68.

Asprey, LB, PG Eller, and SA Kinkead. 1986. "Formation of Actinide Hexafluorides at Ambient Temperatures with Krypton Difluoride." Inorganic Chemistry 25:670-72.

Binenboym, J, U El-Gad, and H Selig. 1974. "Reaction of Ammonium Pertechnetate with Anhydrous Hydrogen Fluoride. Vibrational Spectra of Pertechnetyl Fluoride." Inorganic Chemistry 13:319-21.

Brown, D. 1968. Halides of the Transition Elements. Wiley-Interscience, John Wiley & Sons LTD, New York.

Burg, AB. 1950. "Volatile Inorganic Fluorides." in Fluorine Chemistry, ed. JH Simmons, Vol 1. Academic Press, Inc., New York.

Chilenskas, AA. 1968. "Fluidized-Bed Fluoride Volatility Processing of Irradiated UO_2 Fuels." Nuclear Applications 5:11-19.

Claassen, HH, GL Goodman, JH Holloway, and H Selig. 1970. "Raman Spectra of MoF_6, TcF_6, ReF_6, UF_6, SF_6, SeF_6, and TeF_6 in the Vapor State." J. Chem Physics 53:341-48.

Claassen, HH, H Selig, JG Malm, CL Chernick, and B Weinstock. 1961. "Ruthenium Hexafluoride." Journal of the American Chemical Society 83:2390-91.

Corbin, O, A Vanderschmitt, and M Lucas. 1980. "Ruthenium in Fuel Reprocessing by Fluoride Volatility Process (II)." J Nuclear Science and Technology 17:443 - 47.

Del Cul, GD, AS Icenhour, DW Simmons, and LD Trowbridge. 2002. *Present Status of the Recovery and Processing of ^{233}U from the Oak Ridge Molten Salt Reactor*. in American Nuclear Society 5th Topical Meeting on Spent Nuclear Fuel and Fissile Materials Management. American Nuclear Society, Charleston, South Carolina.

Edwards, AJ, GR Jones, and RJC Sills. 1968. "The crystal structure of a trimeric form of technetium oxide tetrafluoride." Chem. Commun:1177-78.

Edwards, AJ, GR Jones, and RJC Sills. 1970. "Fluoride crystal structures. Part XII: Trimeric technetium oxide tetrafluoride." J. Chem. Soc. A:2521-23.

Fischer, J, LE Trevorrow, GJ Vogel, and WA Shinn. 1962. "Plutonium Hexafluoride Thermal Decomposition Rates." Ind. Eng. Chem. Proc. Des. Dev. 1:47-51.

Galkin, NP, LA Ponomarev, and YD Shishkov. 1990. "Investigation of processes of separation of uranium and plutonium hexafluorides." Radiokhimica 22:754-57.

Galwey, AK. 2004. "Is the science of thermal analysis kinetics based on solid foundations?: A literature appraisal." Thermochimica Acta 413:139-83.

Gendre, R. 1962. CEA-2161. Commissariat a l'Energie Atomique, Paris, France.

Gibson, JK, and RG Haire. 1992. "High-temperature fluorination studies of uranium, neptunium, plutonium and americium." Journal of Alloys and Compounds 181:23-32.

Golja, B, J Barkanic, A Hoff, and J Stach. 1983. "Plasma Etching characteristics of Si and SiO_2 in NF_3/Ar and NF_3/He Plasmas." The Electrochemical Society Extended Abstracts (Washington, D.C. October 9-14, 1983):207-08.

Golja, B, JA Barkanic, and A Hoff. 1985. "A review of nitrogen trifluoride for dry etching in microelectronics processing." Microelectronics Journal 16:5-21.

Gray, J, P Korinko, B Garcia-Diaz, A Visser, and T Adams. 2010. *Reactive Gas Recycle for Used Nuclear Fuel* in FCRD Annual Report, FCRD-SEPA-2010-000177. Savannah River National Laboratory, Aiken, SC.

Henrion, PN, and A Leurs. 1971. "Kinetics of the reaction of UO_2, NpO_2 and (U, Pu)O_2 with fluorine and its chlorine derivatives." Journal of Nuclear Materials 41:1-22.

Herak, R. 1969. "The crystal structure of the high temperature modification of U_3O_8." Acta Crystallographica Section B 25:2505-08.

Homma, S, S Ogata, J Koga, and S Matsumoto. 2005. "Gas-solid reaction model for a shrinking spherical particle with unreacted shrinking core." Chemical Engineering Science 60:4971-80.

Homma, S, Y Uoi, A Braun, J Koga, and S Matsumoto. 2008. "Reaction Model for Fluorination of Uranium Dioxide Using Improved Unreacted Shrinking Core Model for Expanding Sperical Particles." J Nuclear Science and Technology 45:823-27.

Ishii, F, and Y Kita. 2000. in Advanced Inorganic Fluorides, eds. T Nakajima, BZ emva and A Tressaud, pp. 629. Elsevier, Amsterdam.

Iwasaki, M. 1964. "Kinetic studies of the fluorination of uranium oxides by fluorine--I : The fluorination of U3O8 and UO3." Journal of Inorganic and Nuclear Chemistry 26:1853-61.

Iwasaki, M. 1968. "Kinetics of the fluorination of uranium dioxide pellets by fluorine." Journal of Nuclear Materials 25:216-26.

Jarry, RL, and J Stockbar. 1966. ANL-7125. Argonne National Laboratory, Argonne, IL.

Johnson, CE, and J Fischer. 1961. "Kinetics of the Reaction Of Sulfur Tetrafluoride With Uranium Trioxide And Uranyl Fluoride." The Journal of Physical Chemistry 65:1849-52.

Jonke, AA. 1965. "Reprocessing of Nuclear Reactor Fuels by Processes Based on Volatilization, Fractional Distillation, and Selective Adsorption." Journal Name: Atomic Energy Review (Austria) 3:3-60.

Kamoshida, M, F Kawamura, A Sasahira, T Fukasawa, T Sawa, and J Yamashita. 2000. "A new concept for the nuclear fuel recycle system: Application of the fluoride volatility reprocessing." Progress in Nuclear Energy 37:145-50.

Kani, Y, A Sasahira, K Hoshino, and F Kawamura. 2009. "New reprocessing system for spent nuclear reactor fuel using fluoride volatility method." Journal of Fluorine Chemistry 130:74-82.

Kastenmeier, B. 2000. "Gas utilization in remote plasma cleaning and stripping applications." J. Vac. Sci. Technol. A 18:2102.

Kim, KC, and GM Campbell. 1985. "Fourier Transform Infrared Spectrometry Using a Very-Long-Pathlength Cell: Dioxygen Difluoride Stability and Reactions with Plutonium Compounds." Applied Spectroscopy 39:625-28.

Kleykamp, H. 1985. "The chemical state of the fission products in oxide fuels." Journal of Nuclear Materials 131:221-46.

Kleykamp, H, JO Paschoal, R Pejsa, and F Thümmler. 1985. "Composition and structure of fission product precipitates in irradiated oxide fuels: Correlation with phase studies in the Mo-Ru-Rh-Pd and BaO-UO_2-ZrO_2-MoO_2 Systems." Journal of Nuclear Materials 130:426-33.

Kobayashi, H, O Amano, F Kawamura, M Aoi, K Hoshino, A Sasahira, and Y Kani. 2005. "Fluorex reprocessing system for the thermal reactors cycle and future thermal/fast reactors (coexistence) cycle." Progress in Nuclear Energy 47:380-88.

Kwon, SW, EH Kim, BG Ahn, JH Yoo, and HG Ahn. 2002. "Fluorination of Metals and Metal Oxides by Gas-Solid Reaction." Journal of Industrial and Engineering Chemistry 8:477-82.

Labaton, VY. 1959. "The fluorides of uranium--IV Kinetic studies of the fluorination of uranium tetrafluoride by chlorine trifluoride." Journal of Inorganic and Nuclear Chemistry 10:86-93.

Labaton, VY, and KDB Johnson. 1959. "The fluorides of uranium--III Kinetic studies of the fluorination of uranium tetrafluoride by flourine." Journal of Inorganic and Nuclear Chemistry 10:74-85.

Langan, J. 1998. "Electrical impedance analysis and etch rate maximization in NF_3/Ar discharges." J. Vac. Sci. Technol. A 16:2108.

Lau, KH, RD Brittain, and DL Hildenbrand. 1985. "Complex sublimation/decomposition of uranyl fluoride: thermodynamics of gaseous uranyl fluoride (UO_2F_2) and uranium oxide fluoride (UOF_4)." The Journal of Physical Chemistry 89:4369-73.

Levitz, NM, LJ Anastasia, EL Carls, AA Chilenskas, JAE Graae, AA Jonke, RA Kessie, RP Larsen, WJ Mecham, D Ramaswami, MJ Steindler, and GJ Vogel. 1969. *A Conceptual Design Study of a Fluoride-Volatility Plant for Reprocessing LMFBR Fuels*. ANL-7583, Vol ANL-7583. Argonne National Laboratory.

Loopstra, BO. 1970. "The structure of β-U_3O_8." Acta Crystallographica Section B 26:656-57.

Malm, JG, PG Eller, and LB Asprey. 1984. "Low temperature synthesis of plutonium hexafluoride using dioxygen difluoride." Journal of the American Chemical Society 106:2726-27.

Malm, JG, B Weinstock, and EE Weaver. 1958. "The Preparation and Properties of NpF_5; a Comparison with PuF_5." The Journal of Physical Chemistry 62:1506-08.

McEachern, RJ, and P Taylor. 1998. "A review of the oxidation of uranium dioxide at temperatures below 400°C." Journal of Nuclear Materials 254:87-121.

McNamara, B, R Scheele, A Kozelisky, and M Edwards. 2009. "Thermal reactions of uranium metal, UO_2, U_3O_8, UF_4, and UO_2F_2 with NF_3 to produce UF_6." Journal of Nuclear Materials 394:166-73.

Moeller, T. 1973. "The Lanthanides." in Comprehensive Inorganic Chemistry, eds. JC Bailar, et al., Vol 4. Pergamon Press, New York.

O'Hare, PAG, and JG Malm. 1982. "Thermochemistry of uranium compounds XIII. Standard enthalpies of formation at 298.15 K of α-uranium oxide tetrafluoride (UOF_4) and uranyl fluoride (UO_2F_2) Thermodynamics of (uranium + oxygen + fluorine)." The Journal of Chemical Thermodynamics 14:331-36.

Ogata, S, S Homma, A Sasahira, F Kawamura, J Koga, and S Matsumoto. 2004. "Fluorination Reaction of Uranium Dioxide by Fluorine." J Nuclear Science and Technology 41:135-41.

Otey, MG, and RA LeDoux. 1967. "$U_3O_5F_8$--A new compound in the U-O-F system." Journal of Inorganic and Nuclear Chemistry 29:2249-56.

Paine, RT, RR Ryan, and LB Asprey. 1975. "Synthesis, characterization, and structure of uranium oxide tetrafluoride." Inorganic Chemistry 14:1113-17.

Peacock, RD. 1983. in Handbook of Inorganic Chemistry Supplement, eds. HH Kugler and C Keller, Vol 2, pp. 78-84. Springer Verlag, Berlin.

Rard, JA, G Anderegg, H Wanner, and MH Rand. 1999. Chemical Thermodynamics of Technetium. 3, Elesvier Sciences B. V., Amsterdam, the Netherlands.

Roine, A, T Kottiranta, P Lamberg, J Mansikka-aho, P Bjorklund, J-P Kentala, T Talonen, R Ahlberg, A Grohn, O Saarinen, J Myyri, J Sipila, Vartiainen, and etc. 2009. *HSC Chemistry 7.00*. Outotec Research Oy, Pori, Finland.

Sakurai, T. 1974. "Comparison of the fluorinations of uranium dioxide by bromine trifluoride and elemental fluorine." The Journal of Physical Chemistry 78:1140-44.

Scheele, RD, and AM Casella. 2010. *Assessment of the Use of Nitrogen Trifluoride for Purifying Coolant and Heat Transfer Salts in the Fluoride Salt-Cooled High Temperature Reactor*. PNNL-19793. Pacific Northwest National Laboratory, Richland, Washington.

Scheele, RD, BK McNamara, BM Rapko, MK Edwards, AE Kozelisky, RC Daniel, TI McSweeney, RB Kefgen, SJ Maharas, PJ Weaver, and KJ Iwamasa. 2006. *Development of NF_3 Deposit Remoal Technology for the Portsmouth Gaseous Diffusion Plant*. in Waste Management 06, Tucson, AZ.

Schmets, JJ. 1970. "Reprocessing of Spent Nuclear Fuels by Fluoride Volatility Processes." At. Energy Rev. ;8: 3-126 (Mar 1970).

Schwochau, K. 2000. Technetium: Chemistry and Radiopharmaceutical Applications. Wiley-VCH, Weinheim, Federal Republic of Germany.

Seaborg, GT, and HS Brown. 1961. "Preparation of neptunium hexafluoride." 2,982,604.

Selig, H, CL Chernick, and JG Malm. 1961. "The preparation and properties of TcF_6." Journal of Inorganic and Nuclear Chemistry 19:377-77.

Selig, H, and JG Malm. 1963. "The preparation and properties of pertechnetyl fluoride,TcO_3F." Inorg. Nucl. Chem 25:349-51.

Sharp, JH, GW Brindley, and BNN Achar. 1966. "Numerical Data for Some Commonly Used Solid State Reaction Equations." Journal of the American Ceramic Society 49:379-82.

Shatalov, VV, MB Seregin, VF Kharin, and LA Ponomarev. 2001. "Gas-Fluoride Technology for Processing Spent Oxide Fuel." Atomic Energy 90:224-34.

Steindler, MJ, and DV Steidl. 1957. ANL-5759. Argonne National Laboratory, Argonne, IL.

Stephenson, MJ, JR Merriman, and HL Kaufman. 1967. *Removal of Impurities from Uranium Hexafluoride by Selective Sorption Techniques*. USAEC-Report K-1713. USAEC.

Streng, AG. 1963. "The Oxygen Fluorides." Chemical Reviews 63:607-24.

Szekely, J, JW Evans, and HY Sohn. 1976a. Gas-Solid reactions. Academic Press, New York.

Szekely, J, JW Evans, and HY Sohn. 1976b. Gas-Solid Reactions. Academic Press, Inc., New York.

Trevorrow, LE, TJ Gerding, and MJ Steindler. 1968. "The fluorination of neptunium(IV) fluoride and neptunium(IV) oxide." Journal of Inorganic and Nuclear Chemistry 30:2671-77.

Trevorrow, LE, WA Shinn, and RK Steunenberg. 1961. "The Thermal Decomposition of Plutonium Hexafluoride." The Journal of Physical Chemistry 65:398-403.

Uhlíř , J, and M Mareček. 2009. "Fluoride volatility method for reprocessing of LWR and FR fuels." Journal of Fluorine Chemistry 130:89-93.

Vandenbussche, G. 1966. CEA-R-2859. Commissariat a l'Energie Atomique, Paris, France.

Weaver, CF, and HA Friedman. 1967. *A lterature survey of the fluorides and oxy fluorides of molydenum*. Oak Ridge National Laboratory, Oak Ridge, TN.

Weinstock, B, and JG Malm. 1956. "The properties of plutonium hexafluoride." Journal of Inorganic and Nuclear Chemistry 2:380-94.

Weinstock, B, EE Weaver, and JG Malm. 1959. "Vapour-pressures of NpF_6 and PuF_6; thermodynamic calculations with UF_6, NpF_6 and PuF_6." Journal of Inorganic and Nuclear Chemistry 11:104-14.

Wilson, PW. 1974a. "The preparation and properties of uranium oxide tetrafluoride." Journal of Inorganic and Nuclear Chemistry 36:303-05.

Wilson, PW. 1974b. "$U_2O_3F_6$--Its preparation and properties." Journal of Inorganic and Nuclear Chemistry 36:1783-85.

Yahata, T, and M Iwasaki. 1964. "Kinetic studies of the fluorination of uranium oxides by fluorine--II : The fluorination of UO_2." Journal of Inorganic and Nuclear Chemistry 26:1863-67.

Yoo, JH, CS Seo, H Kim, and L Soo. 2008. "A Conceptual Study of Pyroprocessing for Recovering Actinides from Spent Oxide Fuels." Nuclear Engineering and Technology 40:581-92.